

**DOE/NASA/0155-1
NASA CR-165369**

DEMONSTRATION OF CATALYTIC COMBUSTION WITH RESIDUAL FUEL

**W.J. Dodds and E.E. Ekstedt
General Electric Company
Aircraft Engine Business Group**

August 1981

**Prepared for
NATIONAL AERONAUTICS AND SPACE ADMINISTRATION
Lewis Research Center
Under Contract DEN3-155**

**for
U.S. DEPARTMENT OF ENERGY
Fossil Energy
Office of Coal Utilization**

NOTICE

This report was prepared to document work sponsored by the United States Government. Neither the United States nor its agent, the United States Department of Energy, nor any Federal employees, nor any of their contractors, subcontractors or their employees, makes any warranty, express or implied, or assumes any legal liability or responsibility for the accuracy, completeness, or usefulness of any information, apparatus, product or process disclosed, or represents that its use would not infringe privately owned rights.

**DOE/NASA/0155-1
NASA CR-165369**

DEMONSTRATION OF CATALYTIC COMBUSTION WITH RESIDUAL FUEL

**W.J. Dodds and E.E. Ekstedt
General Electric Company
Aircraft Engine Business Group**

August 1981

**Prepared for
NATIONAL AERONAUTICS AND SPACE ADMINISTRATION
Lewis Research Center
Under Contract DEN3-155**

**for
U.S. DEPARTMENT OF ENERGY
Fossil Energy
Office of Coal Utilization**

Page intentionally left blank

Page intentionally left blank

FOREWORD

The work described herein was conducted by the General Electric Aircraft Engine Business Group under Contract DEN3-155. The work was sponsored by the U.S. Department of Energy and was performed under the direction of the NASA Project Manager, Dr. David N. Anderson.

Key General Electric contributors to this program were: E.J. Rogala, Program Manager; E.E. Ekstedt, Technical Program Manager; W.J. Dodds, Principal Investigator; B.T. Keith, Test Section Design; W.E. Kelsey, Fuel Injector Design; M.W. Shayeson, Fuels Consultant; and R.C. Crandall, H.J. Wheeler, and M.P. Kelsey of the Advanced Combustion Laboratory.

Catalytic Reactors were designed and fabricated by Engelhard Industries under the direction of K.R. Burns, Venture Manager; and Drs. I.T. Osgerby and H.C Lee.

Page intentionally left blank

Page intentionally left blank

TABLE OF CONTENTS

Section	Page
1.0 SUMMARY	1
2.0 INTRODUCTION	3
3.0 PROGRAM DESCRIPTION	4
3.1 Task I - Test Section Design and Fabrication	4
3.2 Task II - Lean Catalytic Combustor Testing	4
3.3 Task III - Testing of Backup Reactors with Different Lengths	7
3.4 Task IV - Reports and Records	7
4.0 TEST RIG AND FACILITIES	8
4.1 Catalytic Reactor Test Rig	8
4.1.1 Inlet Section	8
4.1.2 Fuel-Preparation Section	8
4.1.3 Catalytic Reactor	19
4.1.4 Exit Instrumentation Section	26
4.2 Combustor Test Facility	26
4.3 Test Instrumentation	31
4.4 Test Procedures	39
4.5 Test-Fuel Characteristics	41
5.0 RESULTS AND DISCUSSION	47
5.1 Baseline Catalytic Reactor Test Results	47
5.1.1 Baseline Test Description	47
5.1.2 Baseline Catalytic Reactor Emissions and Performance	48
5.2 Backup Catalytic Reactor Test Results	56
5.2.1 Backup Test Description	56
5.2.2 Backup Catalytic Reactor Emissions and Performance	57
5.3 Fuel/Air Mixture-Preparation System Performance	68
6.0 CONCLUDING REMARKS	78
APPENDIX A - TEST DATA SUMMARY	81
APPENDIX B - MULTIPLE CONICAL TUBE INJECTOR	96
APPENDIX C - SYMBOLS	103
REFERENCES	106

LIST OF ILLUSTRATIONS

<u>Figure</u>	<u>Page</u>
1. Baseline Catalytic Reactor.	5
2. Fuel-Preparation Section.	6
3. Catalytic Reactor Test Rig Assembly.	9
4. Air-Assisted Simplex Fuel Nozzle.	11
5. Exploded View of Fuel Nozzle.	12
6. Effect of Air Velocity and Fuel-Flow Rate on Predicted Drop Size.	15
7. Predicted Design-Point Drop Size with No. 6 Oil.	16
8. Ignition Delay of No. 6 Fuel Oil in Air at Elevated Temperature and Pressure.	18
9. Effect of Drop Size on Fuel Vaporization (Design Point).	20
10. Fuel Injector Mounting.	21
11. Comparison of Catalyst Materials.	24
12. Comparison of Catalyst Materials (Second Backup Reactor).	25
13. Catalytic Reactor Mounting.	29
14. Exit Instrumentation Section.	30
15. Heated Residual Fuel System.	32
16. Control Console, Building 306 Advanced Combustion Laboratory.	33
17. Catalytic Reactor Thermocouple Installation.	36
18. Emissions Sampling Probe.	38
19. Test-Fuel Viscosity.	45
20. No. 6 Residual Oil Temperature Rise.	46
21. Baseline Catalytic Reactor Emissions and Performance Characteristics.	49

LIST OF ILLUSTRATIONS (Continued)

<u>Figure</u>	<u>Page</u>
22. Fuel-Bound Nitrogen Conversion.	50
23. Typical Test-Rig Temperature Profiles - Baseline Reactor.	51
24. Baseline Catalytic Reactor Pressure Prop Increase with Operating Time.	53
25. Postrun Condition of Baseline Catalytic Reactor.	54
26. Baseline Catalytic Reactor, Internal Damage.	55
27. Catalytic Reactor Operating Range.	58
28. No. 6 Oil Combustion Efficiency Comparison.	59
29. Relationship Between Combustion Efficiency and NO _x Emissions (No. 6 Oil).	60
30. First Backup Catalytic Reactor Pressure Drop.	61
31. Second Backup Catalytic Reactor Pressure Drop.	62
32. Effect of Inlet Temperature on Emissions and Performance for the Second Backup Reactor.	64
33. Effect on Second Backup Catalytic Reactor of Inlet Temperature/Adiabatic Flame Temperature Correlation.	65
34. Effect on Second Backup Reactor of Reference Velocity on Emissions and Performance.	66
35. Effect of Initial Drop Size on First Backup Catalytic Reactor Emissions and Performance.	69
36. Effect of Pressure on Fuel Evaporation.	70
37. Effect of Air Temperature on Fuel Evaporation.	70
38. Second Backup Catalytic Reactor Axial Temperature Profiles.	71
39. Condition of Inlet Element in the First Backup Catalytic Reactor After Test Run.	72

LIST OF ILLUSTRATIONS (Concluded)

<u>Figure</u>		<u>Page</u>
40.	Postrun Photograph of Second Backup Reactor Elements.	73
41.	Effect of Reference Velocity on Fuel/Air Mixture Uniformity (No. 6 Oil).	75
42.	Effect of Initial Drop Size on Fuel/Air Mixture Uniformity (First Backup Reactor).	76
43.	Fuel-Preparation-System Pressure Drop (First Backup Reactor).	77
44.	Temperature Corrections for $V_T = 19.8$ m/s.	94
45.	Temperature Corrections for $V_T = 30.5$ m/s.	95
46.	Multiple-Conical-Tube Fuel Injectors.	97
47.	Multiple-Conical-Tube Injector Cross Sections.	98
48.	Multiple-Tube Injector Design Details.	99
49.	Multiple-Tube Injector Fuel Tube Installation.	100
50.	Multiple-Tube Injector Inlet.	101

LIST OF TABLES

<u>Table</u>	<u>Page</u>
I. Test Conditions for Original Test Section Design.	10
II. Fuel/Air Mixture-Preparation System Design Guidelines.	13
III. Residual Fuel Properties Assumed for Vaporization Calculations.	17
IV. Catalytic Reactor Design Guidelines.	22
V. Baseline Catalytic Reactor Description.	23
VI. First Backup Catalytic Reactor Description.	27
VII. Second Backup Catalytic Reactor Description.	28
VIII. Instrumentation Listing.	34
IX. Location of Axial Stations (Baseline Reactor).	37
X. Emission Instrument Calibration Gases.	39
XI. Supplementray Test-Point Schedule for Backup Reactors.	40
XII. Measured and Calculated Test Parameters.	42
XIII. Test-Fuel Properties.	44
XIV. Combustion Efficiency and CO Correlation Constants.	67
XV. Test Summary, Run 1.	82
XVI. Temperatures and Exhaust-Gas Concentrations, Run 1.	83
XVII. Test Summary, Run 2.	84
XVIII. Temperatures and Exhaust-Gas Concentrations, Run 2.	85
XIX. Test Summary, Run 3.	86
XX. Temperatures and Exhaust Gas Concentrations, Run 3.	87
XXI. Test Summary, Run 4.	88
XXII. Temperatures and Exhaust-Gas Concentrations, Run 4.	89

LIST OF TABLES (Concluded)

<u>Table</u>	<u>Page</u>
XXIII. Test Summary, Run 5.	90
XXIV. Temperatures and Exhaust-Gas Concentrations, Run 5.	91
XXV. Test Summary, Runs 6-8.	92
XXVI. Temperatures and Exhaust-Gas Concentrations, Runs 6, 7, and 8.	93
XXVII. Multiple-Conical-Tube Injector Design Values.	102

1.0 SUMMARY

A demonstration of catalytic combustion has been conducted with a residual fuel oil. The work was sponsored by the U.S. Department of Energy and managed by NASA Lewis Research Center. The overall objective was to establish basic design data needed for possible future development of low-emissions, catalytic-combustor systems for advanced, stationary-gas-turbine applications. Specific objectives were to demonstrate catalytic combustion of a residual fuel over a range of reactor inlet conditions typical of a large, stationary-gas-turbine combustor, to determine if catalytic reactor performance is affected by incomplete fuel vaporization, and to determine if fuel-droplet size influences catalytic reactor performance.

The experimental effort consisted of lean-combustion testing of three different catalytic reactors, including a baseline and two backup designs, with residual fuel oil. All of the reactors were 11.4-cm (4.5-in.) diameter, multielement configurations consisting of ceramic honeycomb sections catalyzed with palladium. Engelhard Industries designed and supplied all of the catalytic reactors under a subcontract with General Electric. All tests were conducted using a fuel/air-mixture-preparation system consisting of a single-point, air-assisted, simplex injector mounted at the throat of a converging/diverging premixing duct. Fuel-drop size with this system was controlled by varying the atomizing air pressure. The residual oil was heated to 405 K (270° F) for all tests.

The first reactor tested was a baseline configuration designed for operation at a reactor inlet temperature of 589 K (600° F), pressures up to 0.94 MPa (135 psia), and a reactor inlet reference velocity of 19.8 m/s (65 ft/s). These conditions are typical of combustor-inlet conditions for a large, industrial gas turbine. In tests of this baseline reactor, operation at temperatures below about 825 K (1025° F) was precluded due to apparent plugging of the catalytic reactor with residual oil.

In order to reduce plugging, honeycomb materials having larger channel sizes were used in the backup reactors. By increasing the channel size, particularly at the reactor inlet, the operating range was successfully widened to include operation at reactor inlet temperatures down to about 725 K (845° F).

Steady-state performance using residual oil was very good with all of the reactors tested. Combustion efficiency above 99.5% was obtained; pressure drop was less than 5%, and oxides of nitrogen (NO_x) emission indices were about 8 g/kg. Based on limited test results on Jet A/No. 6 oil fuel blends, it has been concluded that the NO_x is almost entirely due to fuel-bound nitrogen and that nearly 100% fuel-bound nitrogen conversion is obtained. The NO_x emission index for operation on Jet A alone was less than 0.5 g/kg. In addition to the widened operating range obtained with the backup reactors, combustion efficiency was slightly improved.

During backup reactor tests, fuel-drop size was varied by decreasing the atomizing airflow. In the range of 10 to 72.5 μm Sauter mean diameter (SMD), the only apparent effect of increasing drop size was a very slight increase in NO_x . Effects were expected to be slight at the temperatures studied because virtually complete evaporation was predicted.

Each of the reactors tested was damaged to some extent during the lean-combustion tests. It is thought that the observed damage (ranging from slight erosion of the reactor inlet to fairly extensive melting of the substrate) was primarily the result of attempts to operate at conditions where partial plugging with residual fuel occurred. In each case, after plugging occurred, the coating of residual oil was burned off; this resulted in high local surface temperatures that probably damaged the reactor.

Results of this experimental program indicate that No. 6 residual oil can be efficiently burned in a catalytic reactor, with acceptable pressure loss, provided the catalytic reactor inlet temperature is high enough. For a typical industrial-gas-turbine engine, either a preburner or a regenerator would probably be required to raise the catalytic reactor inlet temperature. Lean catalytic combustion produces very low thermal NO_x emissions, but NO_x due to fuel-bound nitrogen is not effectively controlled. Although short-term operation on residual oil has been demonstrated, additional durability testing is required to determine the long-term effects of residual oil operation on catalytic reactor performance.

2.0 INTRODUCTION

This report describes the results of an experimental program to demonstrate catalytic combustion of No. 6 residual oil. The use of catalytically supported combustion has been shown to be a promising means for reducing emissions of oxides of nitrogen (NO_x) from stationary-gas-turbine engines. By extending the lean stability limit, combustion catalysts allow operation at combustion temperatures below 1800 K; operation in this temperature range reduces the amount of thermally formed NO_x . The ability of catalytic reactors to operate under steady-state conditions simulating those encountered in gas-turbine engines has been well documented. However, most of the data obtained to date describes catalyst operation with nearly homogeneous fuel/air mixtures containing gaseous or completely vaporized distillate fuel. In order to serve as a practical means of combustion in stationary gas turbines, the catalytic reactor should be able to utilize a wide range of fuels, including heavy residual oils.

In order to begin to establish basic design data for possible later combustor-development efforts, the NASA Lewis Research Center, with U.S. Department of Energy sponsorship, contracted with General Electric to conduct an experimental evaluation of catalytic combustion of a heavy (No. 6) residual fuel oil. An important part of this demonstration was to document the effects of incompletely vaporized droplets entering the reactor and the effects of droplet size.

The program involved the experimental evaluation of three different catalytic reactors operating with No. 6 residual fuel oil. The three reactors consisted of one baseline reactor designed for operation at inlet conditions typical for a large industrial-gas-turbine combustor and two backup designs based on test results obtained with the baseline reactor. A fuel-injection system designed to provide less than 50% fuel vaporization, with uniform fuel/air ratio and velocity profiles at the catalyst inlet at the design operating condition, was used with each of the reactors. The use of an air-assisted nozzle in this injection system enabled the average droplet size to be varied from less than 30 μm to more than 100 μm at the design operating conditions.

Catalytic reactors for this program were noble metal on ceramic honeycomb substrate. Engelhard Industries Division of Engelhard Minerals and Chemicals Corporation designed and fabricated all of the catalytic reactors.

A brief description of the program is presented in Section 3.0 of this report. Details of the test rig, facilities, and procedures used in the experimental program are contained in Section 4.0. Test results are discussed in Section 5.0; concluding remarks are presented in Section 6.0. Appendix A is a summary of the test results, and Appendix B is a discussion of the multiple-conical-tube injector system. A list of symbols and definitions is included as Appendix C.

3.0 PROGRAM DESCRIPTION

The objectives of this experimental program were: (1) to demonstrate steady-state catalytic combustion of a residual fuel oil, (2) to determine the effect of incomplete fuel vaporization on catalytic reactor performance, and (3) to determine if the size of fuel droplets influences performance. The program comprised four tasks. Brief descriptions of the work accomplished in each task are presented below.

3.1 TASK I - TEST SECTION DESIGN AND FABRICATION

The first task comprised the design and fabrication of the baseline catalytic reactor, fuel/air-mixture-preparation systems, and test-section inlet and exit instrumentation. The nominal design-point operating conditions were:

Reactor Inlet Temperature	589 K (600° F)
Reactor Inlet Pressure	0.62 MPa (90 psia)
Reference Velocity	19.8 m/s (65 ft/s)
Adiabatic Combustion Temperature	1400 K (2050° F)
Fuel	No. 6 Residual Oil

The baseline catalytic reactor, shown in Figure 1, was an 11.4-cm (4.5-in.) diameter configuration consisting of three ceramic honeycomb elements catalyzed with palladium. The baseline fuel/air-mixture-preparation system, shown in Figure 2, consisted of an air-assisted, simplex, fuel nozzle mounted at the throat of a converging/diverging, premixing duct. This system was designed to produce average drop sizes of less than 30 μm in the air-assisted mode and drop sizes in the 70 to 150 μm range when operated in the pressure-atomizing mode. Two additional fuel-injection systems of the multiple-conical-tube type originated by Tacina (Reference 1) were designed to produce droplets in the two desired size ranges. These additional injectors were fabricated to be used as backup systems if the baseline system performed inadequately.

3.2 TASK II - LEAN CATALYTIC COMBUSTOR TESTING

Lean-combustion tests were conducted using the baseline catalytic reactor and fuel-injection systems fabricated in Task I. Initially, the catalyst was fueled with Jet A. Increasing proportions of No. 6 oil were added until operation on pure No. 6 oil was attained. Operating limits of the baseline catalytic reactor on No. 6 oil were defined, and gaseous emissions and reactor performance characteristics were measured with injected No. 6 oil drop sizes of less than 30 μm . It was determined that a catalytic reactor inlet temperature well above the original design point was required to maintain steady-state operation with pure residual oil. At temperatures below about 825 K (1025° F), the reactor plugged with the residual oil. Attempts to vary drop size at the high operating temperatures resulted in burning upstream of the catalytic reactor.

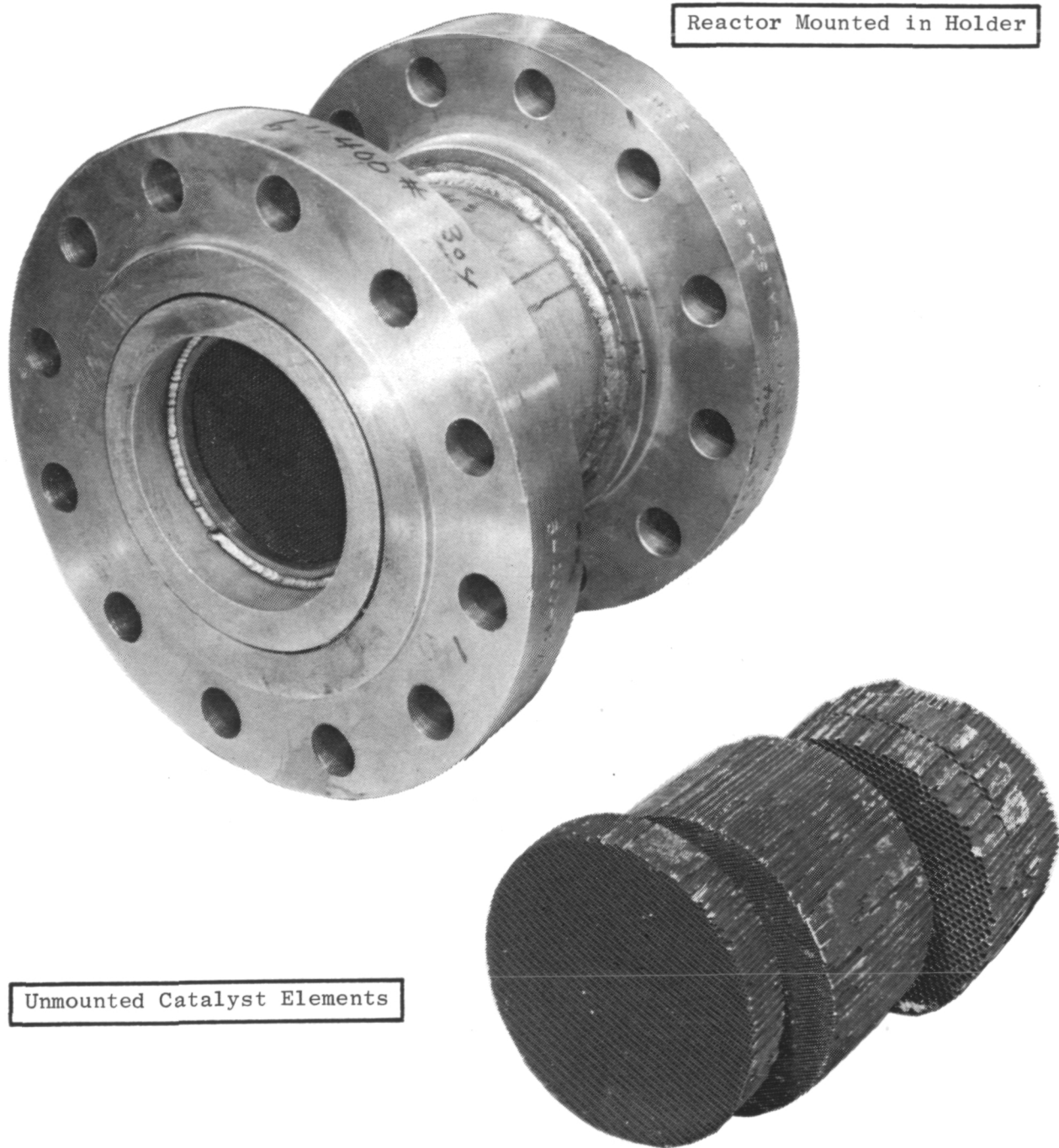


Figure 1. Baseline Catalytic Reactor.

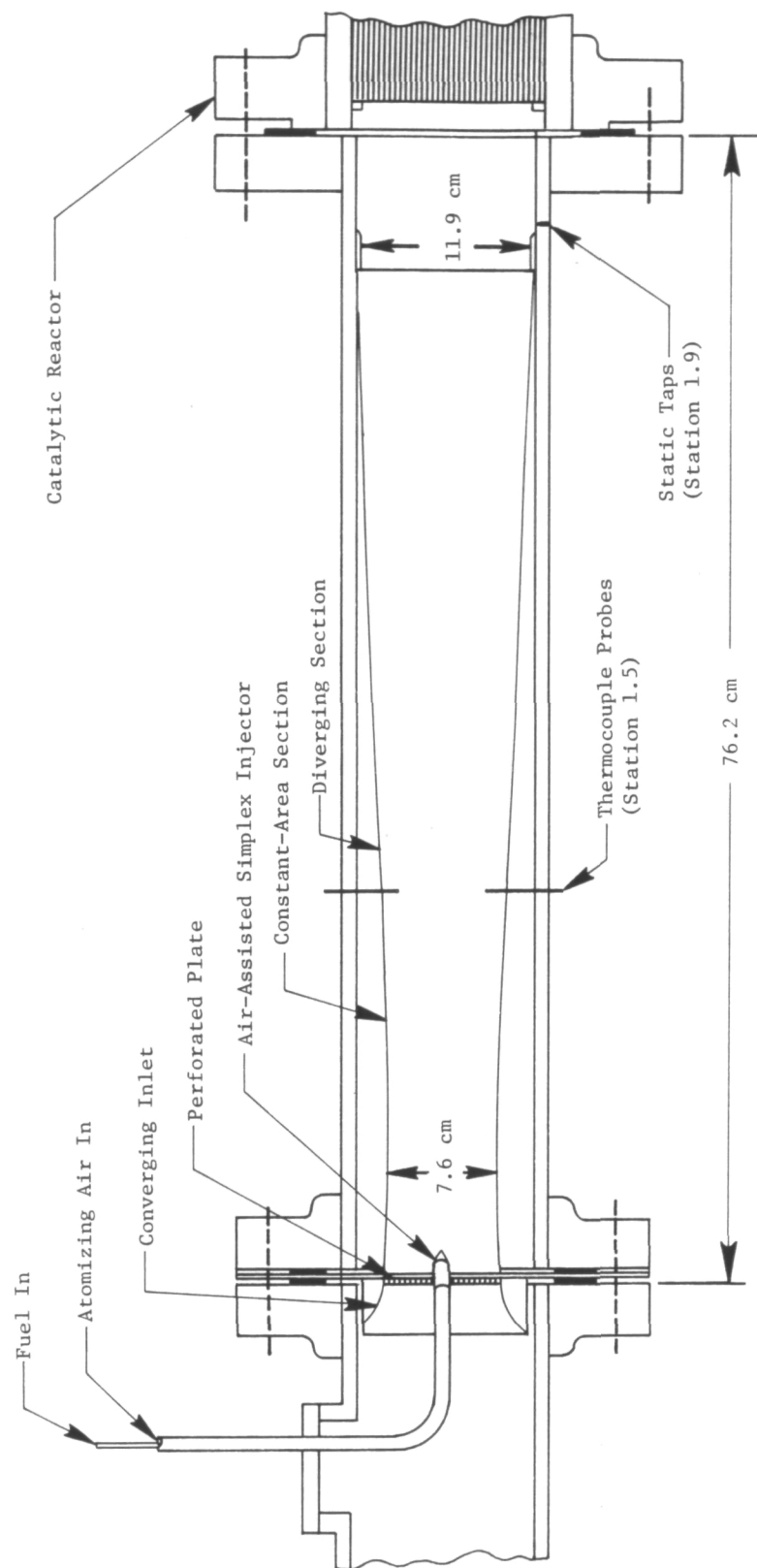


Figure 2. Fuel-Preparation Section.

3.3 TASK III - TESTING OF BACKUP REACTORS WITH DIFFERENT LENGTHS

In Task III of the program, two additional catalytic reactors were designed and tested with the baseline fuel system. These backup reactors were designed with increased-diameter catalyst channels and increased lengths in an attempt to extend the reactor operating range on No. 6 residual oil. These backup reactors were three-element designs consisting of ceramic honeycomb catalyzed with palladium. The operating limits of each configuration were defined by starting at the conditions tested with the baseline reactor and operating at progressively lower inlet temperature and higher reference velocities until steady-state operation could no longer be maintained (due to reactor plugging). Performance and gaseous emissions were measured over the range of inlet temperatures and approach velocities which could be attained by each of the backup reactors.

3.4 TASK IV - REPORTS AND RECORDS

Monthly progress reports were prepared in accordance with the contract requirements. This document constitutes the final report.

4.0 TEST RIG AND FACILITIES

4.1 CATALYTIC REACTOR TEST RIG

The test rig is shown schematically in Figure 3. This assembly contains four major components: (1) inlet section, (2) fuel/air mixture-preparation section, (3) catalytic reactor section, and (4) exit instrumentation section. All of these components have been sized to accommodate a catalytic reactor with a nominal diameter of 11.4 cm (4.5 in.) and have been designed to operate at pressures up to 2.07 MPa (300 psia) at 811 K (1000° F). Air and fuel flow rates over the original design operating range are shown in Table I for this rig. Design details of the major components are described in the following paragraphs.

4.1.1 Inlet Section

The test-rig inlet section consists of a 46-cm (18-in.) length of stainless steel pipe with an inner diameter of 12.2 cm (4.8 in.). A flow-straightening screen is mounted at the upstream end of this pipe to provide a uniform velocity profile to the fuel/air mixture-preparation section. This inlet section is fed by a 10.2-cm (4-in.) flex hose connected to the facility heated air header.

The inlet section is equipped with pads for mounting fuel-injector tubes, thermocouple probes, and static pressure taps as described in Section 4.3.

4.1.2 Fuel-Preparation Section

Design requirements for the fuel/air mixture-preparation section are described in Table II. The single-point, fuel-preparation-system configuration shown in Figure 2 was selected for this application. This system consists of an air-assisted simplex fuel nozzle, a conical flowpath insert, and an outer casing. Multiple-point injectors have most often been selected for recent studies of premixed combustion phenomena because they perform well in short systems; however, preliminary studies indicated the longer, single-point injection system could be used at the relatively low design-point temperature. The air-assisted, simplex injector was preferred because it has proven ability to inject residual oil and the further ability to easily control drop size by varying the atomizing airflow rate. Two multiple-conical-tube injectors based on Tacina designs as described in Reference 1 (one for small drops and one for large drops) were also designed and built as backups for the single-point system, but were not tested. These multiple-point systems are described in Appendix B.

The single-point-injector, fuel/air-mixture-preparation system was built around the air-assisted, simplex nozzle shown in Figures 4 and 5. This injector is a variation of the design used in the "Low NO_x Heavy Fuel Combustor

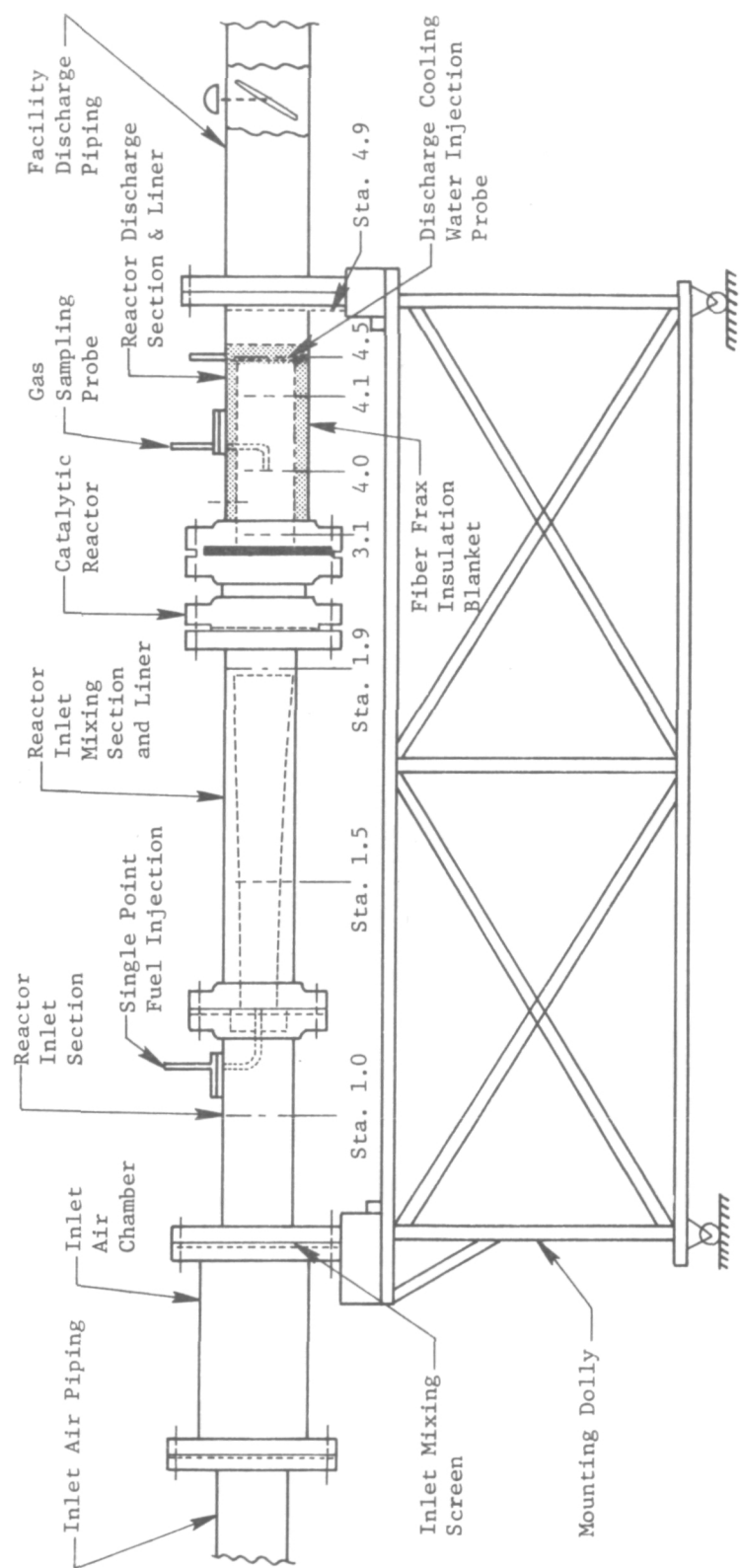


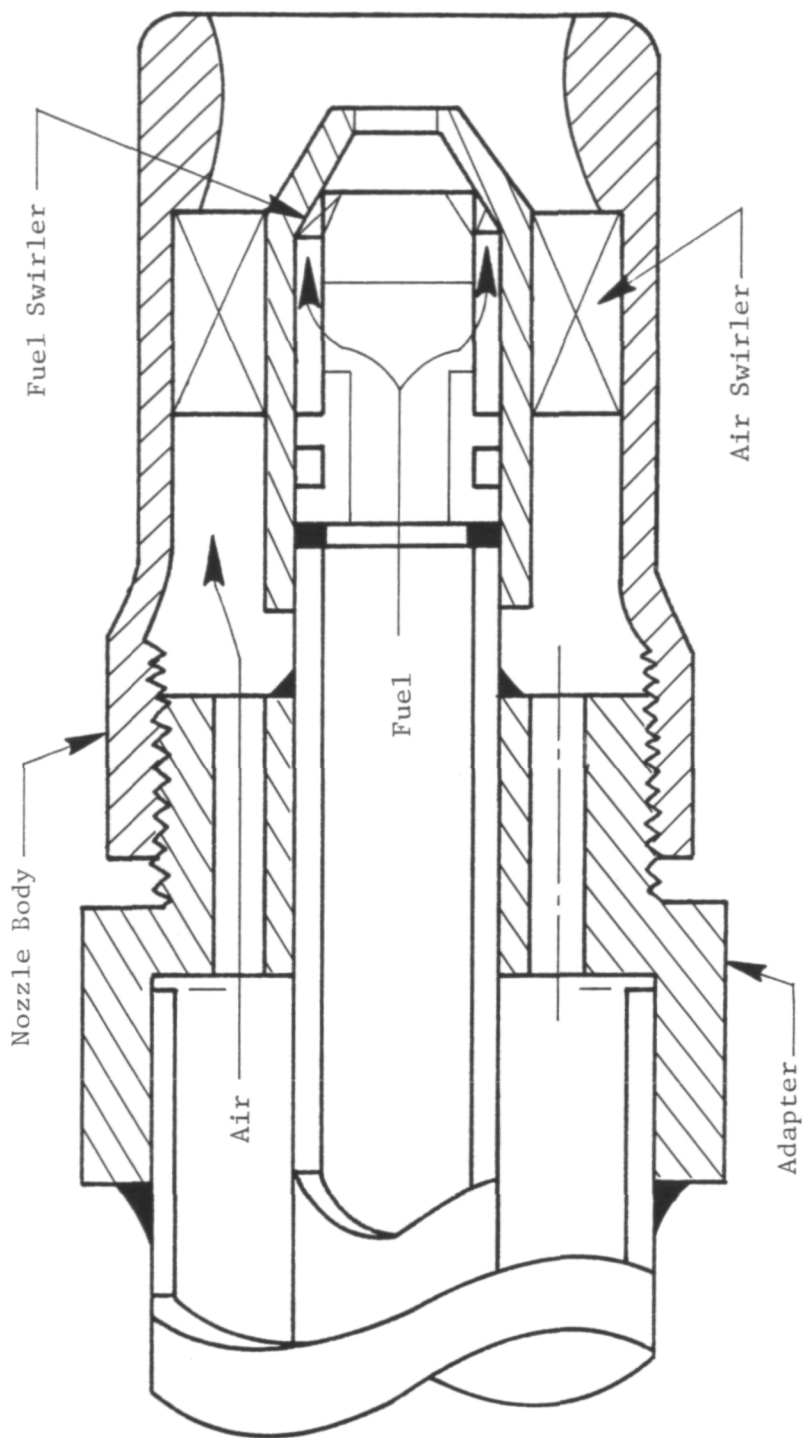
Figure 3. Catalytic Reactor Test Rig Assembly.

Table I. Test Conditions for Original Test Section Design.

● 11.4-cm Diameter Catalytic Reactor

Test Condition	Inlet Air Temperature K (° F)	Test Section Pressure, MPa (psia)	Reference Velocity* m/s (ft/s)	Fuel/Air Ratio	Reactor Airflow, kg/s (lbm/s)
Design Point	589 (600)	0.62 (90)	19.8 (65)	0.016-0.026	0.75 (1.65)
Low Reference Velocity	589 (600)	0.62 (90)	10.7 (35)	0.016-0.026	0.40 (0.89)
High Reference Velocity	589 (600)	0.62 (90)	30.5 (100)	0.016-0.026	1.15 (2.53)
High Pressure	589 (600)	0.93 (135)	19.8 (65)	0.016-0.026	1.12 (2.47)
Low Inlet Temperature	506 (450)	0.62 (90)	19.8 (65)	0.016-0.026	0.87 (1.92)

*Based on a 11.4 cm (4.5 in.) catalytic reactor.



- Fuel Nozzle Specifications 36.5 g/s at 1.0 MPa
- Airflow Effective Area Swirler 28.8 mm²
- Swirler and Adapter 25.3 mm²
- Fuel Spray Cone Angle 84°
- Air-Assist Mode 92°
- Pressure Atomizing

Figure 4. Air-Assisted Simplex Fuel Nozzle.

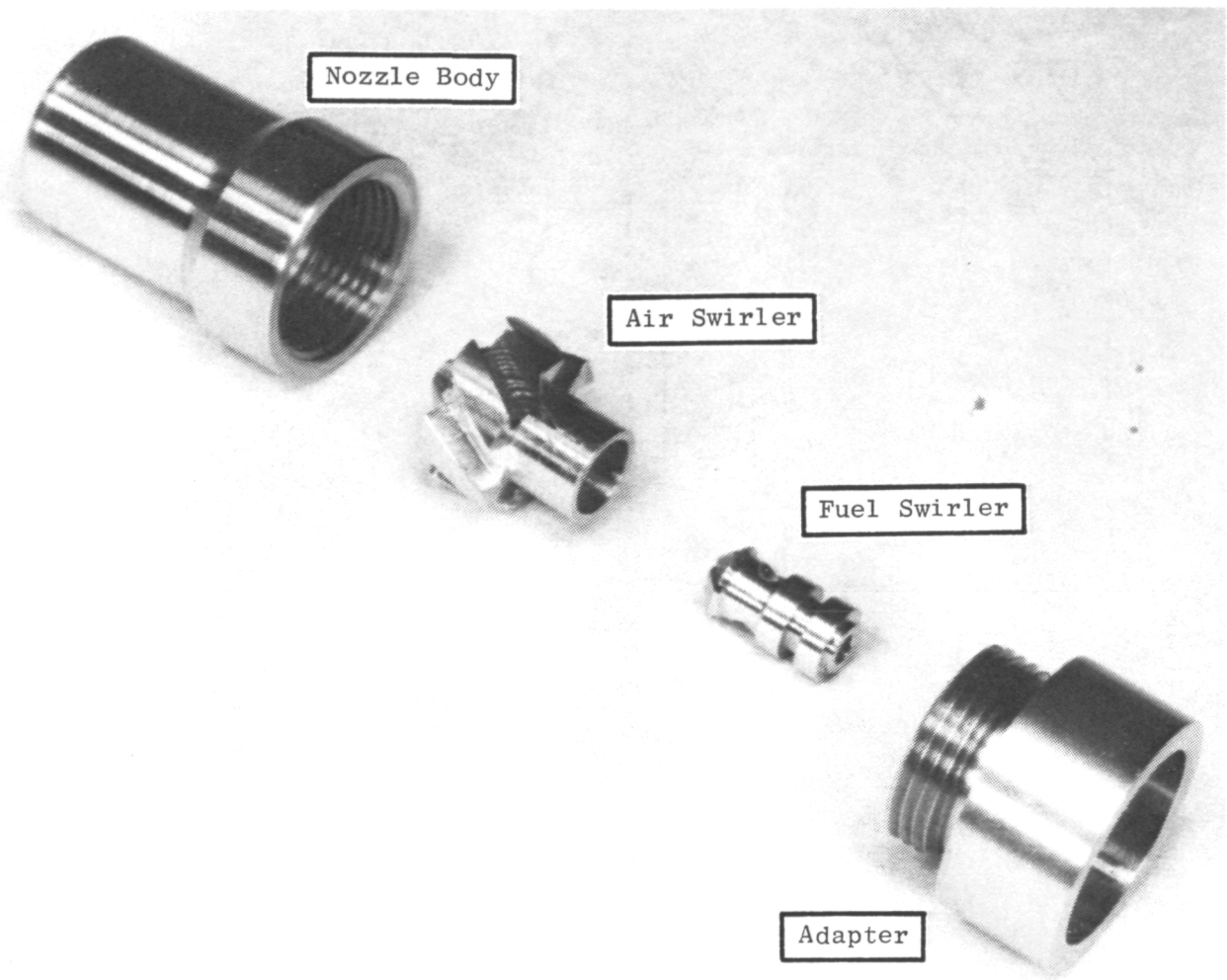


Figure 5. Exploded View of Fuel Nozzle.

Table II. Fuel/Air Mixture-Preparation System Design Guidelines.

- Design Conditions

Inlet Air Temperature	589 K (600° F)
Pressure	0.62 MPa (90 psia)
Reference Velocity	19.8 m/s (65 ft/s)
Fuel/Air Ratio	20.0 g/kg (0.020 lbm/lbm)
Fuel Flow	14.9 g/s (118.5 lbm/hr)
Fuel	No. 6 Residual Oil

- Less Than 50% Fuel Evaporation

- Fuel/Air Ratio Uniformity Within $\pm 10\%$ of Mean at Catalytic Reactor Inlet

- Velocity Profile Within $\pm 10\%$ of Mean at Catalytic Reactor Inlet

- Average Fuel-Drop Size at Catalytic Reactor Inlet:

Small Drop Mode	< 30 μm
Large Drop Mode	70 - 150 μm

Concept" program conducted for NASA by General Electric (Reference 2). The only modifications to that design were resizing internal components to meet fuel-flow requirements and recontouring the nozzle exit to increase the fuel-spray angle. The core of this injector is essentially a simplex nozzle consisting of a fuel swirler, spin chamber, and orifice. When no atomizing air is supplied, this injector functions exactly as a simplex, pressure-atomizing nozzle. Improved atomization is obtained by using high-velocity atomizing air ducted through an annular passage in the injector body to the air swirler.

Atomization with this air-assisted, simplex injector design was predicted using a correlation reported in Reference 3. The form of this correlation is:

$$\text{SMD} = K_8 (t_f^*)^{0.375} (\rho_{AR})^{-0.325} [W_F / (W_F V_F - C W_A V_A)]^{0.55} (K_{FR})$$

where: t_f^* is a hypothetical fuel-film thickness calculated from the volumetric fuel-flow rate, fuel nozzle orifice diameter, and axial fuel velocity assuming that the entire nozzle pressure drop is converted to axial velocity; ρ_{AR} is atomizing-air density normalized by sea-level, room-temperature air density; W_F and W_A are fuel and atomizing-air flow rates; V_F and V_A are the velocities of the fuel and atomizing-air flow, respectively, as calculated from the corresponding density and pressure drop; and K_{FR} is a fuel-property correction factor given by the following equation.

$$K_{FR} = \rho_{FR}^{0.25} \eta_{FR}^{0.06} \sigma_{FR}^{0.375}$$

where ρ_{FR} , η_{FR} , and σ_{FR} are fuel density, absolute viscosity, and surface tension, respectively, divided by corresponding values for standard calibrating fluid at room temperature.

The factor K_8 in the drop-size correlation is a constant that depends on details of nozzle design and manufacture. For several nozzles and a wide range of flow ratings, the range of values reported in Reference 3 was from 104 to 156. An intermediate value of 122, taken from an earlier version of this correlation, was used for the drop-size predictions of the current study. Also, in accordance with Reference 3, the constant C was taken to be 1.0.

The effect of air velocity and fuel-flow rate on predicted initial drop size with the air-assisted simplex nozzle is shown in Figure 6. It should be noted that, although air velocity is used as the independent variable, atomizing airflow and pressure drop are directly related to velocity since the flow area is constant for this nozzle. At all fuel-flow rates, initial drop size decreases monotonically as atomizing-air velocity is increased; however, this effect is much stronger at the lower fuel flows.

Initial drop size is shown in Figure 7 as a function of fuel flow at two selected air velocities. Over the planned range of fuel flows, drop sizes in the lower size range (less than 30 μm) were obtained with the atomizing-air velocity set at 140 m/s; this corresponds to an atomizing-air pressure ratio of 1.12 at the design conditions. When the nozzle is operated in the pressure-atomizing mode (with no atomizing airflow) initial drop sizes are very close to the middle of the 70 to 150 μm range at the design point and are in this size range over most of the design fuel flow range.

The above discussion has focused on initial drop size, but the design guidelines specify drop size at the reactor inlet. Although some reduction in drop size will occur as the fuel evaporates, even the specified maximum of 50% evaporation will result in only about 20% reduction in the size of a fuel droplet.

Selection of fuel/air preparation system length for a premixing combustor involves several considerations. Normally, the minimum acceptable length will be determined by fuel/air mixture uniformity, velocity profile, or fuel-vaporization requirements; the maximum permissible length will be limited by

- Catalytic Reactor Inlet Pressure = 0.62 MPa (90 psia)
- Test Rig Inlet Temperature = 589 K (600° F)
- No. 6 Oil (Fuel) Temperature = 400 K (260° F)
- Atomizing-Air Temperature = 300 K (80° F)

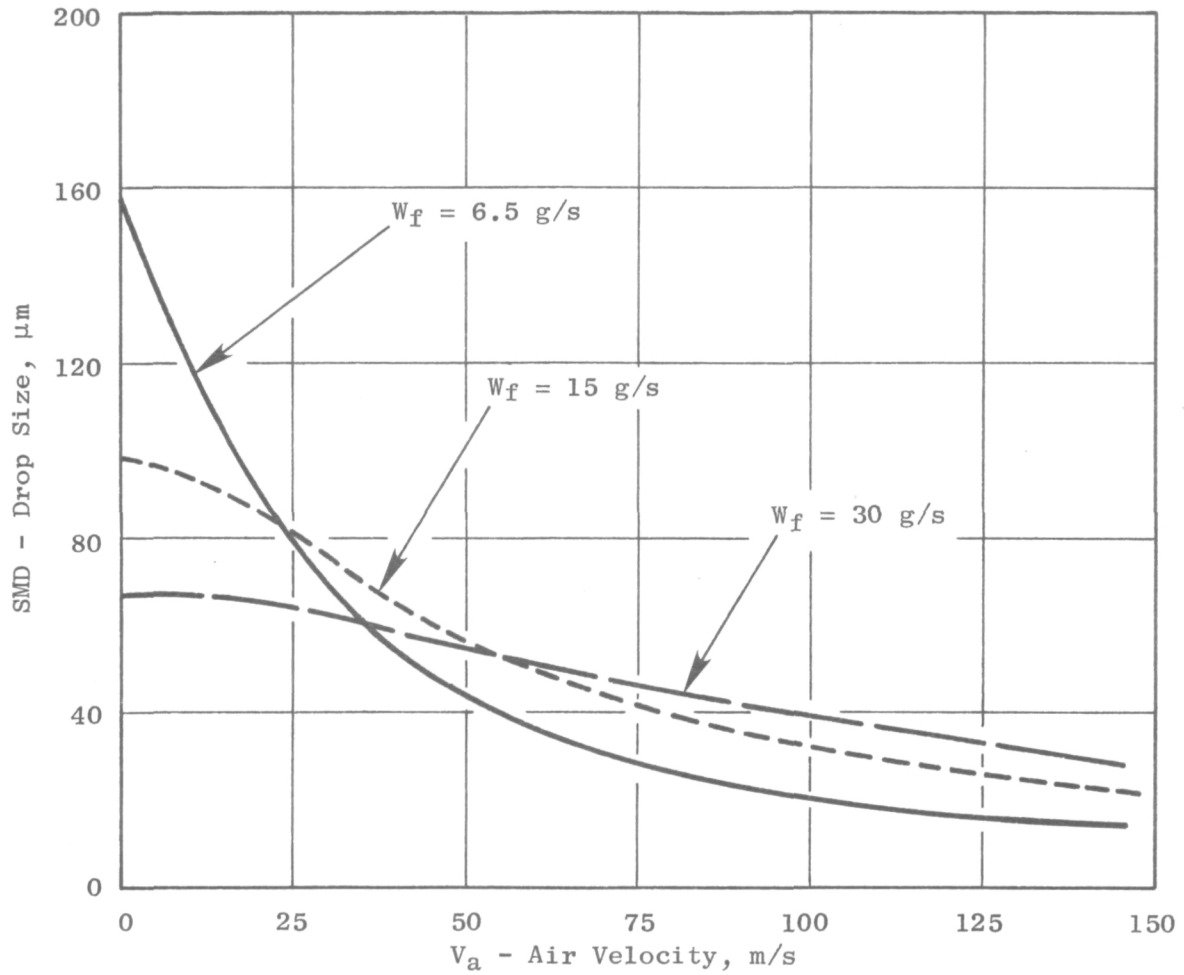


Figure 6. Effect of Air Velocity and Fuel-Flow Rate on Predicted Drop Size.

- Catalytic Reactor Inlet Pressure = 0.62 MPa (90 psia)
- Test Rig Inlet Temperature = 589 K (600° F)
- No. 6 Oil (Fuel) Temperature = 400 K (260° F)
- Atomizing-Air Temperature = 300 K (80° F)

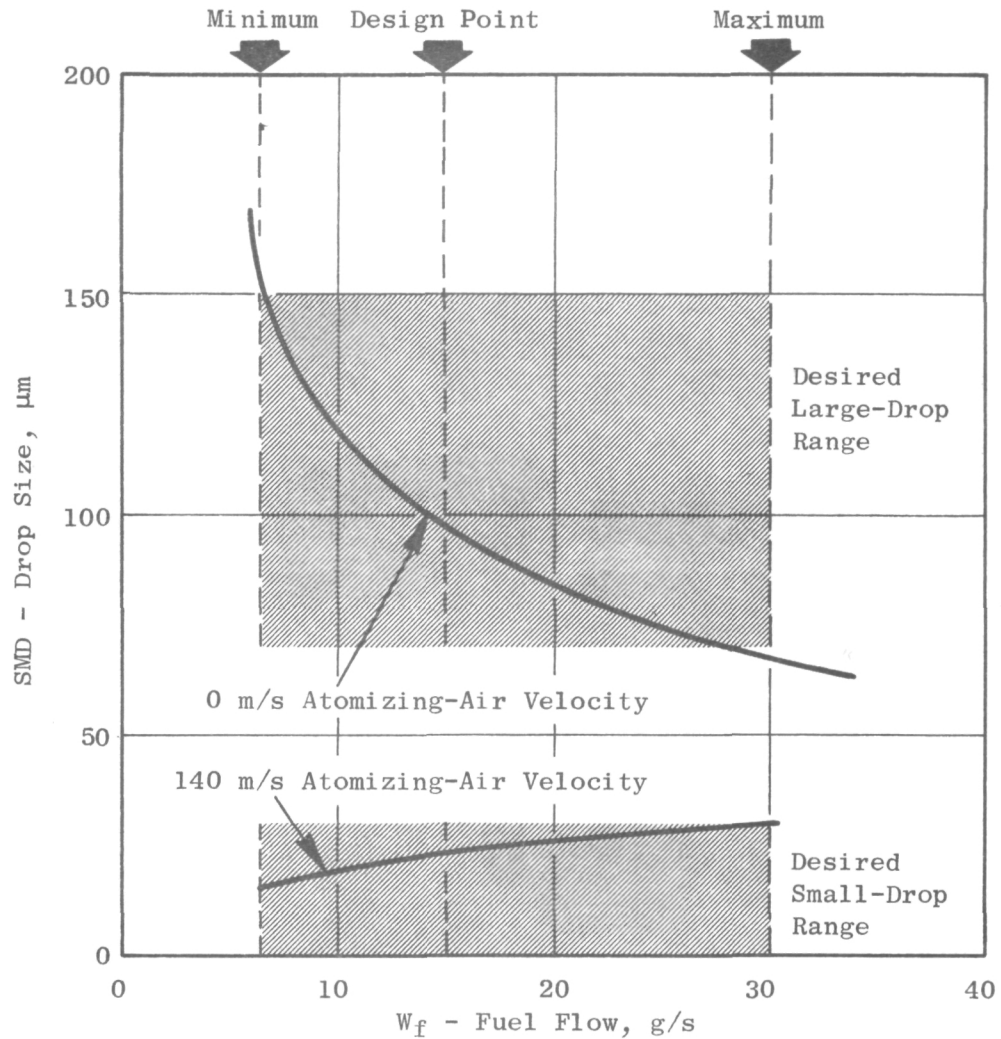


Figure 7. Predicted Design-Point Drop Size with No. 6 Oil.

available space or autoignition. However, for the present program, the length was also limited by the requirement for less than 50% fuel vaporization at the design point.

Measured ignition delay times for No. 6 oil are shown in Figure 8 (from Reference 4). This figure indicates that autoignition would not be expected at 600 K, even with residence times in excess of 100 ms (corresponding to a duct length of more than 1 meter at the minimum design reference velocity, 10 m/s). Thus, system length is not limited by autoignition.

Fuel vaporization for No. 6 oil was calculated using a computerized, mathematical model based on work reported in Reference 5. This model consists of equations for heat transfer, mass transfer, and drop velocity; the equations are solved using a triple-iteration technique. For a single drop, radius, temperature, percent vaporization, distance from injection point, velocity, and elapsed time are calculated at incremental drop temperatures until the droplet heat-up period is complete (wet-bulb temperature is reached), at which point a time increment is used. Typical residual oil properties from References 6 and 7 were used for vaporization calculations (Table III).

Table III. Residual Fuel Properties Assumed for Vaporization Calculations.

Fuel Property	Value		
Temperature, K	311	422	589
Vapor Pressure, Pa	9	965	68,950
Specific Heat, kJ/kg	1.05	1.26	1.58
Heat of Vaporization, kJ/kg	353	318	244

There are several reasons to expect that the vaporization levels obtained during actual tests would be somewhat lower than the predicted values. First, it is assumed in the program that there is no interaction between droplets. Thus the temperature, pressure, and partial pressure of fuel in the surrounding air are treated as constants. In practice, air temperature will decrease, and partial pressure of the fuel vapor will increase as the droplets evaporate - slowing the heat- and mass-transfer rates. A second assumption is that droplet composition does not change during the evaporation process. Actually, as the lighter fractions are vaporized, the partial pressure of the fuel will be decreased, and cracking of the heavier fractions may become more important than vaporization. Thirdly, the properties of No. 6 oil can vary widely. The residual oil used for these tests (described in Section 4.5) was found to be somewhat heavier than the typical residual oil assumed for design calculations.

● Reference 4

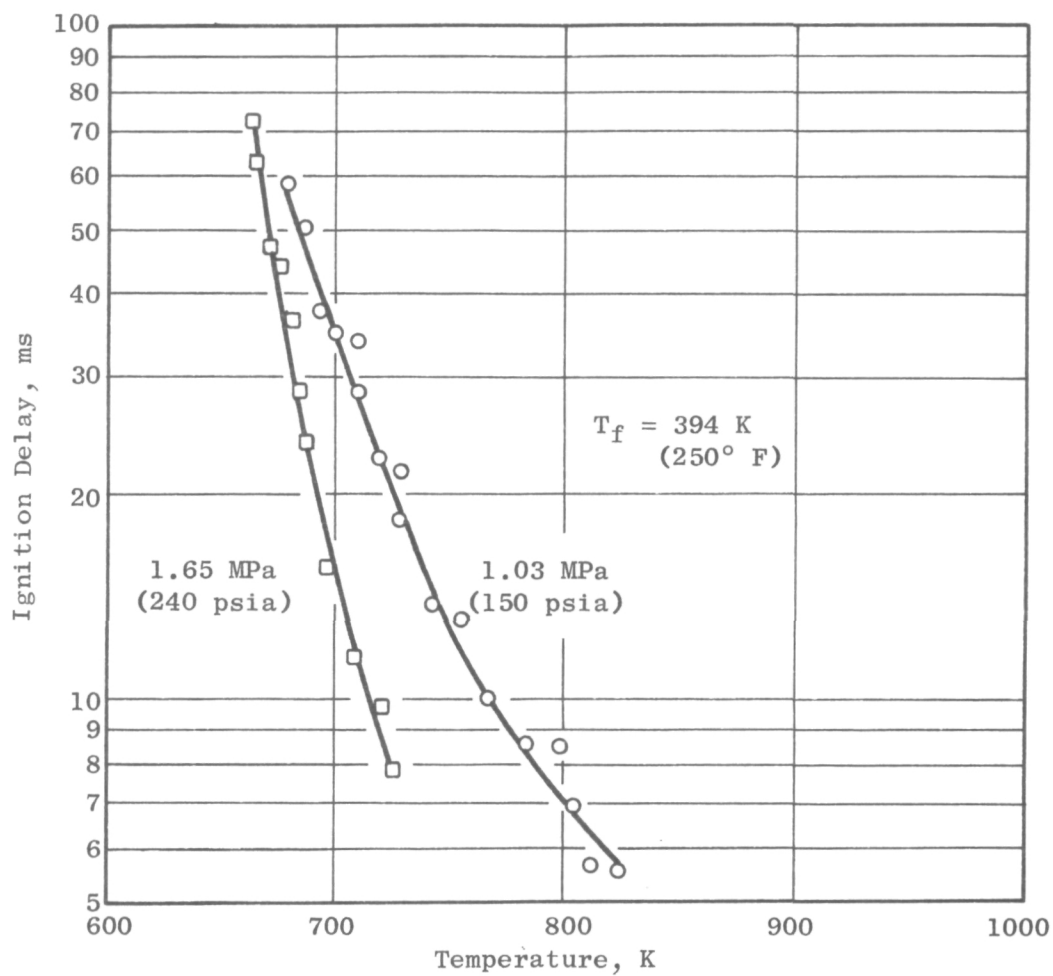


Figure 8. Ignition Delay of No. 6 Fuel Oil in Air at Elevated Temperature and Pressure.

Droplet vaporization was calculated at the design-point temperature and pressure for several different values of airstream velocity. Results of these calculations, shown in Figure 9, indicate that at the design inlet temperature and pressure, and over the range of airstream velocities considered, fuel vaporization is a function of residence time and drop size. Thus, for a 30- μm drop, about 35 to 40 ms is required to achieve 50% vaporization. This corresponds to a distance of about 0.6 m for a constant-cross-sectional-area duct at the design reference velocity of 19.8 m/s. For the diverging duct used in the current catalytic combustor test rig, the design-point residence time is about 25 ms; this corresponds to approximately 37% vaporization with 30- μm drops and only about 5% vaporization with 100- μm drops.

Mixture uniformity at the catalytic reactor inlet depends on the initial fuel and air dispersion at the point of fuel injection and, to some extent, on turbulent diffusion. In order to improve the initial dispersion of fuel, the cross-sectional area of the duct was reduced at the point of fuel injection by installing a conical insert. This method has been used in previous experimental studies to improve the performance of fuel-preparation systems having single-point injectors (References 8 and 9).

A photograph of the inlet to the reduced-area section is shown in Figure 10. The airflow is accelerated into a smooth, rounded inlet and through a perforated plate that positions the nozzle directly in the center of the duct and provides a uniform velocity profile. The plate also serves as a turbulence generator to improve mixing. The injector tip is located about 1.5 cm downstream of the perforated plate. The fuel nozzle tip is designed to provide a relatively high spray angle both in the pressure-atomizing mode and in the air-assist mode (80° to 90° included angle) to give good initial fuel penetration.

A constant-area section 7.6 cm (3 in.) in diameter and 15.2 cm (6 in.) long is provided downstream of the perforated plate. This section allows the fuel-injector wake to mix out before the flow enters the diffuser section. The 2.38° half-angle, conical-diffuser insert has an area ratio of 2.45.

The studies reported in References 8 and 9 have shown that fuel/air mixture uniformity within $\pm 10\%$ can be obtained with single-point injector systems having length-to-inlet-diameter ratios as low as 5.0 if an external swirler is mounted around the fuel injector to improve fuel spreading. With the conical insert, the system used in the current study was designed for a length-to-diameter ratio of 10.0 in order to provide adequate mixing length for operation without an external swirler.

4.1.3 Catalytic Reactor

The catalytic reactor configurations for these tests were specified and supplied by Engelhard Industries Division of the Engelhard Minerals and Chemicals Corporation. Three different reactor configurations were built and tested. All of the reactors consisted of noble metal catalyst on ceramic honeycomb substrates.

- Air Temperature = 589 K (600° F)
- Pressure = 0.62 MPa (90 psia)
- No. 6 Oil (Fuel) Temperature = 394 K (250° F)

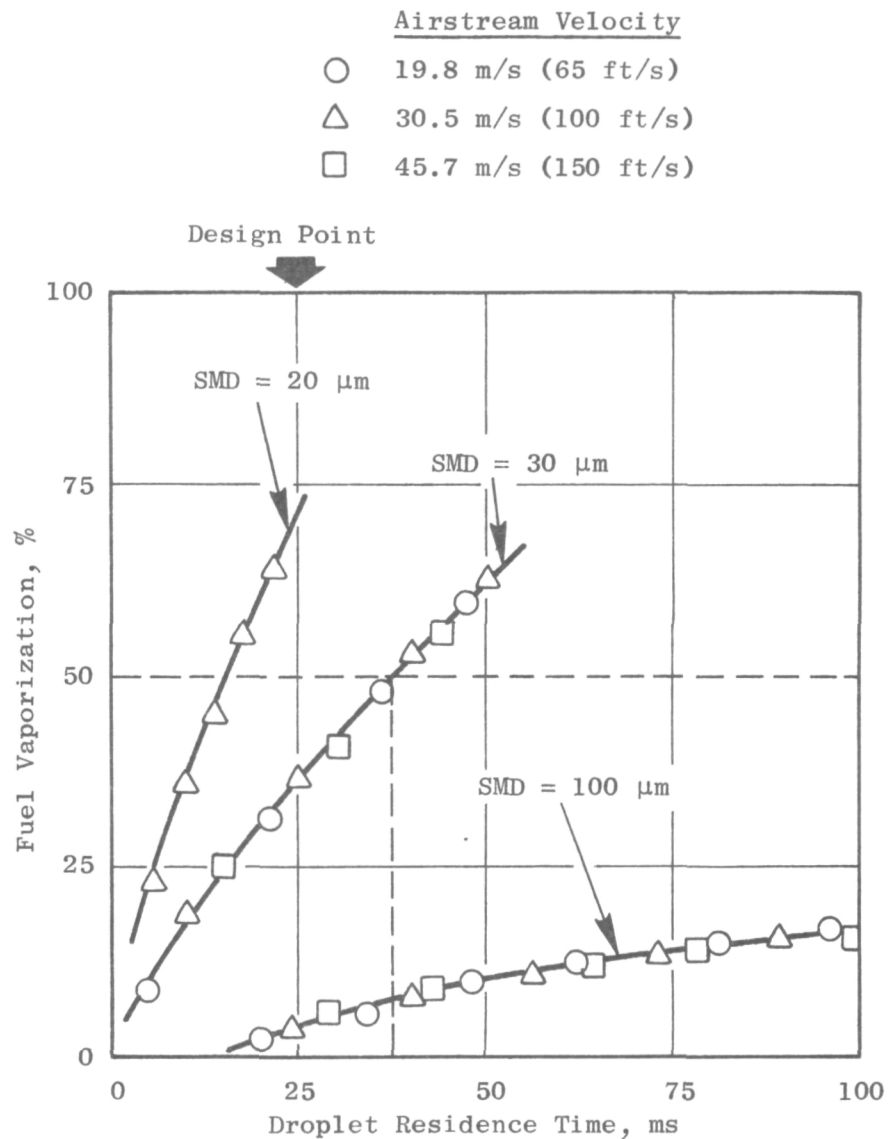


Figure 9. Effect of Drop Size on Fuel Vaporization (Design Point).

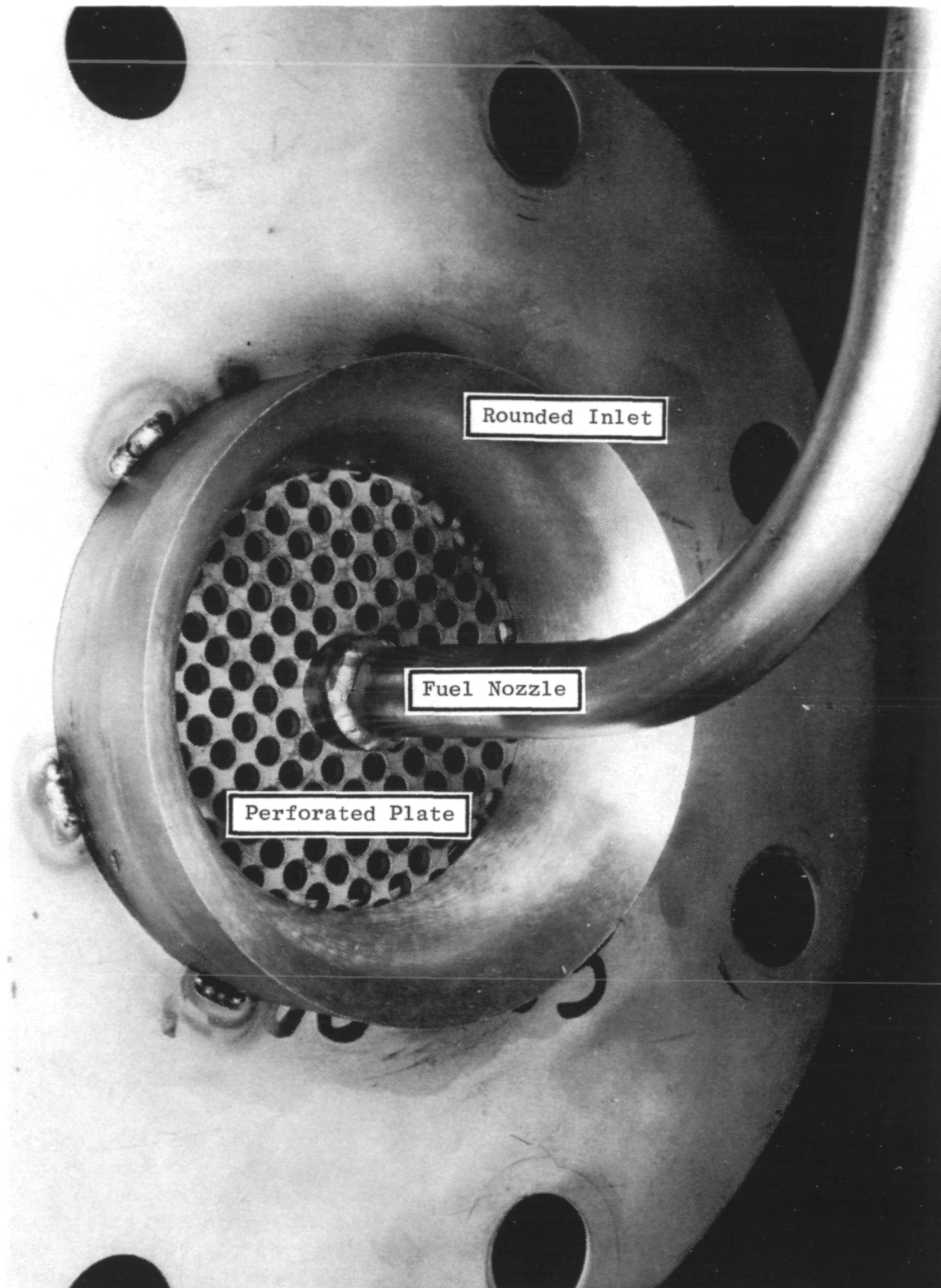


Figure 10. Fuel Injector Mounting.

Catalytic reactor design guidelines are summarized in Table IV. After an initial review of these requirements, the catalyst supplier recommended that the design inlet temperature be increased to at least 633 K (680° F) to ensure acceptable light-off and steady-state performance. The actual catalytic reactor design studies assumed operation at this increased temperature with the understanding that operation would be attempted at both 589 and 633 K (600 and 680° F). These initial design studies were also based on data obtained using distillate fuel oil because the effect of using residual oil was not well documented.

Table IV. Catalytic Reactor Design Guidelines.

- Design Conditions

Inlet Air Temperature	589 K (600° F)
Pressure	0.62 MPa (90 psia)
Reference Velocity	19.8 m/s (65 ft/s)
Adiabatic Combustion Temperature	1400 K (2050° F)
Fuel	No. 6 Residual Oil

- 11.4-cm (4.5-in.) Diameter Reactor
- Pressure Drop Less Than 5% of Upstream Total Pressure
- Combustion Efficiency at Least 99.5% at Design Conditions
- Reactor Heat Loss Less Than 5% of Reaction Heat Release

The three reactor designs included a baseline and two backup configurations. The baseline and first backup configurations were specified prior to the start of testing. The second backup was specified after test results with the first two configurations had been reviewed.

The baseline catalytic reactor design is described in Table V, and samples of the catalyst are shown in Figures 11 and 12. This baseline reactor is a three-element design; the first and second elements are sized to provide mass-transfer area as required to meet the design combustion-efficiency goal. A correlation of combustion efficiency as a function of adiabatic flame temperature and catalyst mass-transfer units was used to size these two elements. (The concept of the mass-transfer unit is described in Reference 10.) The third element was sized primarily to provide adequate residence time for catalytically supported thermal reactions. Pressure drop was predicted using

Table V. Baseline Catalytic Reactor Description.

Parameters	Catalyst [†] Configuration			Overall
	Inlet-Segment	Intermediate	Downstream	
Length, cm	2.5	8.9	7.6	20.3
Channel Density Cells/cm ²	47.0	47.0	9.0	
Substrate	Corning Cordierite	Corning Cordierite	DuPont Torvex Alumina	
L/D _H	21.9	76.6	27.5	
Channel Reynolds* Number	4000	4000	9810	
Pressure Loss**	---	---	---	3.2%
Average Sherwood* Number	15.0	8.2	---	
Mass Transfer Units*	0.43	0.82	---	

Notes: [†]Engelhard proprietary Pd/alumina

*Catalyst inlet conditions

**Design conditions

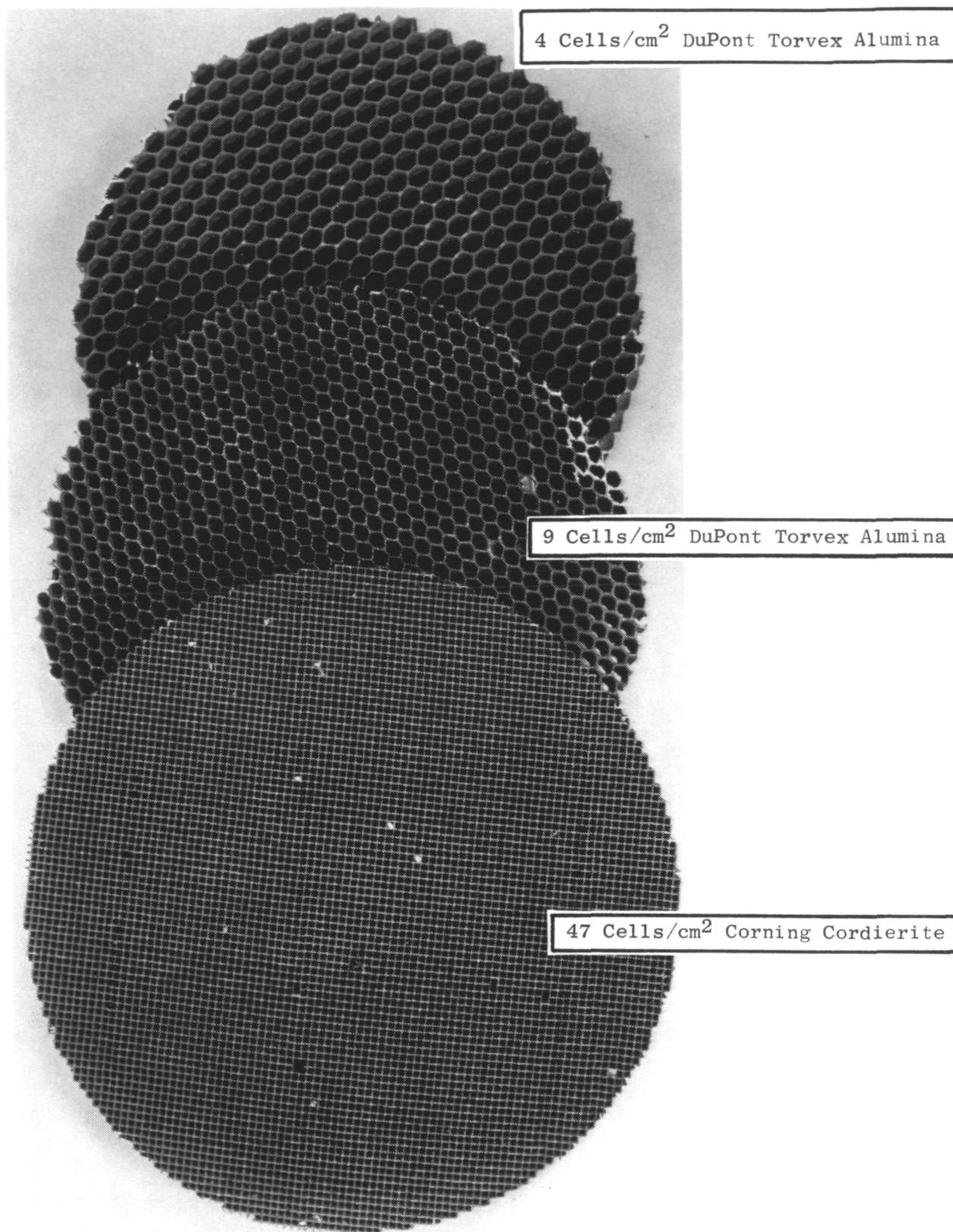


Figure 11. Comparison of Catalyst Materials.

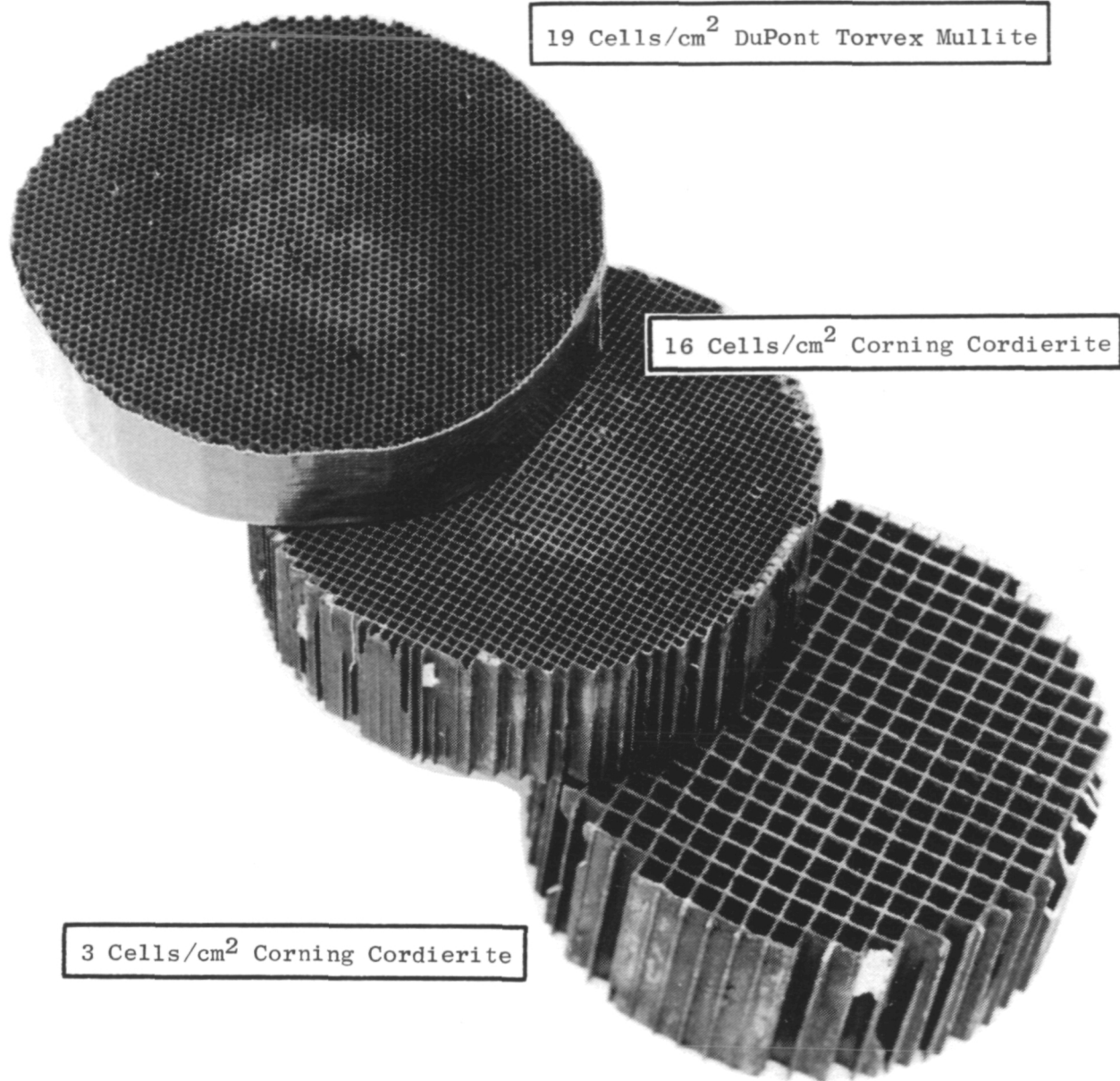


Figure 12. Comparison of Catalyst Materials (Second Backup Reactor).

an empirical friction-factor correlation. All of the elements were catalyzed with a proprietary (Engelhard) preparation of palladium on stabilized alumina.

The first backup reactor configuration is described in Table VI. In this configuration, an increased cell size is used in the first element; the second and third elements are identical to those used in the baseline reactor. The objective of this configuration was to reduce the probability of reactor plugging due to the impingement of residual fuel droplets. The length of the first element was increased relative to the baseline design in order to provide approximately the same mass-transfer conversion and pressure drop.

The second backup reactor configuration, described in Table VII, has larger cells than either the baseline or the first backup reactor. Again, this increase in cell size of the inlet elements was to prevent reactor plugging. The cell size of the exit element was reduced, and overall length was increased to provide the mass-transfer surface area required to obtain the desired combustion efficiency.

All of the reactors were contained in thick-wall spool pieces as shown in Figure 13. Each element was wrapped with an insulating, compliant layer of ceramic fiber material and was constrained axially by stainless steel rings. These rings provided an open-face diameter of 11.4 cm. Design-point reactor heat loss with this housing was calculated to be less than 1% of the reaction heat release.

4.1.4 Exit Instrumentation Section

The catalytic reactor is mounted on an insulated, instrumented, exit section (Figure 14) that consists of a 50-cm length of stainless steel pipe, with an inner diameter of 15.4 cm, and a concentrically mounted, 41-cm long, replaceable, metallic liner having an inner diameter of 11.4 cm. The annular space between the casing and the liner is packed with ceramic fiber insulation to maintain nearly adiabatic flow.

Bosses are provided for a water quench bar as well as the sampling rake, thermocouple probes, and pressure taps described in Section 4.3. The downstream end of the exit section attaches to facility-exit ducting containing a back-pressure valve and a filter/separator system. A description of the test facility used for these tests is presented in the following section.

4.2 COMBUSTOR TEST FACILITY

All catalytic reactor testing in this program was conducted in the Building 306 Advanced Combustion Laboratory at Evendale, Ohio. This laboratory is designed and equipped to accommodate a variety of experimental investigations of moderate-size combustion systems. The laboratory contains two test bays, one on either side of the central control room. Each bay has provisions for four test stands, and each bay has a separate control console.

Table VI. First Backup Catalytic Reactor Description.

Parameters	Catalyst [†] Configuration			Overall
	Inlet-Segment	Intermediate	Downstream	
Length, cm	5.0	8.9	7.6	23.0
Channel Density Cells/cm ²	4.0	47.0	9.0	
Substrate	Corning Cordierite	Corning Cordierite	DuPont Torvex Alumina	
L/D _H	16.2	76.6	27.5	
Channel Reynolds [*] Number	10460	4000	9810	
Pressure Loss ^{**}	---	---	---	3.0%
Average Sherwood [*] Number	31.2	8.2	---	
Mass Transfer Units [*]	0.25	0.82	---	

Notes: [†]Engelhard proprietary Pd/alumina^{*}Catalyst inlet conditions^{**}Design conditions

Table VII. Second Backup Catalytic Reactor Description.

Parameters	Catalyst [†] Configuration			Overall
	Inlet - Segment	Intermediate	Downstream	
Length, cm	5.0	3.8	7.6	10.2
Channel Density Cells/cm ²	2.6	16.0	19.0	19.0
Substrate	Corning Cordierite	Corning Cordierite	DuPont Torvex Mullite	DuPont Torvex Mullite
L/D _H	9.9	18.7	41.1	54.9
Channel Reynolds Number*	15920	6465	7290	7290
Pressure Loss**	---			---
Average Sherwood Number*	43.9	20.4	11.0	11.0
Mass Transfer Units*	0.14	0.31	0.32	0.43
				4.1%

Notes: [†]Engelhard proprietary Pd/alumina

*Catalyst inlet conditions

**Design conditions

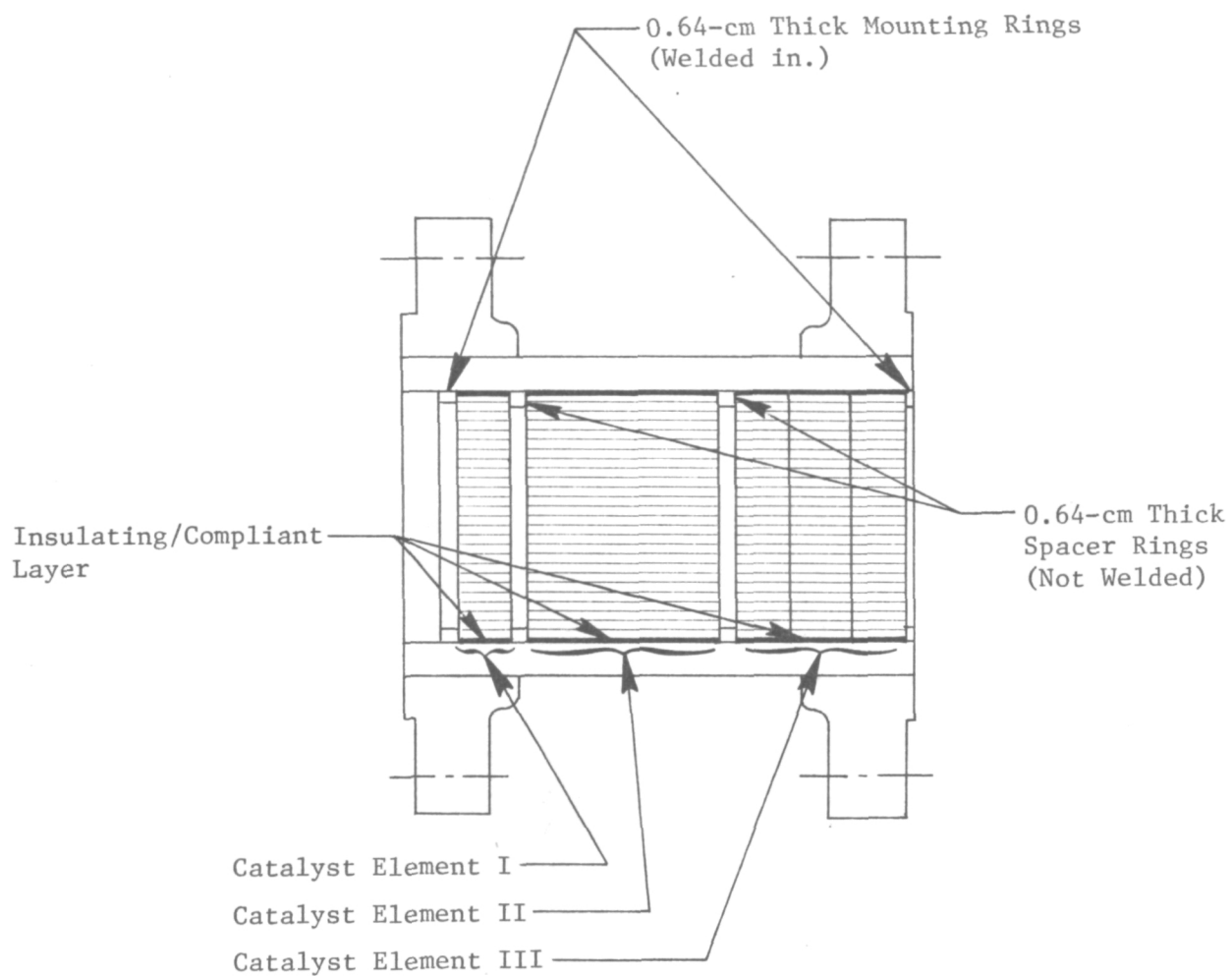


Figure 13. Catalytic Reactor Mounting.

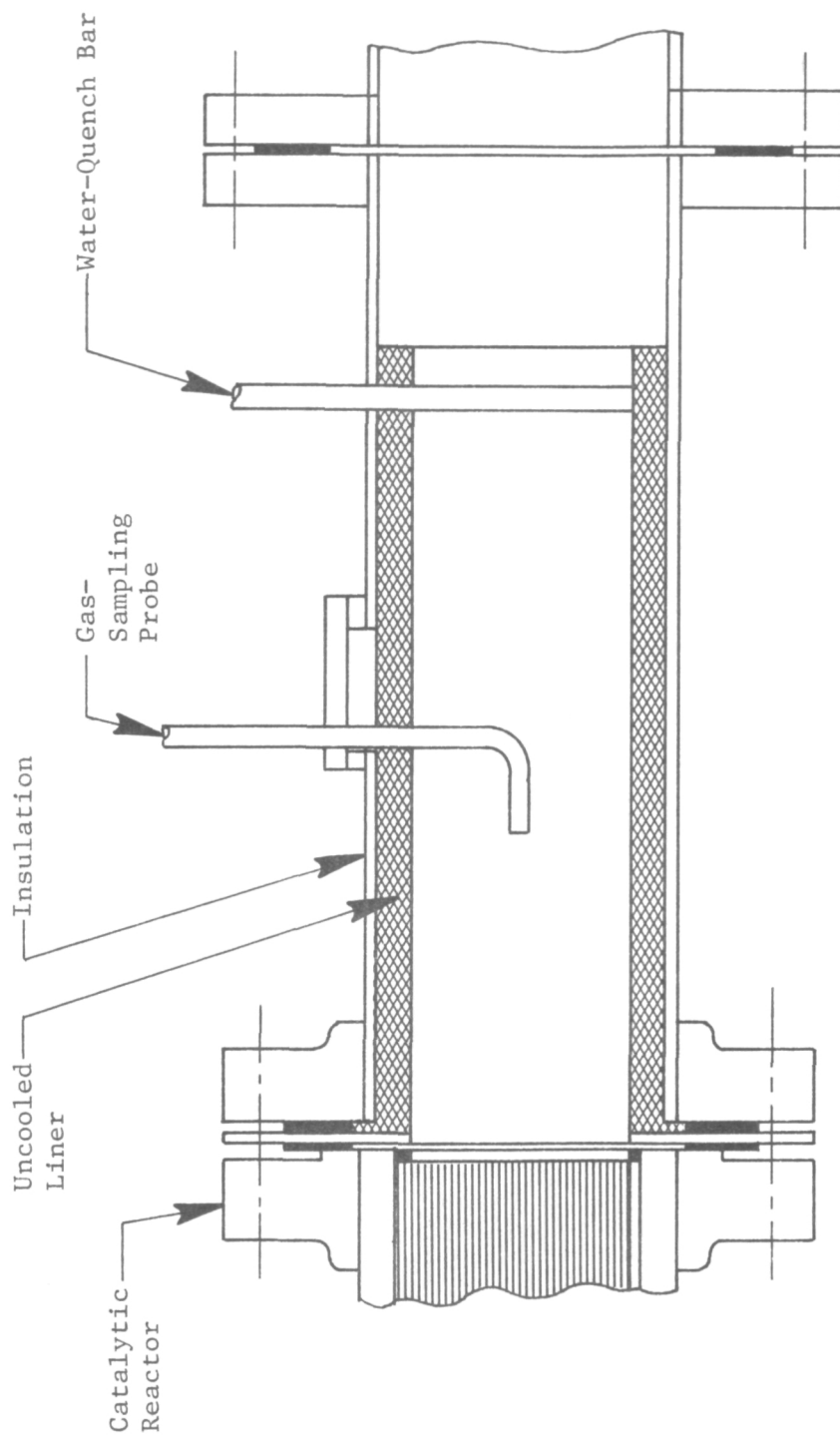


Figure 14. Exit Instrumentation Section.

The laboratory is supplied with all services needed for combustion testing. Air at pressures up to 2.1 MPa (300 psia) is piped from a central air-supply system at flow rates up to 4.5 kg/s (10 lbm/s). Jet A and JP-4 fuels are supplied by pipeline from large storage tanks located elsewhere in the plant.

The heated fuel system, shown schematically in Figure 15, was used for the residual oil tests. With this system, the residual oil is maintained at about 350 K (170° F) in a steam-heated, 25-m³ (2000-gal), storage trailer. The trailer incorporates an air-driven boost pump and an internal bypass line to continuously circulate the fuel. Either heated residual oil, distillate (Jet A) from the facility tanks, or a combination of the two can be supplied to the inlet of the main steam/fuel heat exchanger. Saturated steam to this heat exchanger is supplied at 1.2 MPa (175 psia), providing a maximum fuel preheat capability up to about 450 K (350° F). Fuel leaving the heat exchanger is filtered and then input to the high-pressure pump that can provide fuel pressures up to 10.3 MPa (1500 psia). Total fuel flow is metered with a turbine flowmeter. When a mixture of residual and distillate fuel is used, the distillate flow is measured with a second turbine flowmeter.

A remotely operated valve, located at the fuel nozzle inlet, is available to divert the fuel flow to a waste fuel tank. This valve is used to preset fuel temperature and is also used for emergency shutdown.

Test-rig inlet conditions were controlled and monitored from a console located in the control room adjacent to the test cell (Figure 16). Other permanently mounted, control-room facilities used in combustor tests included digital recorders to monitor and record thermocouple outputs and an array of manometers and gages to monitor system pressures. Emissions analysis instrumentation and associated readout equipment were also located in this control room.

4.3 Test Instrumentation

A listing of the test-rig and related facility instrumentation used in this test program is presented in Table VIII. The axial stations indicated in this table are described in Table IX.

All temperatures were measured with either chromel-alumel (Type K) or sheathed platinum (Type B) thermocouples (T/C), as indicated in Table VIII. Chromel-alumel thermocouples were read and logged with a digital printer. Platinum thermocouple output was read out on a digital voltmeter and hand-logged. System pressures were read out on pressure gages and were also hand-logged. Fuel injector, atomizing air, and catalytic reactor pressure drops were read by means of mercury manometers.

Catalyst substrate temperatures were measured with sheathed thermocouples installed in the catalyst channels. These thermocouples were led in from the aft end of the reactor, as shown in Figure 17, and were held in place with ceramic cement. Sufficient cement was used to completely close the channel.

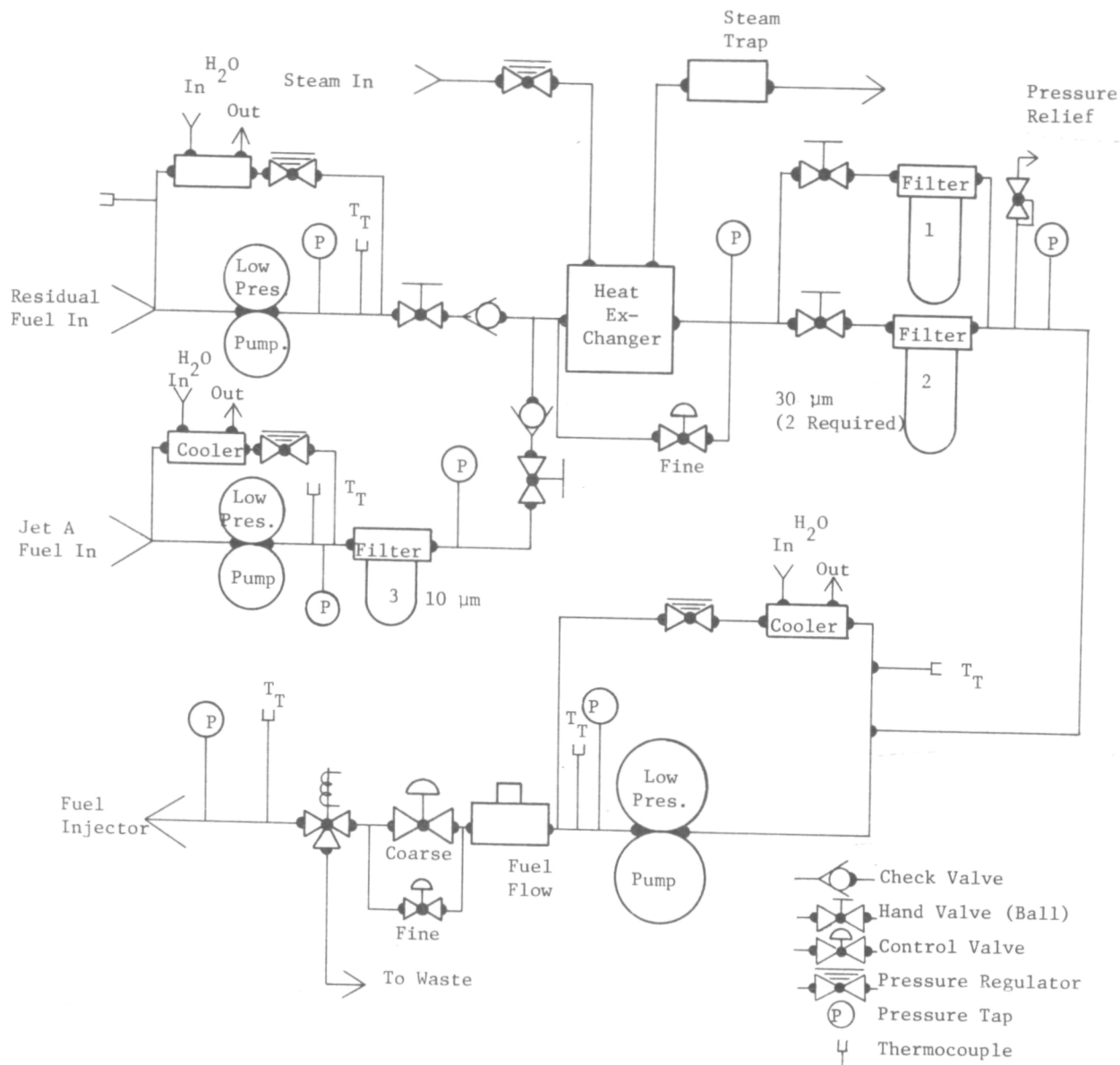


Figure 15. Heated Residual Fuel System.



Figure 16. Control Console, Building 306 Advanced Combustion Laboratory.

Table VIII. Instrumentation Listing.

Axial Location	Radial Distance From Centerline, cm	Instrumentation Designation	Item Number	Angular Location
1.0	0.0	Inlet Total Temperature	Tt 1.090	90°
1.0	2.0	Inlet Total Temperature	Tt 1.0270	270°
1.0	6.1	Inlet Wall Static Pressure	Ps 1.045	45°
1.0	6.1	Inlet Wall Static Pressure	Ps 1.0315	315°
1.5	2.2	Nozzle Discharge Temperature	Tt 1.545	45°
1.5	2.2	Nozzle Discharge Temperature	Tt 1.5315	315°
1.9	6.1	Wall Static Pressure	Ps 1.945	45°
1.9	6.1	Wall Static Pressure	Ps 1.9315	315°
1.9	7.0	Mixer Discharge Skin T/C	Ts 1.900	0°
1.9	7.0	Mixer Discharge Skin T/C	Ts 1.990	90°
1.9	7.0	Mixer Discharge Skin T/C	Ts 1.9180	180°
1.9	7.0	Mixer Discharge Skin T/C	Ts 1.9270	270°
2.0	0.0	Reactor T/C Plat 10% Rh-Pt	Ts 2.0A	---
2.0	2.5	Reactor T/C Plat 10% Rh-Pt	Ts 2.0B	---
2.0	5.0	Reactor T/C Plat 10% Rh-Pt	Ts 2.0C	---
2.5	0.0	Reactor T/C Plat 10% Rh-Pt	Ts 2.5A	---
3.0	0.0	Reactor T/C Plat 10% Rh-Pt	Ts 3.0A	---
3.0	5.0	Reactor T/C Plat 10% Rh-Pt	Ts 3.0B	---
3.1	0.0	Catalyst Discharge Temperature	Tt 3.1105	105°
3.1	2.5	Catalyst Discharge Temperature	Tt 3.1225	225°
3.1	5.0	Catalyst Discharge Temperature	Tt 3.1345	345°
3.1	5.7	Discharge Liner Skin T/C	Ts 3.100	0°
3.1	5.7	Discharge Liner Skin T/C	Ts 3.190	90°
3.1	5.7	Discharge Liner Skin T/C	Ts 3.1180	180°
3.1	5.7	Discharge Liner Skin T/C	Ts 3.1270	270°
3.1	5.7	Liner Static Press	Ps 3.145	45°
3.1	5.7	Liner Static Press	Ps 3.1315	315°

Table VIII. Instrumentation Listing. (Concluded)

Axial Location	Radial Distance From Centerline, cm	Instrumentation Designation	Item Number	Angular Location
4.0	0.0	Gas-Sampling Probe	GS 4.000	0°
4.0	1.9	Discharge Temperature	Tt 4.090	90°
4.0	2.5	Discharge Temperature	Ts 4.0270	270°
4.0	5.7	Liner Skin T/C	Ts 4.045	45°
4.0	5.7	Liner Skin T/C	Ts 4.0135	135°
4.0	5.7	Liner Skin T/C	Ts 4.0225	225°
4.0	5.7	Liner Skin T/C	Ts 4.0315	315°
4.1	0.0	Discharge Total Temperature	Tt 4.190	90°
4.1	2.5	Discharge Total Temperature	Tt 4.1270	270°
1.0-3.1	---	ΔP Ps Across Injector	Ps Δ 1.03.1	45°
1.9-3.1	---	ΔP Ps Across Catalyst	Ps Δ 1.93.1	315°
4.9	8.4	Discharge Skin T/C	Ts 4.900	0°
4.9	8.4	Discharge Skin T/C	Ts 4.990	90°
4.9	8.4	Discharge Skin T/C	Ts 4.9180	180°
4.9	8.4	Discharge Skin T/C	Ts 4.9270	270°
---	---	Residual Fuel Flow	RFF PPH0	---
---	---	Residual Fuel Inlet Temp.	Tt RF	---
---	---	Residual Fuel Inlet Pressure	Ps RF	---
---	---	Injector Fuel Atmo. Air Temp.	Tt EFA	---
---	---	Injector Fuel Atmo. Air Press.	Ps EFA	---
---	---	Airflow Inlet Temp.	Tt AFI	---
---	---	Airflow Inlet Press.	Ps AFI	---
---	---	Airflow Orifice ΔP .	Ps Δ AO	---
---	---	Probe Cooling H ₂ O Press.	Ps PCH	---

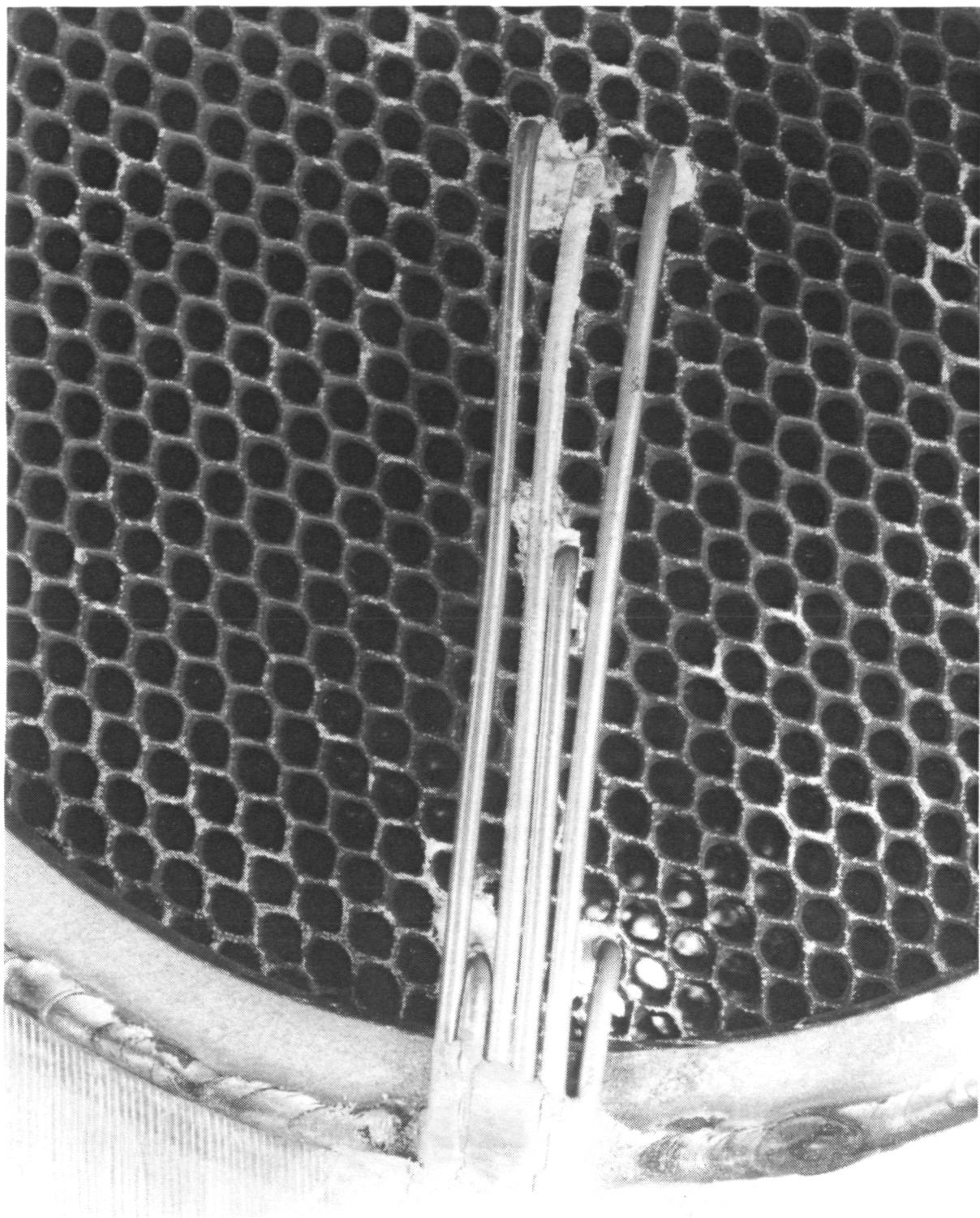


Figure 17. Catalytic Reactor Thermocouple Installation.

Table IX. Location of Axial Stations (Baseline Reactor).

Feature	Axial Location, cm From Fuel-Injection Panel
Station 1.0	-20.0
Fuel Injector	0.0
Station 1.5	8.0
Station 1.9	68.6
Catalytic Reactor Inlet	76.2
First Catalyst Element Inlet (Baseline)	81.3
Station 2.0	83.2
Station 2.5	88.3
Station 3.0	100.3
Last Catalyst Element Exit	101.0
Catalytic Reactor Exit	101.6
Station 3.1	104.1
Station 4.0	116.8
Station 4.1	132.1
Station 4.5	139.7

At steady-state conditions, with this method of installation, the measured temperature is representative of the substrate-wall temperature (rather than the gas temperature) provided the reactions continue undisturbed in all channels surrounding the closed-end channel. With a total of six substrate thermocouples, the blockage due to closure of the instrumented channels was less than 1% for all reactors tested.

Gas samples were withdrawn through a single-point, water-cooled probe mounted on the duct centerline 15.2 cm (6 in.) downstream from the catalytic reactor exit. As shown in Figure 18, this probe is constructed with three concentric tubes. Cooling water is supplied through the outermost annular passage to protect the outer shell and the probe tip. This water is then led out through the inner annulus to an external drain. During the test runs, the cooling flow was controlled to maintain the cooling-water exit temperature at about 350 K (170° F) to provide sufficient sample quenching and probe cooling without overcooling the sample tube.

Samples were routed from the probe to the sample-analysis system through a stainless steel sample line. This line was steam-heated to maintain the sample temperature close to 423 K (300° F).

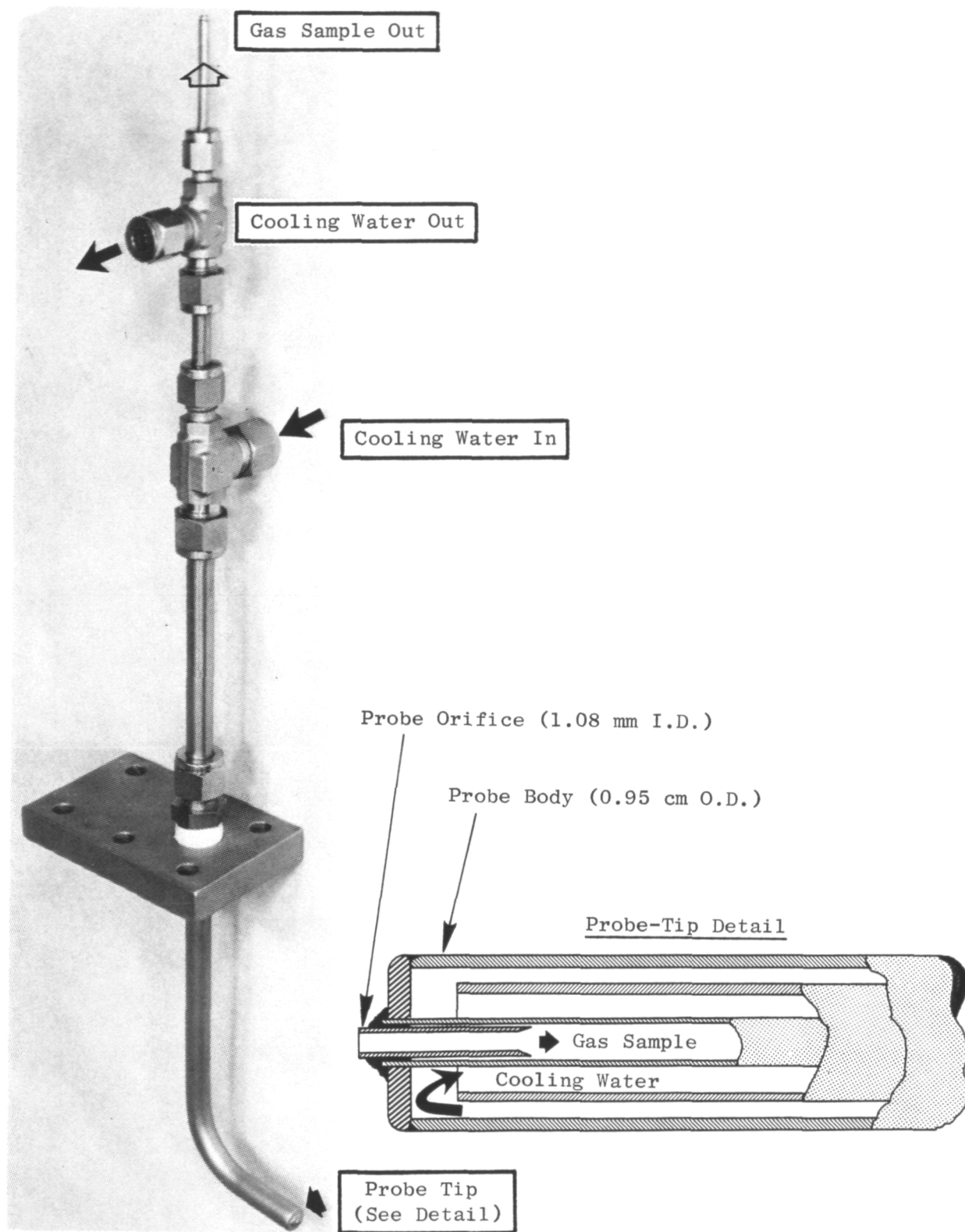


Figure 18. Emissions Sampling Probe.

The Contaminants Analyzed and Recorded On-Line (CAROL) system was used to measure gaseous emissions. This system conforms to SAE ARP 1256 and consists of four basic instruments: a flame-ionization detector (FID) for measuring total HC concentrations, two nondispersive infrared analyzers for measuring CO and CO₂, and a heated, chemiluminescent analyzer for measuring NO and NO₂. The CAROL system was calibrated, before each run, using the calibration gases indicated in Table X.

Table X. Emission Instrument Calibration Gases.

Gas Constituent	Instrument Range	Nominal Full-Scale Reading	Span Gases			
			1	2	3	4
CO ₂ , %	1	10	2.48	3.96	5.85	7.95
CO, ppm	1	2500	233	447	945	2380
HC*, ppm	3	300	268	---	---	---
	4	1500	268	699	1440	---
NO _x **, ppm	3	125	29.8	68	---	---
	4	300	29.8	68	287	---
*Calibrated in ppm CH ₄ using C ₃ H ₈ span gas. **Calibrated with NO span gas.						

Outputs from the CO, CO₂, HC, and NO_x analyzers of the CAROL system were continuously recorded on strip-chart recorders and manually recorded for later input to an emissions-data-reduction computer program that calculates exhaust-emission concentration indices, combustion efficiency, and sample fuel/air ratio.

4.4 TEST PROCEDURES

The program consisted of three test series to evaluate the lean-combustion performance of the baseline and two backup catalytic reactors operated on No. 6 fuel oil. All of the tests were conducted in the Building 306 Combustion Laboratory, using the test rig described in Section 4.1.

The initial test plan was to operate the baseline catalytic reactor over the entire range of test points indicated in Table I. The backup reactors were to be operated only at the design-point conditions indicated in Table I.

Prior to the baseline catalytic reactor test series, preliminary results of other catalytic reactor tests being conducted with residual oil, by NASA, indicated a potential problem with upstream burning of the residual oil at the design point. Those results also indicated that the autoignition problem was less severe as inlet temperatures were increased. Based on these reports, it was concluded that the probability of success in initial tests would be increased if an inlet temperature above 755 K (900° F) were used, and the supplementary test-point schedule shown in Table XI was defined. In this test-point schedule, the inlet pressure is limited to 0.414 MPa (60 psia) at inlet temperatures above 800 K because of test-facility pressure limitations. The minimum reference velocity is limited to 19.8 m/s (65 ft/sec) above 800 K to ensure that the bulk fuel/air mixture residence time is less than the autoignition delay time.

Table XI. Supplementary Test-Point Schedule for Backup Reactors.

- Three Fuel/Air Ratios at Each Condition

Sequence	Inlet Pressure, MPa (psia)	Rig Inlet Temperature, K (° F)	Reference Velocity, m/s (ft/s)
1	0.41 (60)	867 (1100)	19.8 (65)
2	0.41 (60)	867 (1100)	30.5 (100)
3	0.41 (60)	811 (1000)	19.8 (65)
4	0.41 (60)	811 (1000)	30.5 (100)
5	0.41 (60)	756 (900)	19.8 (65)*
6	0.62 (90)	756 (900)	10.7 (35)*
7	0.62 (90)	756 (900)	30.5 (100)*
8	0.62 (90)	756 (900)	19.8 (65)
9	0.93 (135)	756 (900)	19.8 (65)
10	0.62 (90)	700 (800)	19.8 (65)
11	0.62 (90)	644 (700)	19.8 (65)
12	0.62 (90)	589 (600)	19.8 (65)*

*Attempt Drop-Size Variation

Following the initial check, Jet A fuel flow was started and increased until peak catalytic reactor temperatures, between 1255 K (1800° F) and 1478 K (2200° F), were indicated. After stable operation was established, transition to No. 6 fuel oil was accomplished by gradually decreasing Jet A flow while increasing No. 6 oil flow. During this transition, which normally took about 15 minutes, total fuel flow was controlled to maintain the peak catalytic reactor temperature in the desired range.

During the baseline catalytic reactor tests, transition from Jet A to residual oil was accomplished in stages by establishing stable operation with fuel mixtures containing 0, 25, 50, 75, and finally 100% residual fuel. A complete reading, including emissions, was taken for each test mixture.

Generally, light-off on distillate fuel and transition to operation on residual fuel were accomplished at a rig inlet temperature of 867 K (1100° F), a pressure of 0.41 MPa (60 psia), and a reference velocity of 19.8 m/s (65 ft/s); this corresponds to the first set of inlet conditions described in Table XI. Fuel/air ratio was then varied at these inlet conditions in order to evaluate the effect of changes in flame temperature. After the fuel/air ratio variation was completed, reference velocity was increased to 30 m/s to set the second set of inlet conditions shown in Table XI. Fuel/air ratio was then varied at these inlet conditions. Inlet conditions were varied in the order shown in Table XI, varying fuel/air ratio at each set of inlet conditions, until the catalytic reactor operating limits (either due to auto-ignition or poor performance) were defined.

Emission and performance readings were generally obtained at a minimum of three different fuel/air ratios at each set of inlet conditions. These fuel/air ratios were selected during the test based on peak catalytic reactor substrate temperature and combustion-efficiency criteria.

After setting the inlet conditions, fuel flow was adjusted to obtain a peak substrate temperature of about 1350° K (1970° F). At this condition, the combustion efficiency was normally above 99%. After the emission levels stabilized at this point, the range and voltage level from each analyzer were recorded. Operating pressures, temperatures, and fuel flow were logged simultaneously. Fuel flow was then reduced until a combustion efficiency of about 90% was indicated by the hydrocarbon analyzer output. After emission levels stabilized, a second reading was obtained at this fuel flow. A third reading was then obtained after stabilizing at an intermediate fuel/air ratio.

At each test condition, all of the parameters shown in Table XII were recorded and/or computed.

4.5 TEST-FUEL CHARACTERISTICS

The primary test fuel for this program was No. 6 residual fuel oil. Residual fuels are the materials remaining in crude oil after light and medium products have been removed by distillation. All refiners distill crude oil under atmospheric pressure, and the residual material is termed

Table XII. Measured and Calculated Test Parameters.

Parameter	Symbol	Unit	Measured	Calculated	Comments
Reactor Airflow	\dot{W}_c	kg/s		X	Sum of main airflow (ASME orifice) plus atomizing airflow (\dot{W}_{AA})
Reactor Inlet Temperature	$T_{1.5}$	K	X		Thermocouple in premixing duct
Reactor Inlet Pressure	$P_{1.9}$	mPa	X		Flow-weighted average of rig inlet and atomizing air temperatures
Fuel Flow	\dot{W}_f	g/s	X		Average of measurements from 2 static pressure taps
Metered Fuel/Air Ratio	f_m	g/kg			Turbine flowmeter
Humidity	h	g/kg	X		\dot{W}_f/\dot{W}_c
Atomizing Airflow	\dot{W}_{AA}	kg/s		X	Dew-point hygrometer
Main-Stream (Rig Inlet) Temperature	$T_{1.0}$	K	X		Nozzle airflow calibration
Atomizing-Air Temperature	T_{AA}	K	X		Two thermocouple probes in inlet section
Atomizing-Air Pressure Drop	ΔP_{AA}	kPa		X	Thermocouple probe in air line at nozzle inlet
Fuel Temperature	T_f	K	X		Static pressure tap in air line at nozzle inlet
Fuel Pressure Drop	ΔP_f	MPa		X	Thermocouple probe in fuel line at nozzle inlet
Reference Velocity	V_r	m/s		X	Static pressure tap in fuel line at nozzle inlet
Initial Drop Size	d_o	μm		X	$\dot{W}_c/\rho_{1.9} A_{catalytic\ Reactor}^*$
Reactor Substrate Temperatures	T_c	K			Reference 3 Equations
Reactor Exit Temperatures	T_{ex}	K	X		Three type K thermocouples in inlet element (0.6 cm from aft face of element 1), One type S thermocouple in center of second element, plus 2 type S thermocouples located 0.6 cm from reactor exit
Gas-Sample Fuel/Air Ratio	f_s	g/kg		X	Seven thermocouple probes located at three different stations downstream of reactor exit (2.5, 15.2, and 30.5 cm from exit plane)
Gas-Sample CO Emission Index	EICO	g/kg		X	Single-Point, gas-sampling probe. ARP 1256 Equations
Gas-Sample HC Emission Index	EIHC	g/kg		X	
Gas-Sample NO_x Emission Index	EINO _x	g/kg		X	
Gas-Sample Combustion Efficiency	η_g	%		X	Gas-sample analysis
Thermocouple Combustion Efficiency	η_{tc}	%		X	Ratio of measured temperature rise (based on average of two measured exit temperatures, Station 3.1, $r = 0.0$ cm and $r = 2.5$ cm) to calculated temperature rise (based on f_m)

* $\rho_{1.9}$ is the fluid density at the catalytic reactor inlet.

"atmospheric residuum." In many large, modern refineries this material is subjected to additional distillation under vacuum to produce heavier distillates. The residual material from this process is called "vacuum residuum."

The relative quantities of the residuum produced, and the characteristics, are dependent on the properties of the crude oil and the refining processes applied. In general, atmospheric residuum amounts to 45 to 50% of the original crude; vacuum residuum amounts to about 15 to 20%. Since the metal-containing impurities found in all crude oils are nonvolatile, they become concentrated in the residuum, more so in vacuum residuum than in atmospheric residuum.

The sulfur-containing compounds found in all crude oils always occur at higher concentrations in the higher boiling fractions. Therefore, the sulfur content of residuum is always higher than that of the original crude, and it is more so in vacuum than in atmospheric residuum.

Since the properties of residuals from diverse sources can vary widely, it is common practice to dilute them with "cutter stocks" to reach some viscosity within established limits (e.g., 180 to 1800 cSt at 100° F for No. 6 oil). Also, for environmental reasons, it is necessary to limit the sulfur content of such fuels to 0.8% maximum for new engines. If the cutter stocks cannot achieve this result, then a desulfurized cutter stock must be used for this purpose.

An analysis of the No. 6 oil used in this program is presented in Table XIII. This table also shows a typical range of properties for No. 6 oil and typical properties of the distillate fuel (Jet A) that was used for light-off. Based on discussions with the refiner, the No. 6 test fuel is believed to be a vacuum residuum containing 20 to 30% cutter stock. As indicated in Table XIII, the test fuel was quite thick; both viscosity and pour point were in the upper range. However, levels of sulfur and metals were relatively low.

A plot of viscosity as a function of fuel temperature is presented in Figure 19. During operation, the fuel was heated to about 400 K (260° F) to obtain a viscosity close to 10 cSt.

Equilibrium adiabatic flame temperatures for the test fuel as a function of fuel/air ratio at the design-point temperature and pressure are shown in Figure 20.

Table XIII. Test-Fuel Properties.

Property	No. 6 Oil		Jet A (Typical)
	Typical	Test	
Specific Gravity (289/289 K)	0.95	0.944	0.81
Hydrogen Content, wt %	---	11.52	14
Sulfur Content, wt %	<0.8*	0.47	0.01
Nitrogen Content, wt %	---	0.22	---
Vanadium, ppm	0-150	26	---
Total Ash, %	---	0.022	---
Minor Constituents (Qualitative Analysis)	Fe, Ni	Ca, Ni	---
Net Heat of Combustion, MJ/kg	---	41.3	43
Viscosity, cSt at 311 K	180-1800	1345	1.65
Surface Tension, N/m at 339 K	---	0.0329	0.020
Pour Point, K	<289*	294	---
Distillation, K			
Initial Burning Point (IBP)	---	460	450
10%	560-617	541	470
40%	---	809**	---
50%	---	---	490
90%	---	---	510
Final Burning Point (FBP)	---	---	630

*ASTM Specification D396

**Max. Distillation Temperature

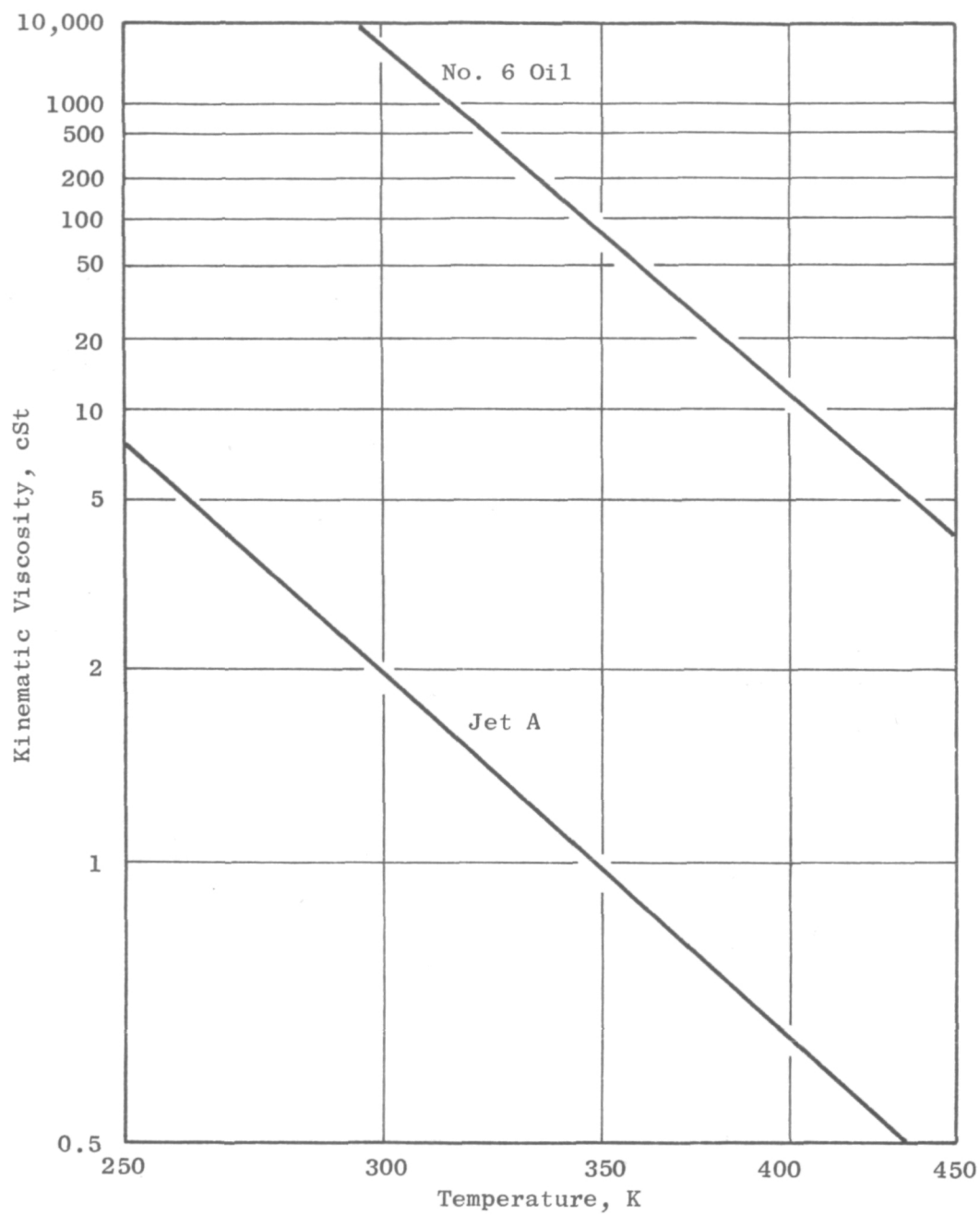


Figure 19. Test-Fuel Viscosity.

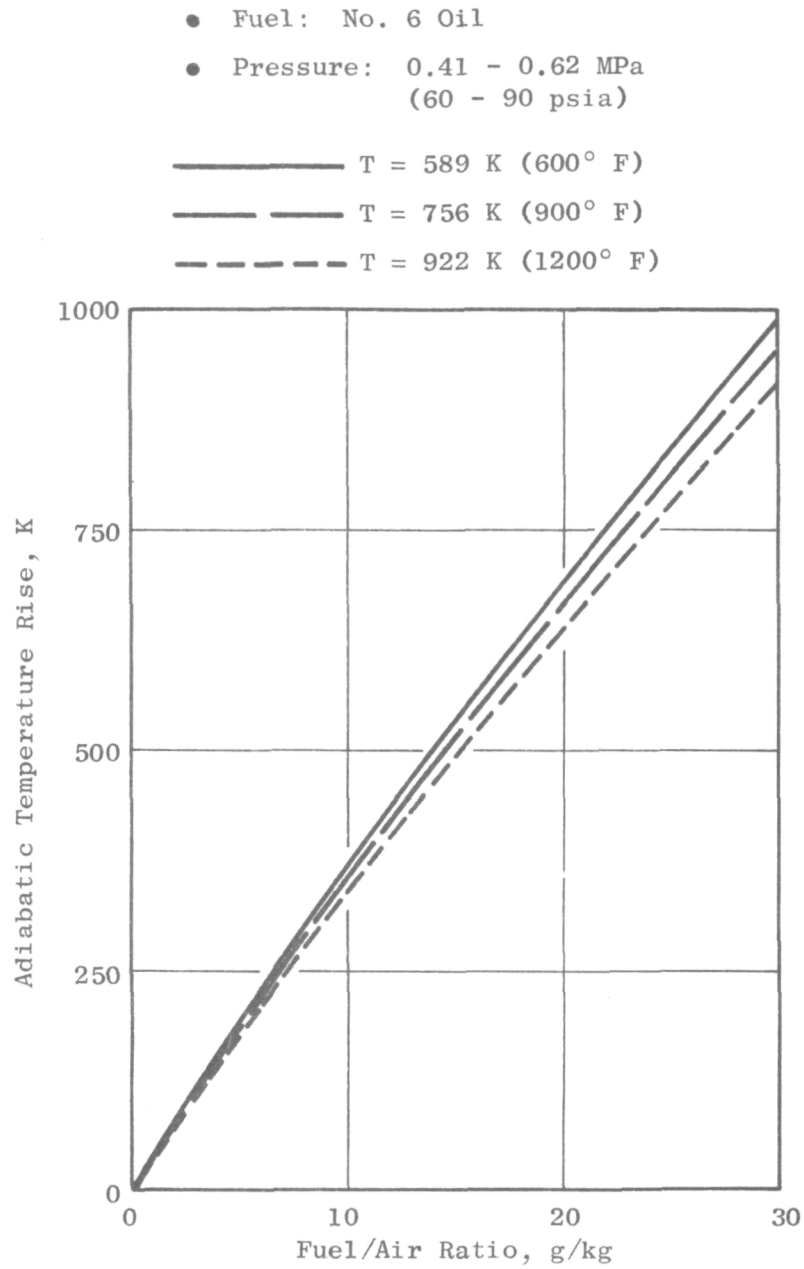


Figure 20. No. 6 Residual Oil Temperature Rise.

5.0 RESULTS AND DISCUSSION

5.1 BASELINE CATALYTIC REACTOR TEST RESULTS

5.1.1 Baseline Test Description

The baseline catalytic reactor test series consisted of two test runs; a total of 20 test points were obtained. The baseline reactor configuration was successfully operated on No. 6 residual oil after initial problems with catalyst plugging during the transition from distillate fuel.

The first test run consisted of repeated attempts to establish steady-state operation on residual fuel. Initially, light-off (on Jet A) and transition to operation on No. 6 oil was attempted at a rig inlet temperature of 756 K (900° F), 0.414 MPa (60 psia), and a reference velocity of 19.8 m/s (65 ft/s). Transition to operation on 50% residual oil was attempted several times at these conditions. In each case, the catalytic reactor pressure drop began to increase very rapidly before the transition could be completed, apparently due to plugging of the catalyst channels with a coating of the residual fuel. When this increase in pressure drop occurred, fuel flow to the reactor was immediately terminated. It was found that the normal reactor pressure drop could be reestablished by purging the catalytic reactor with air at about 783 K (950° F) for 10 to 15 minutes.

After unsuccessful attempts to transition over a range of fuel/air ratios, rig inlet temperature was increased to 811 K (1000° F). At this condition, steady-state operation on fuel mixtures containing first 25% and then 50% residual oil was established.

The first run was terminated due to a problem with the test-facility control system. The reactor was damaged during a momentary increase in fuel flow during shutdown. All catalytic reactor elements were replaced and reinstrumented prior to the second test run.

The second test run was initiated by setting the 811 K (1000° F), 50% residual oil condition that had already been demonstrated during the first run. Transition to 75% residual oil was attempted but reactor plugging prevented completion.

Operation on 100% No. 6 oil was finally accomplished by increasing the rig inlet temperature to 867 K (1100° F) while maintaining catalytic reactor inlet pressure at 0.414 MPa (60 psia) and reference velocity at 19.8 m/s (65 ft/s). Performance and emission data were then recorded over a range of fuel/air ratios at these inlet conditions.

Attempts to vary initial-drop size below about 15 μm at the above conditions were unsuccessful because of burning upstream of the catalytic reactor. Upstream burning was indicated by two thermocouples mounted in the mixing duct a short distance downstream of the fuel injector ($T_{1.5}$). An automatic shut-off was used to terminate fuel flow when the thermocouple reading exceeded the rig inlet temperature by more than 140 K (250° F).

Attempts to operate at a higher reference velocity were also unsuccessful due to catalytic reactor plugging. Operation at higher temperature, higher pressure, and lower reference velocity were not attempted because of expected autoignition.

5.1.2 Baseline Catalytic Reactor Emissions and Performance

Operating characteristics of the baseline catalytic reactor on No. 6 residual oil are shown as a function of gas-sample fuel/air ratio in Figure 21. The gas-sample fuel/air ratio is based on a carbon balance of measured CO, CO₂, and unburned hydrocarbon concentrations. It has been used in Figure 21, rather than the metered fuel/air ratio (based on measured fuel and air flows). As will be discussed in Section 5.3, the fuel/air ratio produced by the single-point injector was somewhat center-peaked. Emissions and performance parameters measured near the duct centerline are therefore best represented by the fuel/air ratio as measured by the gas sample.

As indicated in Figure 21, combustion efficiency (calculated from CO and HC content) above 99.5% was obtained at fuel/air ratios above about 17 g/kg. The measured NO_x emissions index was slightly above 7 g/kg at the higher fuel/air ratios and decreased approximately in proportion to combustion efficiency as fuel/air ratio was reduced.

The magnitude of the NO_x emission index and its relationship to combustion efficiency both indicate that the NO_x is due primarily to fuel-bound nitrogen. As shown in Figure 22, NO_x emissions are approximately proportional to fuel-bound nitrogen content when mixtures of Jet A and No. 6 oil were used. With pure JP-5, which has negligible fuel-bound nitrogen, NO_x levels were below 0.5 g/kg. This indicates very low thermal NO_x production; this is characteristic of catalytic combustion. With pure No. 6 oil, NO_x emissions were close to 7.2 g/kg and correspond to 100% fuel-bound nitrogen conversion (0.22% nitrogen, by weight, in the test fuel). The approximate proportionality between NO_x emissions and combustion efficiency indicates that the fuel-bound nitrogen is retained in the unburned hydrocarbons in about the same concentration as in the parent fuel.

Measured temperature profiles with a 50% mixture of No. 6 oil and Jet A are shown in Figure 23. These profiles are typical of those obtained with all fuel mixtures. The profiles reflect the drop in temperature between the rig inlet (Station 1.0) and the mixing duct (Station 1.5) due to fuel vaporization and the addition of cold, atomizing air. The rapid increase in temperature at the catalytic reactor inlet indicates good ignition capability, and the center-peaked fuel distribution is evident from the lower temperatures near the outer wall (5.0-cm radius). In the exit section, temperatures on the centerline and along the wall decrease gradually downstream of the reactor, probably due to heat losses to the sampling probe and the exit section wall, respectively. At a radial position midway between the reactor centerline and wall ($r = 2.5$ cm), the measured temperature continues to increase downstream

Nominal Operating Conditions

$T_{1.5} = 823 \text{ K} (1021^\circ \text{ F})$

$P_{1.5} = 0.41 \text{ MPa} (60 \text{ psia})$

$V_r = 21.5 \text{ m/s} (71 \text{ ft/s})$

Fuel: No. 6 Oil, SMD = $10 \mu\text{m}$

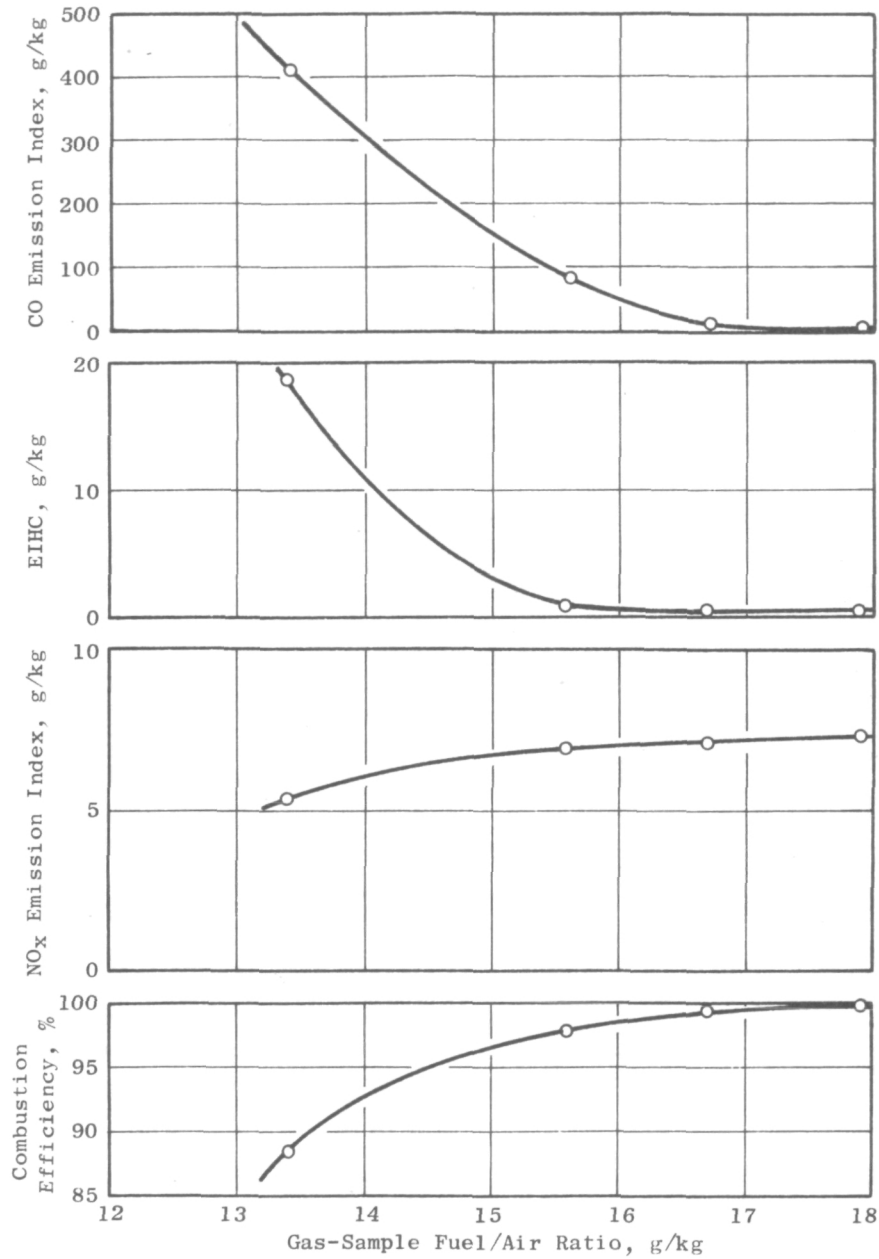


Figure 21. Baseline Catalytic Reactor Emissions and Performance Characteristics.

- Catalyst Inlet Temperature = 767 - 840 K (920 - 1050° F)
- Pressure = 0.41 MPa (60 psia)
- Fuel/Air Ratio = 10 - 15 g/kg
- Approach Velocity = 20 - 22 m/s (65 - 72 ft/s)

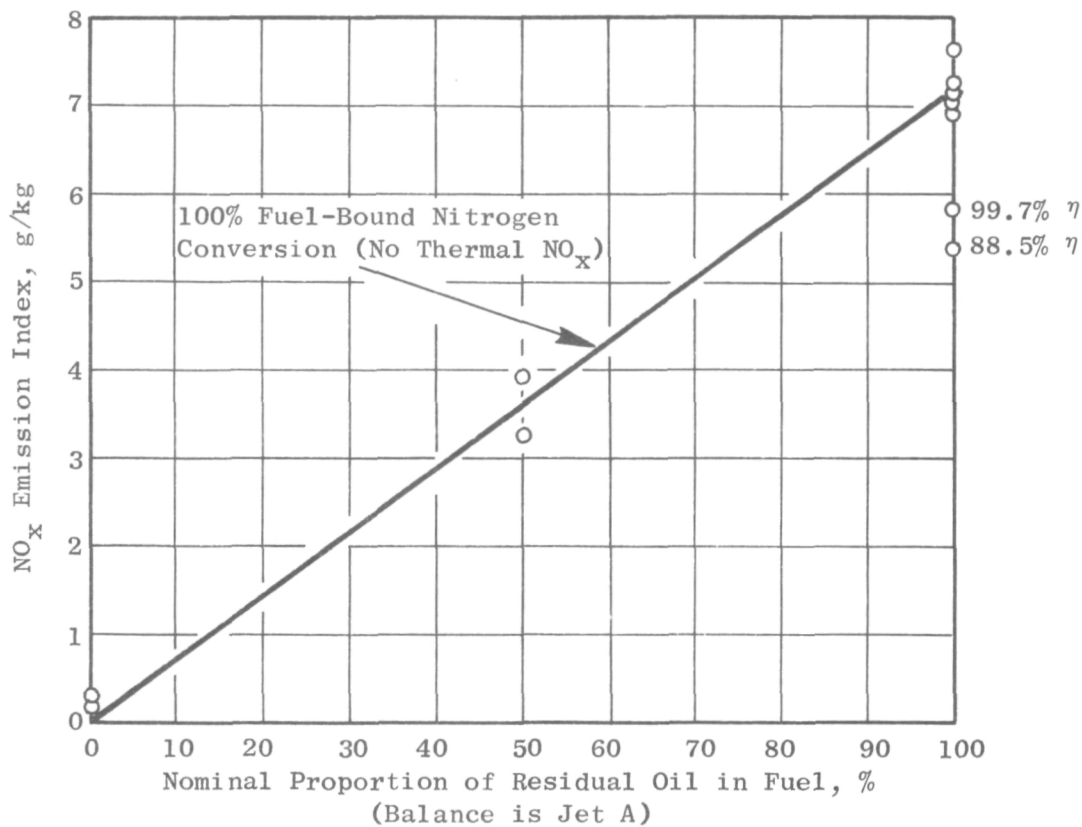


Figure 22. Fuel-Bound Nitrogen Conversion.

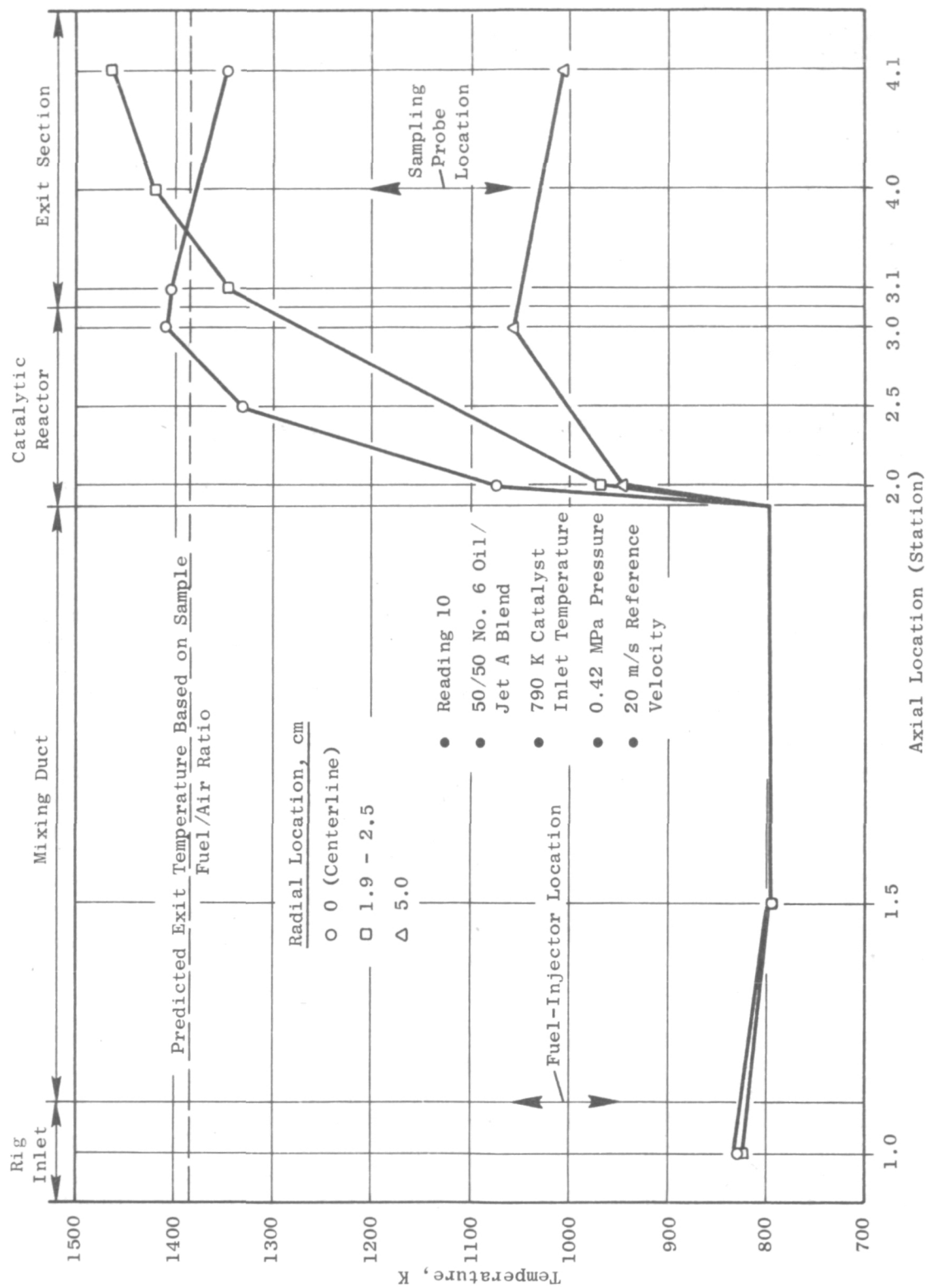


Figure 23. Typical Test-Rig Temperature Profiles - Baseline Reactor.

of the reactor. This temperature rise could be due to continued combustion downstream of the reactor. This effect could also be attributed in part to uncertainty in thermocouple correction factors (corrections for radiation and conduction are as high as 188 K for the exit thermocouple) and to nonaxisymmetric temperature profiles. (Recall that the thermocouple probes at $r = 2.5$ cm were at different circumferential positions so that the same streamline was not measured by all of the probes.)

On the reactor centerline, the measured temperatures did not increase downstream of the reactor, and measured reactor exit temperatures were generally within about 25 K (45° F) of the flame temperature predicted based on an analysis of gas samples attained on the centerline. These data indicate that combustion was very nearly complete at the reactor exit, at least on the reactor centerline.

Catalytic reactor pressure drop was close to the design value of 3.2% at the beginning of each run. As the run progressed, however, pressure drop increased. This effect is shown in Figure 24 where catalytic reactor pressure drop, corrected to design-point inlet conditions, is shown as a function of reading number.

The reason for increased catalytic reactor pressure drop was revealed in postrun inspections. The catalytic reactor condition after the first run is shown in Figures 25 and 26. Externally, the reactor appeared to be in good condition except for a small amount of erosion of the inlet face (Figure 25). However, there was significant internal damage due to overtemperature and subsequent melting of the catalyst substrate (Figure 26). In the baseline reactor, melting of the cordierite substrates indicates local temperatures in excess of 1700 K (2600° F). It is thought that most of this damage occurred when the catalytic reactor became plugged with fuel. Pressure drop was steady during steady-state operations, and measured substrate temperatures were well below 1700 K.

All internal test-rig surfaces were clean except for very slight carboning on the fuel nozzle. No indications of burning in the mixing duct were found; this indicates that the setting on the automatic autoignition shutoff was conservative.

Overall, the baseline test results were encouraging; good catalytic reactor performance was obtained with No. 6 residual oil. The reactor operating range, however, was very narrow and required a catalytic reactor inlet temperature more than 220 K (400° F) above the original design point in order to obtain steady-state operation without reactor plugging. Significant damage to the catalytic reactor occurred during each of the baseline test runs, but the reactor damage is believed to have occurred during transients (particularly during catalytic reactor plugging).

When reactor plugging occurred, airflow decreased slightly as reactor pressure drop increased, but fuel flow remained constant. This resulted in a momentary increase in fuel/air ratio and increased reactor temperatures.

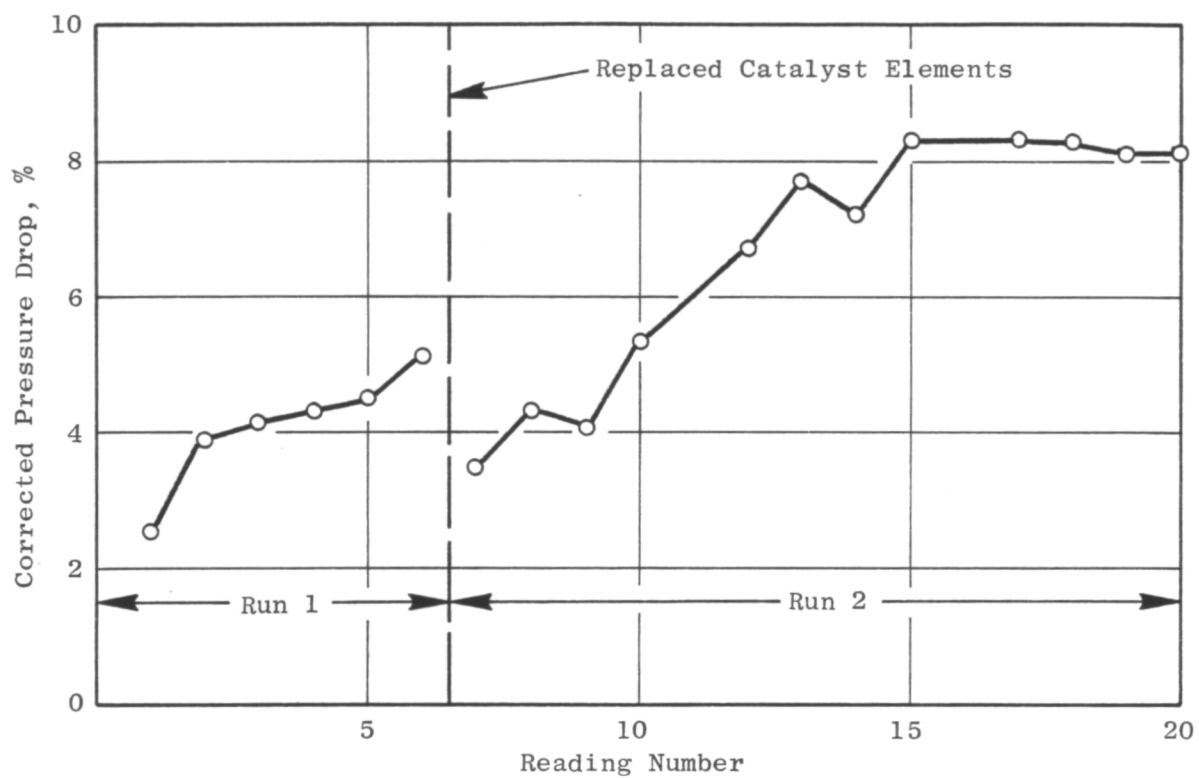


Figure 24. Baseline Catalytic Reactor Pressure Drop Increase with Operating Time.

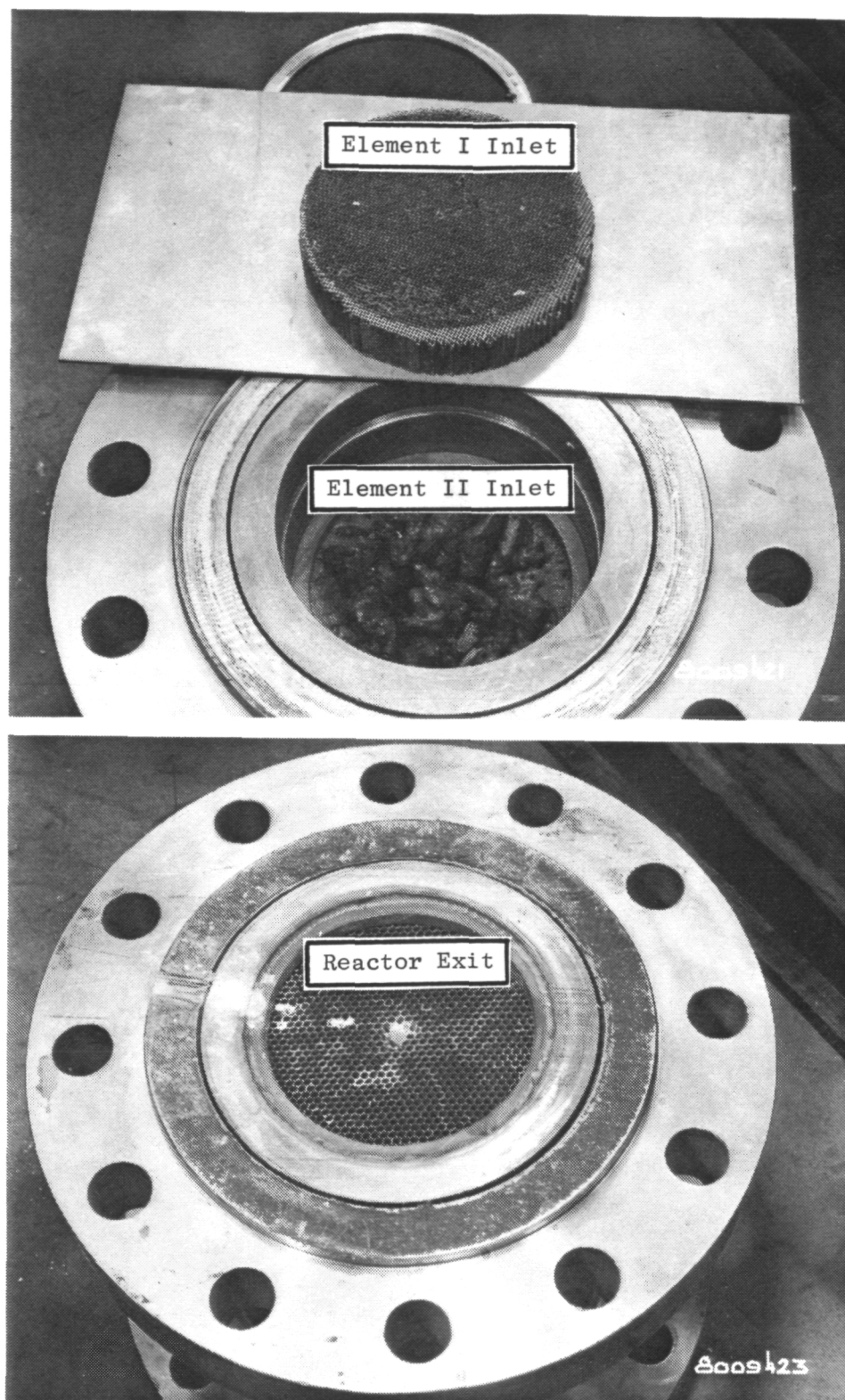


Figure 25. Postrun Condition of Baseline Catalytic Reactor.

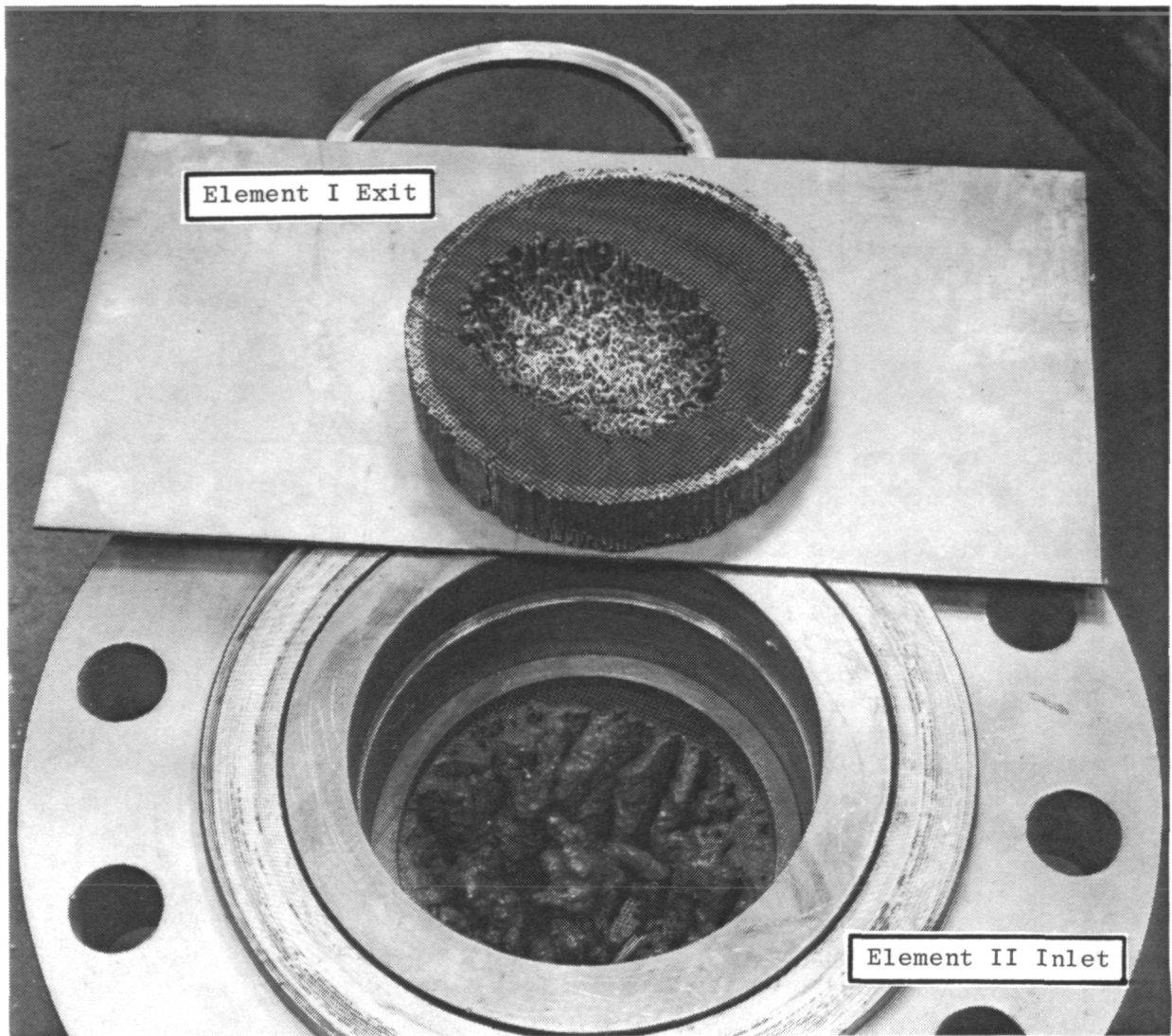


Figure 26. Baseline Catalytic Reactor, Internal Damage.

Reactor surface temperatures were also increased as the carbon coating burned off after fuel flow had been terminated. There was no indication of reactor deterioration during steady-state operation; however, in order to demonstrate operation over a wider range of operating conditions, and particularly at lower catalytic reactor inlet temperatures, a series of backup reactor tests was planned.

5.2 BACKUP CATALYTIC REACTOR TEST RESULTS

5.2.1 Backup Test Description

As discussed in Section 4.1, the first and second backup catalytic reactors had successively larger cells in the inlet catalyst element in order to reduce the probability of plugging with residual oil. With both backup reactors, the test inlet conditions were varied, as shown in Table XI, starting at the operating condition which had been demonstrated with the baseline reactor and progressing to higher reference velocities and lower inlet temperatures until the reactor operating limits were defined.

The operating ranges of each of the backup catalytic reactors were significantly wider than that of the baseline reactor, as shown in Figure 27. The first backup reactor, with increased cell size in the inlet element, could be operated at reference velocities up to about 30 m/s at a reactor inlet temperature of 825 K (1025° F) or down to 775 K (935° F) inlet temperature at the design-point reference velocity. However, plugging still occurred when reference velocity was increased and inlet temperature was simultaneously reduced. The second backup reactor, which had increased cell size in both the inlet and center element, never actually plugged to the point where fuel flow had to be terminated. However, operation was unsteady at inlet temperatures below about 750 K (890° F) with a nominal pressure of 0.414 MPa (60 psia). At these conditions, catalytic reactor pressure drop and reactor substrate temperature both cycled at about 10- to 15-second intervals. Pressure drop varied by about 50% of the nominal value, and the peak substrate temperature fluctuated by as much as ± 80 K (144° F).

The unsteady operation of the second backup catalytic reactor at the lower reactor temperature appeared to be due to coating and partial plugging of the catalyst channel with residual oil, followed by ignition and burning of the coating. This process was evidenced by a gradual increase in reactor pressure drop, accompanied by decreasing reactor substrate temperatures, followed by a more rapid reduction in pressure drop with increased substrate temperatures.

Stable operation at 725 K (845° F) and 20 m/s (65 ft/s) was established by increasing inlet pressure above 0.6 MPa (90 psia), but even at this pressure operation became unsteady as reference velocity was increased to 30 m/s (98 ft/s). Operation was also attempted at 11 m/s (36 ft/s) and 0.6 MPa, but burning occurred upstream of the reactor as reference velocity was being reduced.

The apparent upstream-burning phenomenon that prevented variation of drop size in the baseline tests was studied further in tests of the backup catalytic reactors. Based on posttest inspections of the baseline configuration, it was concluded that the automatic upstream-burning shutoff setting [140 K (250° F) above rig inlet temperature] was conservative. Therefore, during the first backup tests, the shutoff setting was increased to 278 K (500° F) above rig inlet temperature. With this setting, it was possible to operate over a wider range of drop sizes and inlet temperatures. Increased temperature was indicated occasionally on the two thermocouple probes located in the premixing section (Station 1.5), but this temperature rise appeared to be a very local phenomenon. Although the two premixing section thermocouples were only about 5 cm apart, an increase in temperature was often indicated on one thermocouple probe while output from the other remained constant. It appeared either that small flames had been stabilizing in the wake of the thermocouples or that fuel droplets were impinging on these probes, then igniting and burning. For tests of the second backup reactor, the thermocouple probes were removed, and mixing-section temperature was monitored using surface-mounted thermocouples. With these surface-mounted thermocouples, the indicated mixing-section temperature was stable except for one occasion when upstream burning occurred at low reference velocity with Jet A fuel. This incident did not damage the test section or reactor.

5.2.2 Backup Catalytic Reactor Emissions and Performance

Combustion efficiencies of the backup catalytic reactors are compared with baseline reactor efficiency at similar operating conditions in Figure 28. At constant flame temperature, combustion efficiency was slightly improved with the first backup reactor and significantly improved with the second.

NO_x emission levels were similar for all three reactors although data taken during Run 3, with the first backup reactor, were about 10% higher than levels obtained in other runs. NO_x emissions were primarily due to fuel-bound nitrogen and varied linearly with combustion efficiency over a wide range of operating conditions as shown in Figure 29.

Catalytic reactor pressure drop was much more consistent with the backup configurations than it was with the baseline. Measured pressure drop, corrected for reactor inlet flow function, is shown for each of the backup reactors in Figures 30 and 31. Design-point pressure drop for both of the reactors was less than 4%. As expected, the pressure drop of both reactors increased as fuel/air ratio (and temperature rise) was increased.

Parametric variations in reactor inlet temperature, reference velocity, and initial drop size were run with each of the backup reactors. In general, combustion efficiency decreased with reduced inlet temperature and increased reference velocity; initial drop size had little effect at the conditions studied.

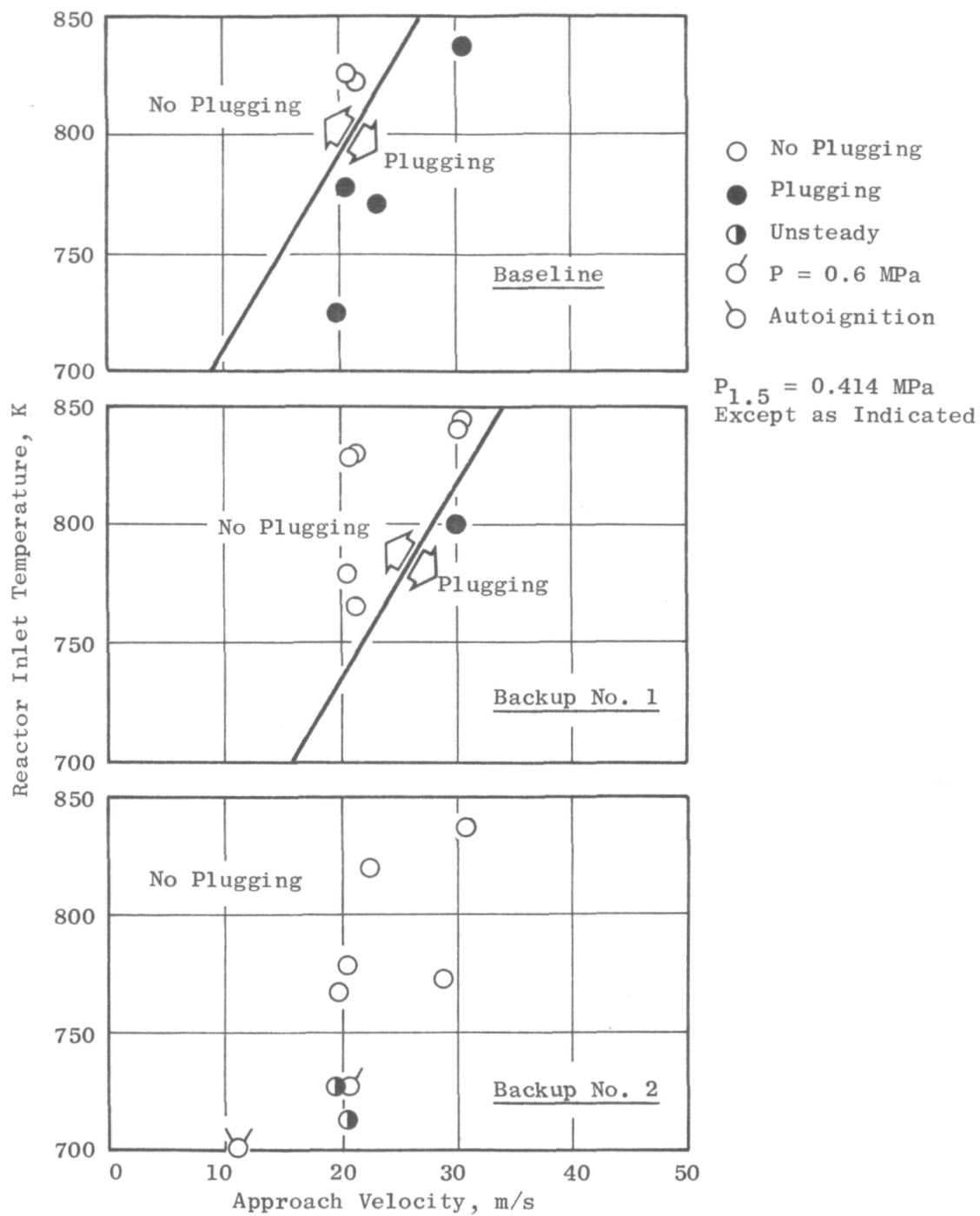


Figure 27. Catalytic Reactor Operating Range.

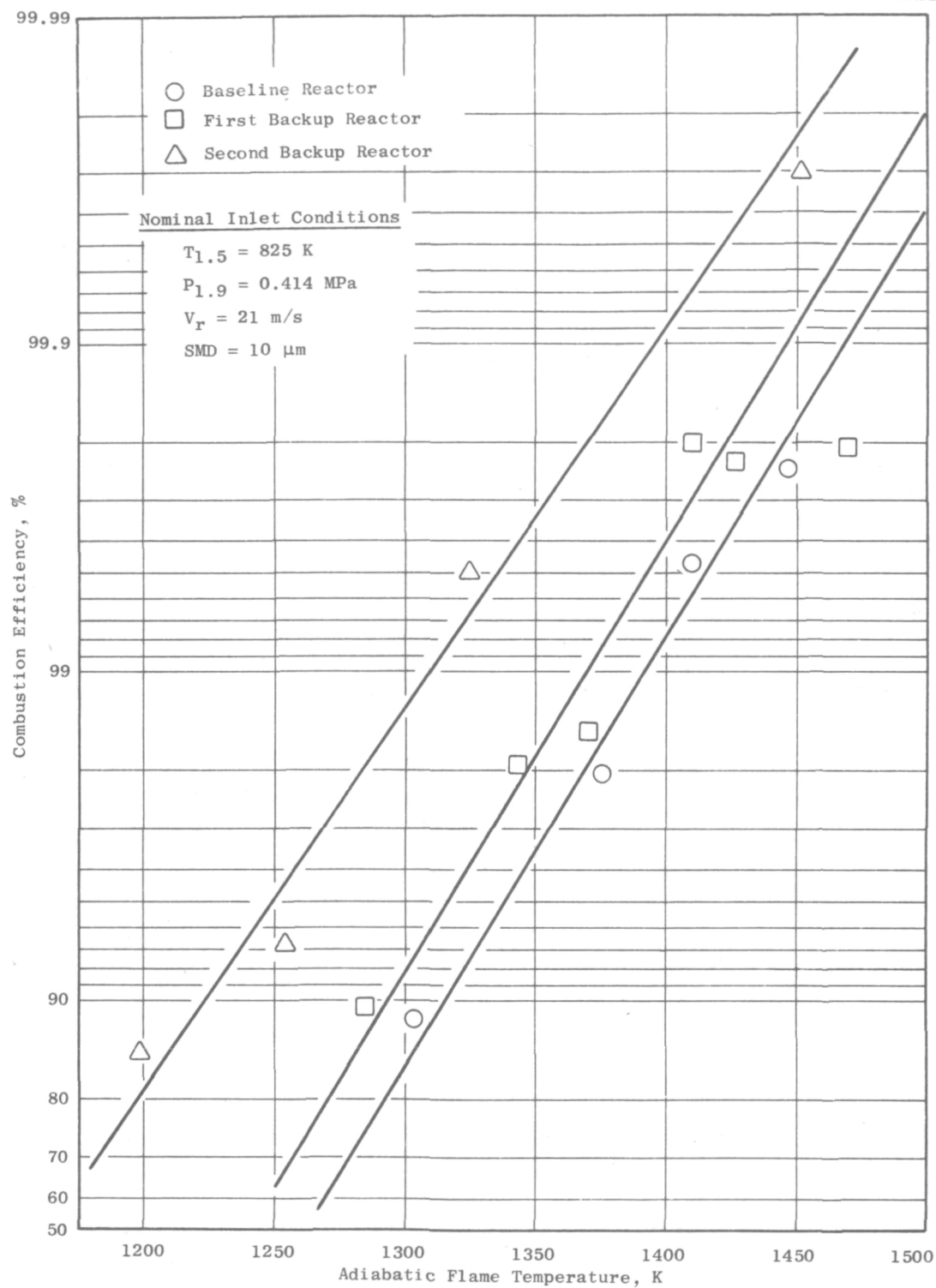


Figure 28. No. 6 Oil Combustion Efficiency Comparison.

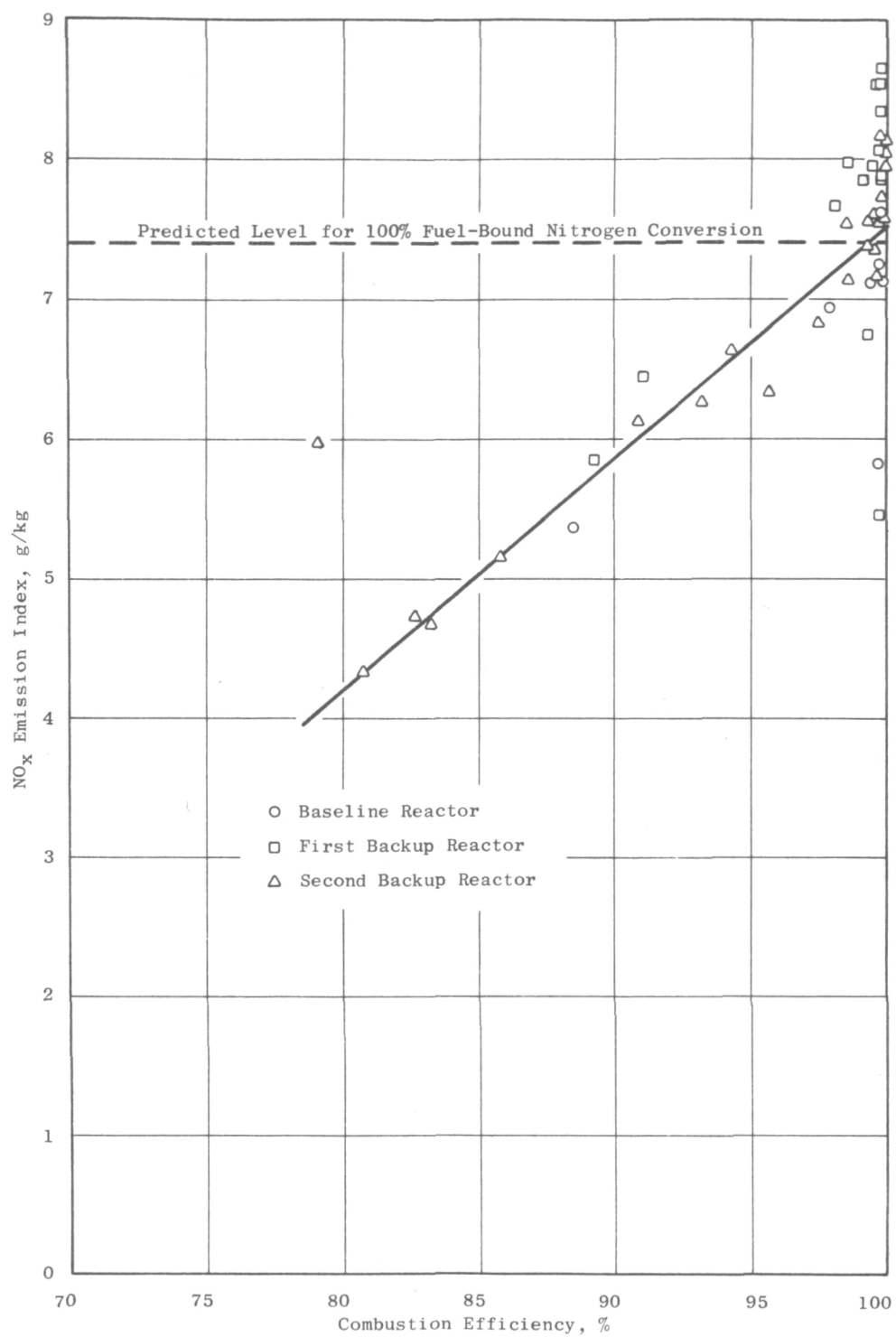


Figure 29. Relationship Between Combustion Efficiency and NO_x Emissions (No. 6 Oil).

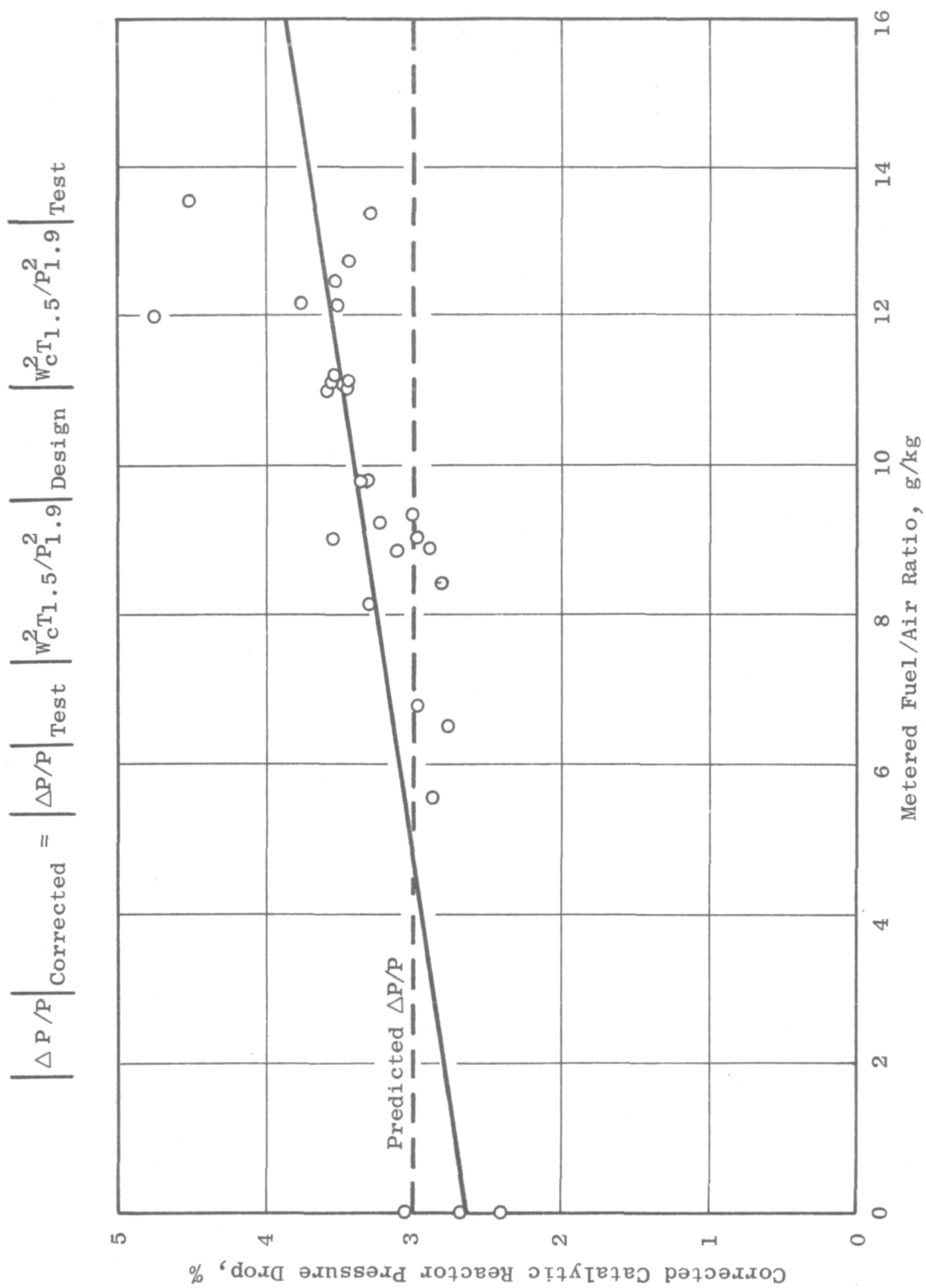


Figure 30. First Backup Catalytic Reactor Pressure Drop.

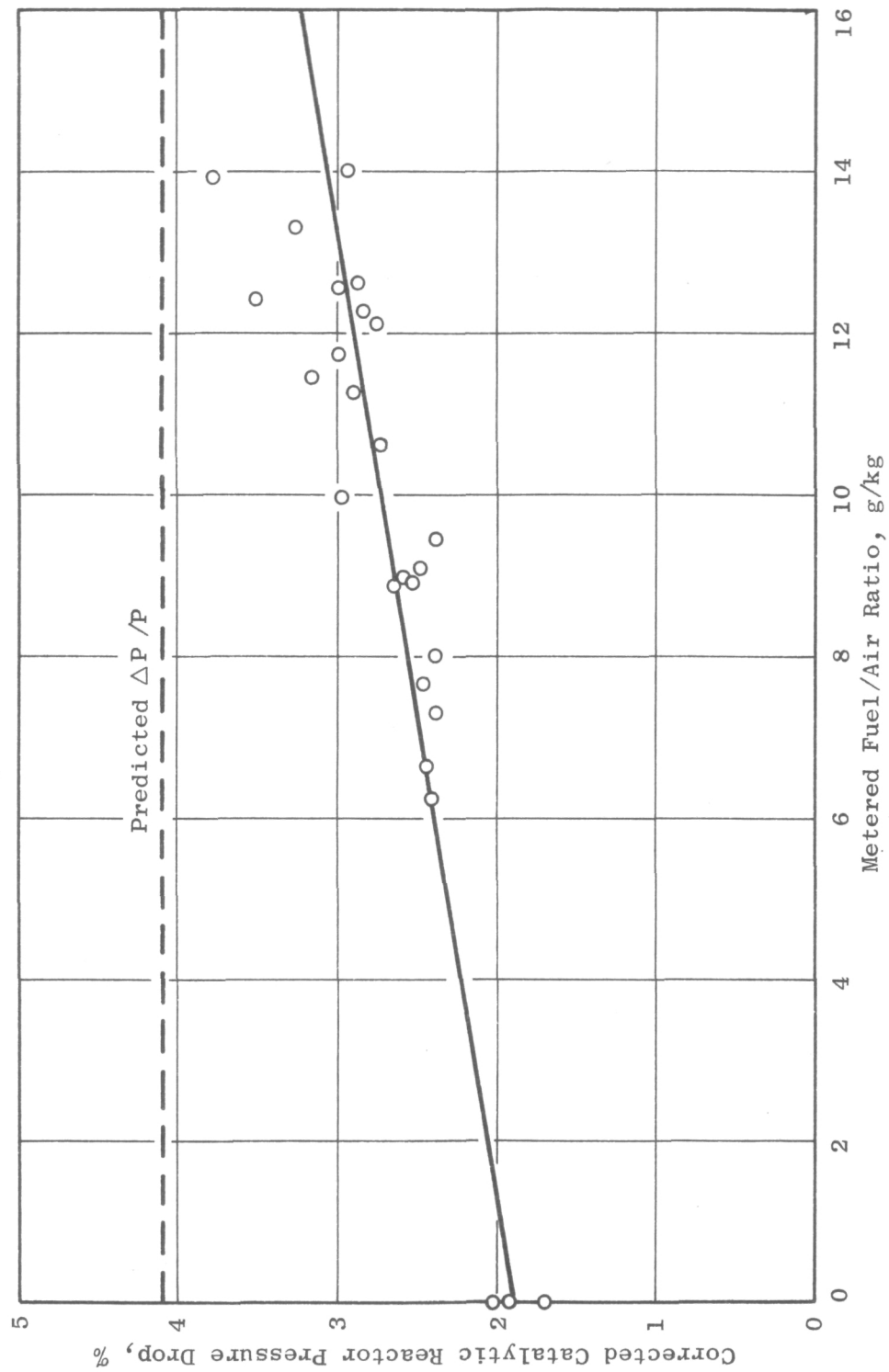


Figure 31. Second Backup Catalytic Reactor Pressure Drop.

The effect of inlet temperature and fuel/air ratio on emissions and performance for the second backup reactor is shown in Figure 32. The indicated behavior is also typical of results obtained with the first backup reactor. With reduced temperature, all of the performance curves are shifted to the right, toward higher fuel/air ratio; this suggests that reactor performance is primarily dependent on adiabatic flame temperature. As shown in Figure 33, reactor emissions and performance at the inlet temperatures studied correlate fairly well with adiabatic flame temperature.

The effect of reference velocity on catalytic reactor emissions and performance is shown in Figure 34. As reference velocity increased, both NO_x and combustion efficiency decreased.

The combined effects of reference velocity and adiabatic flame temperature on combustion efficiency and CO emissions were correlated using a multiple-regression analysis. The following functional forms were selected for this regression analysis:

$$100 - \eta = A (V_r/19.8)^B \exp [(T_{ad} - 1400)/C]$$

$$\text{EICO} = D (V_r/19.8)^E \exp [(T_{ad} - 1400)/F]$$

where V_r and T_{ad} are the reference velocity and adiabatic flame temperature, respectively, and A, B, C, D, E, and F are constants to be determined by the regression analysis. The constants 19.8 and 1400 are the design values of reference velocity and adiabatic flame temperature, respectively. The use of these constants implies that the constant A represents the design-point inefficiency and D is the design-point carbon monoxide emission index. Functional forms similar to that shown above have proven useful in previous correlations of emissions from conventional gas-turbine combustors (Reference 11).

Results of the above regression analysis are described in Table XIV. The selected functional form provides an excellent correlation with good agreement among the correlation constants obtained with the different catalytic reactors. Based on the similarity of these constants, over the range of operation conditions studied, combustion efficiency can be approximated by:

$$\eta = 100 - A (V_r/19.8)^{3.1} \exp [(T_{ad} - 1400)/-40]$$

and CO emissions can be approximated by:

$$\text{EICO} = D (V_r/19.8)^{3.4} \exp [(T_{ad} - 1400)/-39]$$

Values for A and D appear in Table XIV. These equations can also be used to derive correction factors for comparison of data obtained at different operating conditions. Additionally, NO_x (or fuel-bound nitrogen conversion) can be estimated using the NO_x - efficiency relationship shown in Figure 29.

Nominal Reactor Inlet Conditions

Pressure = 0.413 MPa

Reference Velocity = 21.3 m/s

Fuel: No. 6 Oil

Initial SMD = 9.0 μm

Δ 767 K Temperature

\circ 820 K Temperature

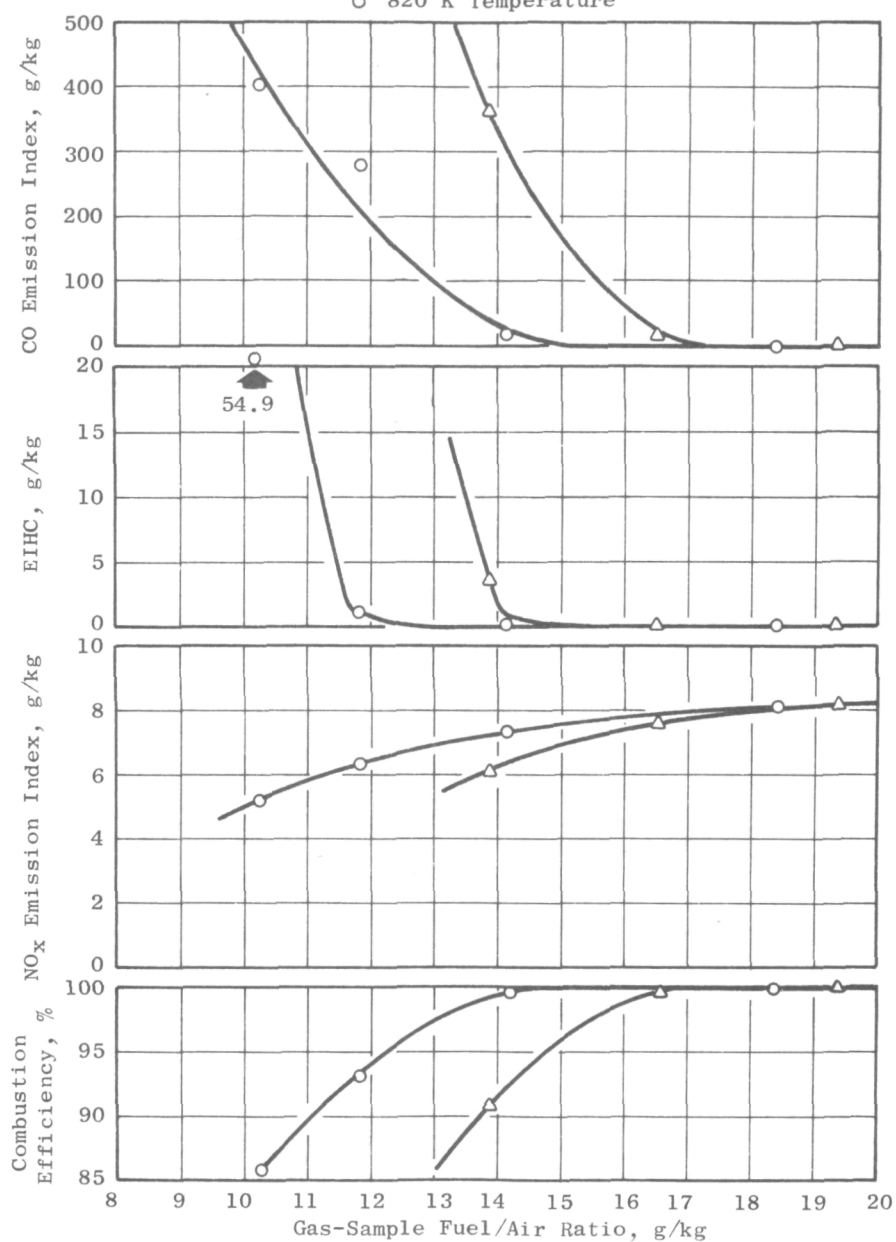


Figure 32. Effect of Inlet Temperature on Emissions and Performance for the Second Backup Reactor.

Nominal Reactor Inlet Conditions

Pressure = 0.413 MPa

Reference Velocity = 21.3 m/s

Fuel: No. 6 Oil

Initial SMD = 9.0 μm

Δ 767 K Temperature

\circ 820 K Temperature

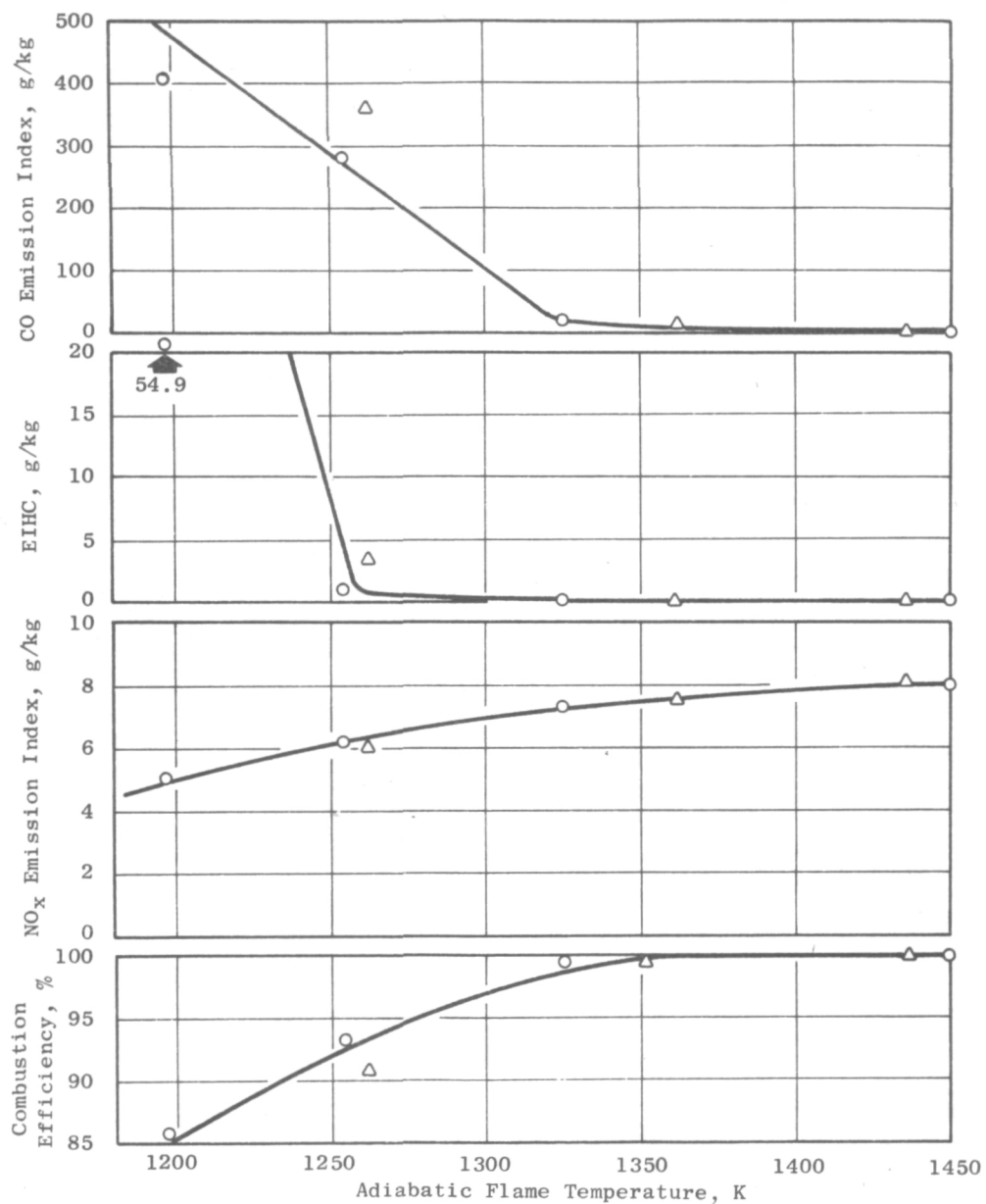


Figure 33. Effect on Second Backup Catalytic Reactor of Inlet Temperature/Adiabatic Flame Temperature Correlation.

Nominal Reactor Inlet Conditions

Pressure = 0.413 MPa

Temperature = 829 K

Fuel: No. 6 Oil

Initial SMD = 9.0 μm

○ 22.3 m/s Reference Velocity

● 31.0 m/s Reference Velocity

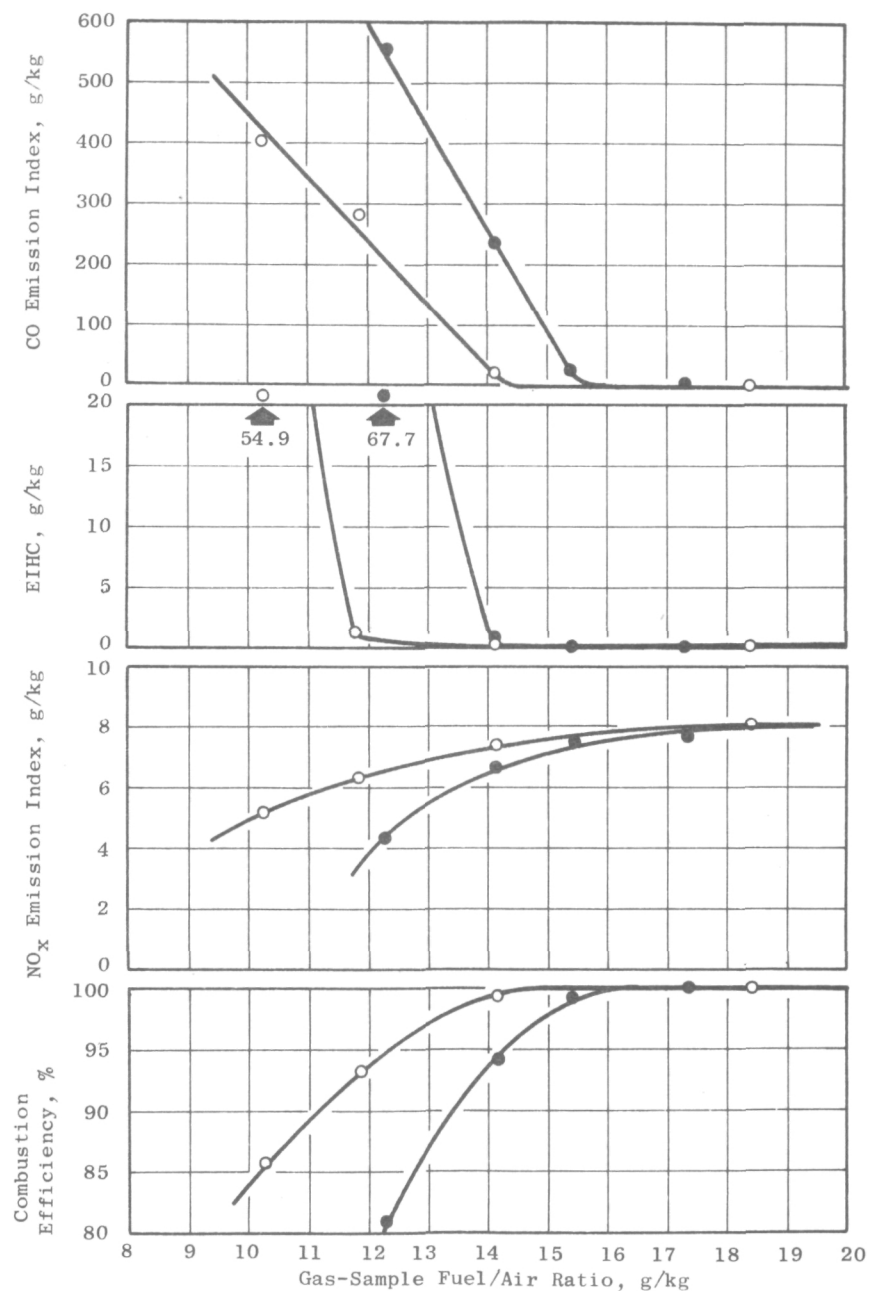


Figure 34. Effect on Second Backup Reactor of Reference Velocity on Emissions and Performance.

Table XIV. Combustion Efficiency and CO Correlation Constants.

	Correlation							
	$100 - \eta_b = A \left(\frac{V_r}{19.8} \right)^B \exp \left(\frac{T_{ad}-1400}{C} \right)$				$EICO = D \left(\frac{V_r}{19.8} \right)^E \exp \left(\frac{T_{ad}-1400}{F} \right)$			
	A	B	C	R*	D	E	F	R*
Catalytic Reactor								
Baseline	0.815	N/A**	-35.99	0.9921	25.4	N/A**	-32.61	0.9893
First Backup	0.438	3.243	-39.89	0.9581	14.3	3.684	-36.33	0.9752
Second Backup	0.130	2.978	-40.84	0.9637	4.9	3.044	-41.03	0.9611

* Correlation coefficient for transformed equation $\left[\text{e.g. } \ln(1 - \eta_b) = \ln A + B \ln \left(\frac{V_r}{19.8} \right) + \left(\frac{T_{ad}-1400}{C} \right) \right]$

** No data available for velocity variation with baseline reactor.

The effect of initial drop size was studied during tests of the first backup reactor; droplet SMD was varied from 12.8 to 72.5 μm . Combustion efficiency and CO emission index, corrected to design-point velocity and flame temperature, and measured NO_x emission index are shown as a function of drop size in Figure 35. Over the range of variation, drop size had very little effect on catalytic reactor emissions and performance. Combustion efficiency and CO levels are quite close to levels predicted for drop sizes less than 10 μm and show no clear-cut trend with increasing drop size. NO_x levels appear to increase very slightly as drop size is increased, but this effect is very weak.

The small effect of initial drop size is not surprising if it is recalled that the fuel/air-preparation system was designed to provide less than 50% evaporation at 589 K (600° F) and 0.621 MPa (90 psia), while the actual testing was conducted at 853 K (1075° F) and 0.421 MPa (61 psia). As shown in Figures 36 and 37,, evaporation increases very rapidly as pressure is reduced and inlet temperature is increased. At the actual high-temperature, reduced-pressure test conditions virtually complete evaporation is predicted over the range of drop sizes tested.

Normalized catalytic reactor temperature axial profiles for high-efficiency operation over a range of reactor inlet temperatures and reference velocities are shown in Figure 38. The shape of these profiles was virtually unchanged by variation in the inlet conditions.

Postrun inspection of the second backup reactor revealed some erosion on the inlet face of the first catalyst element, as shown in Figure 39. This element was damaged (delaminated) during disassembly. Delamination of the substrate occurred with several of the Torvex elements, but in all cases the elements appeared to be intact before they were removed from the catalyst holder. Some melting occurred in the second section of the second backup reactor, as shown in Figure 40.

5.3 FUEL/AIR MIXTURE-PREPARATION SYSTEM PERFORMANCE

The single-point injector fuel/air mixture-preparation system performed well throughout the test series, particularly in consideration of the minimal pretest development of the overall system. Although it was operated at temperatures much higher than the original design point, the air-assisted simplex fuel injector performed very well; there were no signs of plugging or serious carboning. Overall fuel-preparation-system pressure drop was low (generally less than 2% at the design point) and consistent throughout the tests, and the system was generally very clean and carbon free at the end of each test. As described in the previous section, upstream burning occurred in early tests, but the system was undamaged. In later tests, this phenomenon was eliminated by removing two premixing-section thermocouple probes that apparently had been acting as flameholders. The most serious fault with the fuel-preparation system was the center-peaked fuel/air ratio profile at the catalytic reactor inlet.

Nominal Operating Conditions

Reactor Inlet Temperature = 853 K (1075° F)

Pressure = 0.420 MPa

Reference Velocity = 30.4 m/s (100 ft/s)

Fuel: No. 6 Residual Oil

Note: EICO and Combustion Efficiency are Corrected to Design-Point Velocity and Flame Temperature.

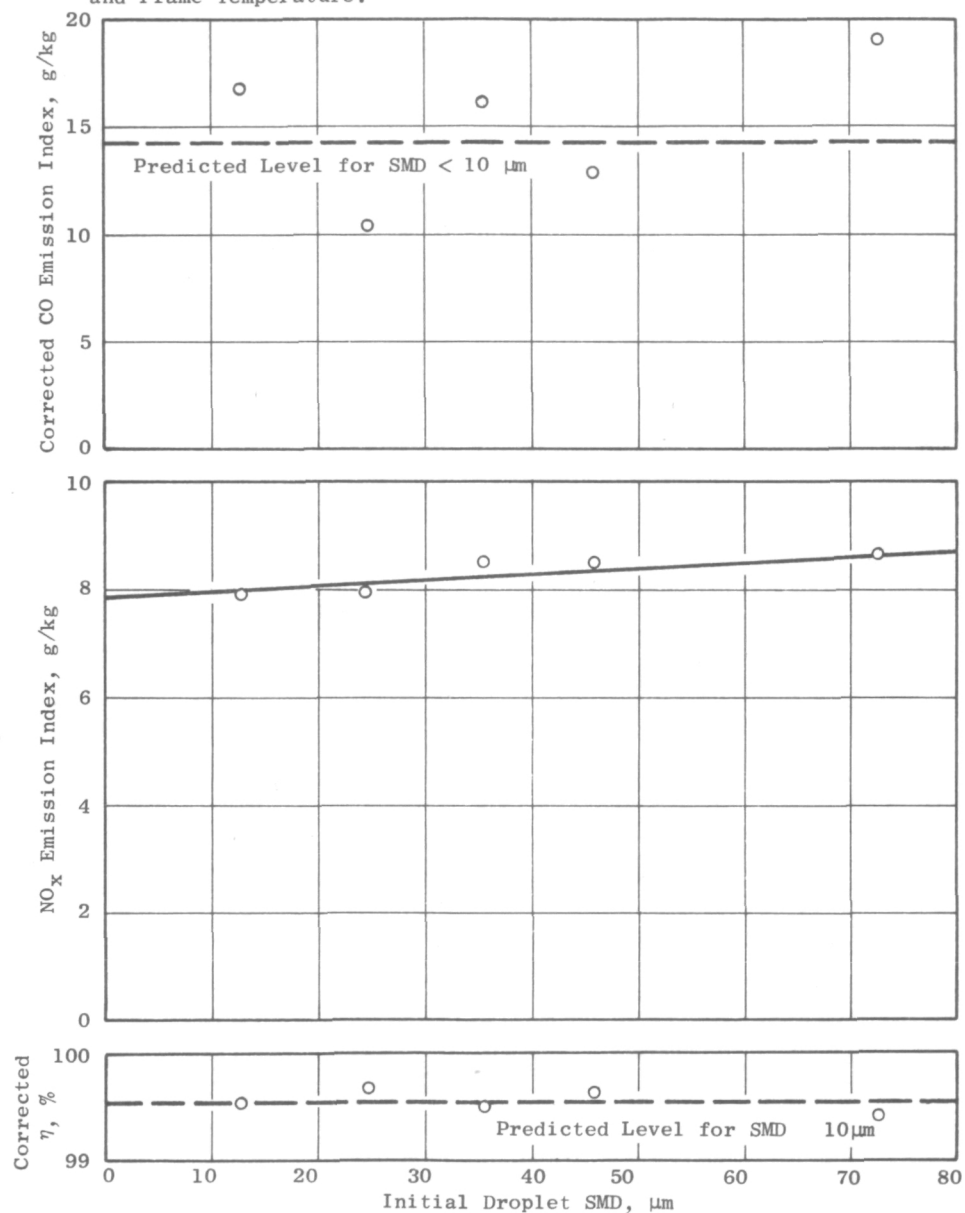


Figure 35. Effect of Initial Drop Size on First Backup Catalytic Reactor Emissions and Performance.

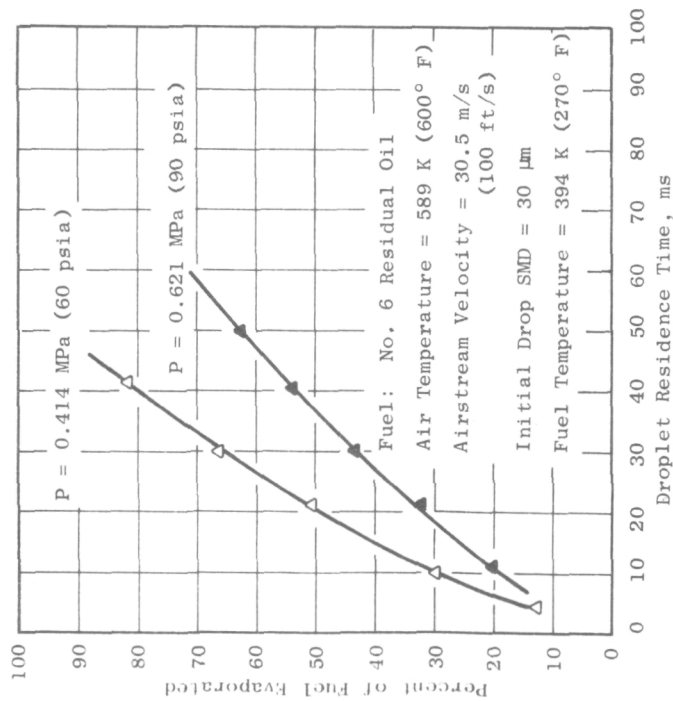


Figure 36. Effect of Pressure on Fuel Evaporation.

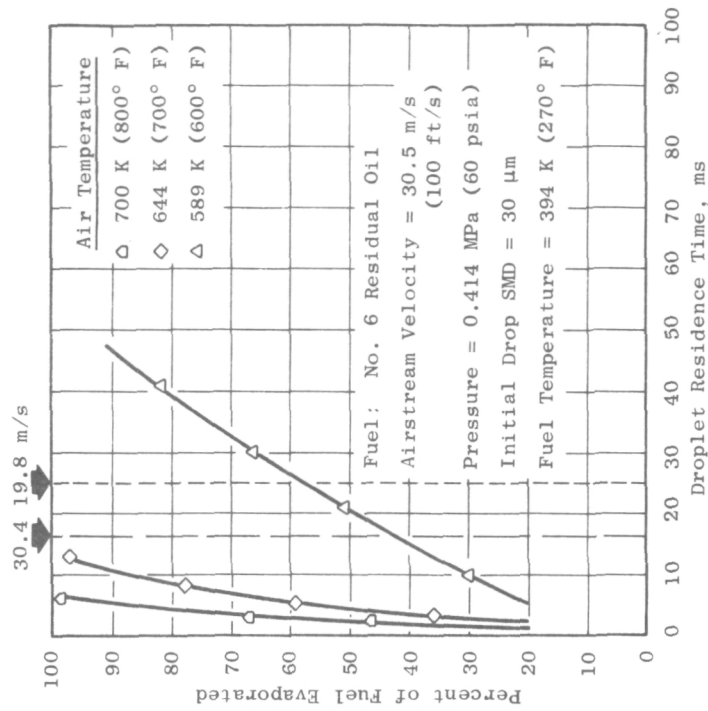


Figure 37. Effect of Air Temperature on Fuel Evaporation.

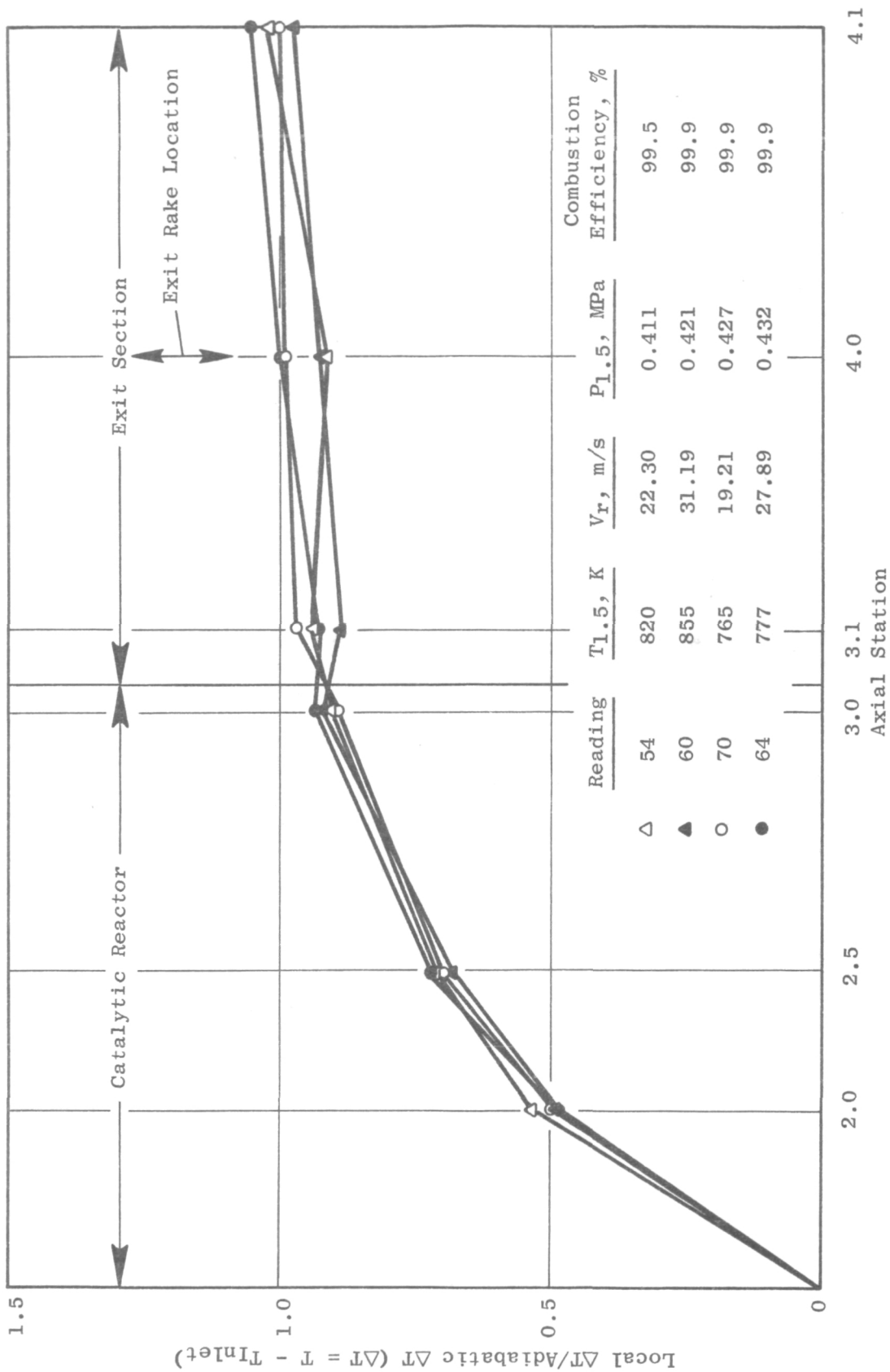


Figure 38. Second Backup Catalytic Reactor Axial Temperature Profiles.

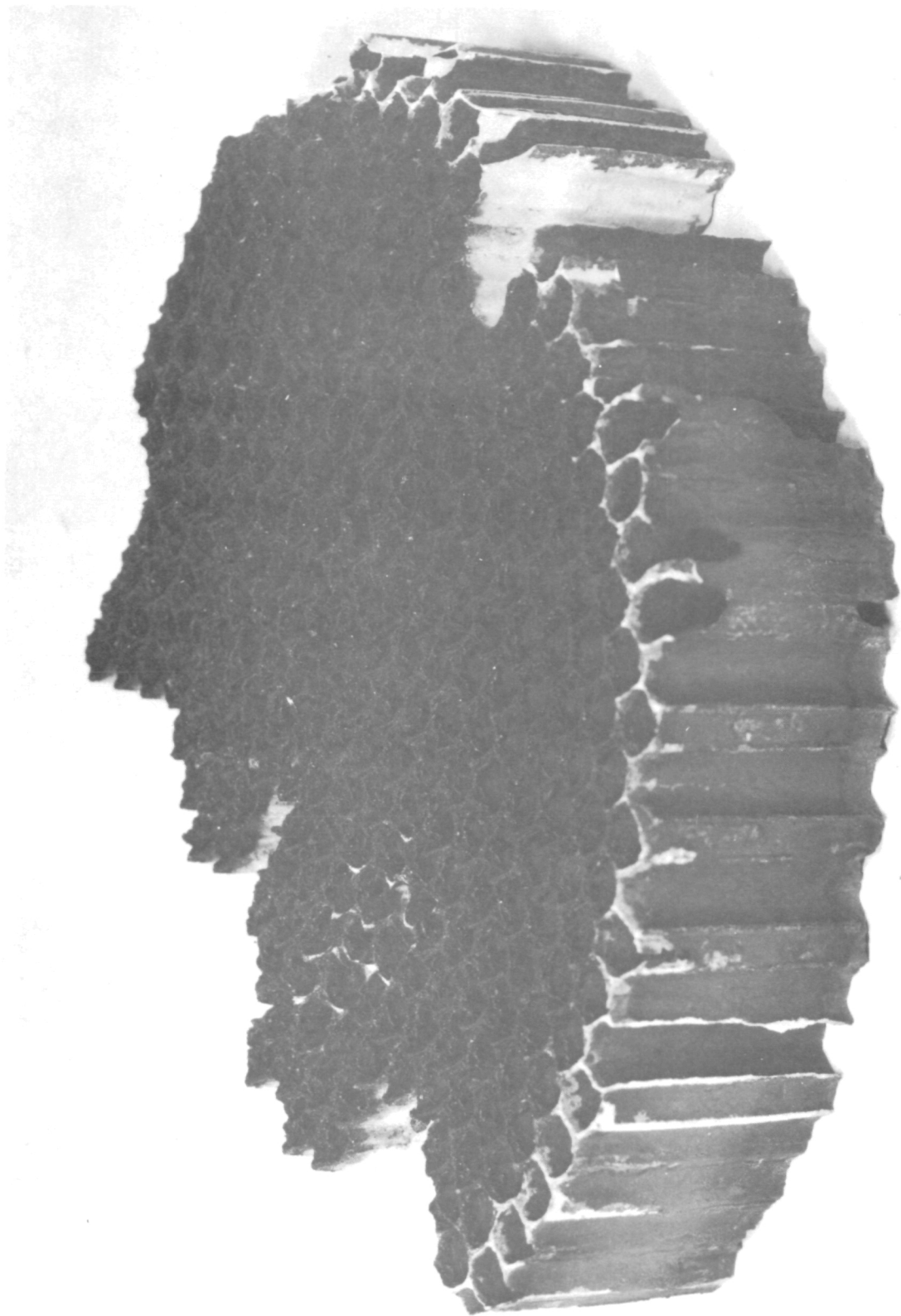


Figure 39. Condition of Inlet Element in the First Backup Catalytic Reactor After Test Run.

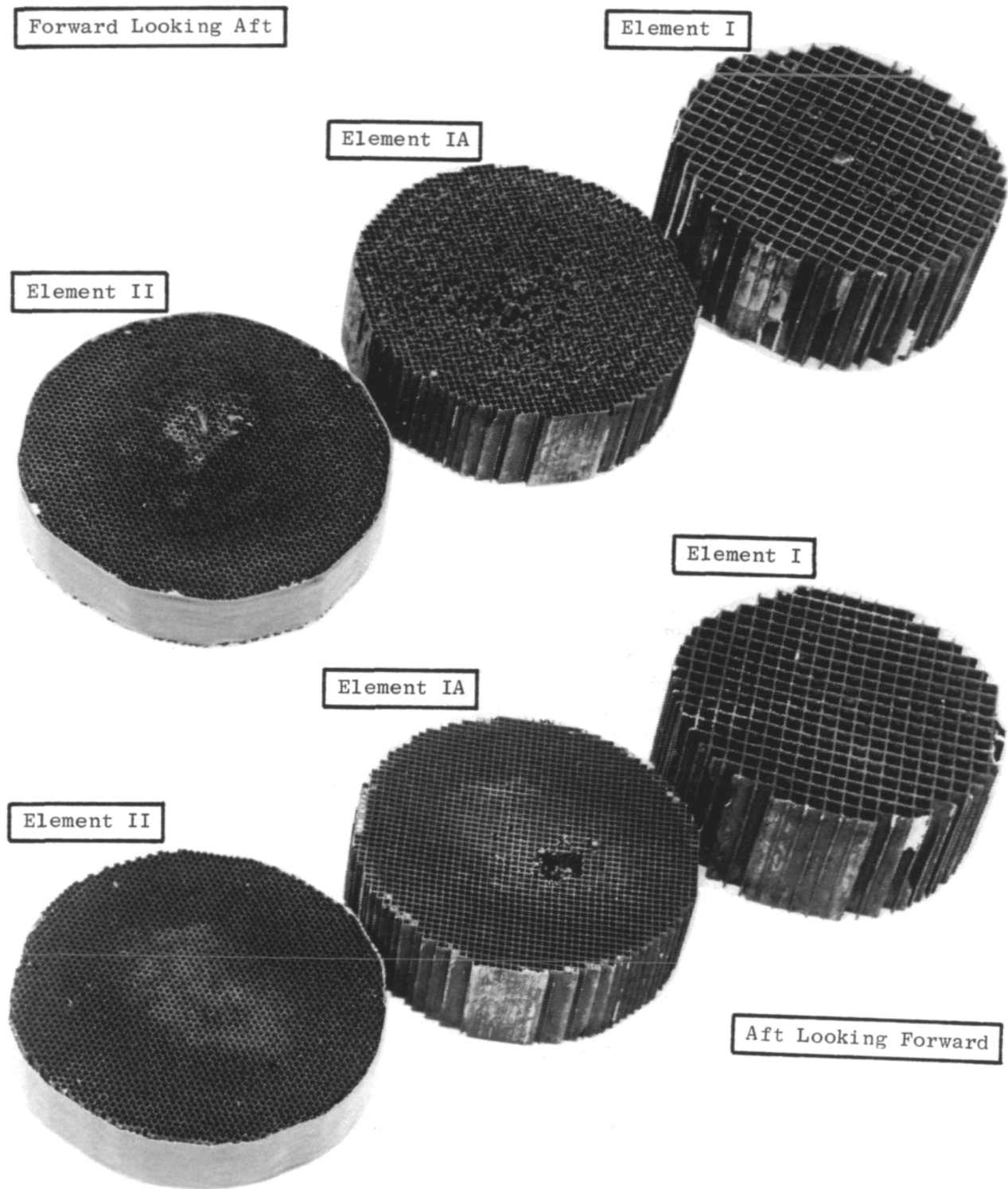


Figure 40. Postrun Photograph of Second Backup Reactor Elements.

The catalyst inlet fuel/air ratio profile was center-peaked at all operating conditions, as evidenced by measured radial temperature profiles within and downstream of the catalytic reactor (see Figure 23) and high local fuel/air ratios determined through analyses of gas samples obtained on the duct centerline downstream of the catalytic reactor. The ratio of the fuel/air ratio determined from the gas sample (f_{sample}) to the overall fuel/air ratio calculated from measured fuel and air flows (f_{metered}) was used throughout the test series as a measure of the fuel/air mixture nonuniformity at the catalytic reactor inlet. Measured temperatures on the catalytic reactor centerline within and just downstream of the aft reactor element compared well with predicted temperature based on gas-sample fuel/air ratio, indicating that little radial mixing occurs between the reactor exit and the sampling point. The ratio of gas-sample to metered fuel/air ratios is therefore thought to be representative of profiles within the reactor.

In initial tests using Jet A fuel at the design reference velocity, peak fuel/air ratios 10 to 20% above the average were indicated. After transition to No. 6 oil, the peak increased to about 40% above the average. As shown in Figure 41, uniformity was also quite sensitive to reference velocity, with the peak fuel/air ratio increasing to about 80% above the average at a reference velocity of 30 m/s.

Initial drop size also had a strong effect on mixture uniformity, as indicated in Figure 42. As droplet size increased, the mixture became much more uniform. It is thought that this effect was due primarily to the reduction in atomizing airflow and air velocity as drop size is increased. In the small-drop, air-atomizing mode the high-velocity atomizing air penetrates the main stream. This improves the initial fuel dispersion and mixing. But in the large-drop, pressure-atomizing mode the momentum of the fuel spray did not appear to be sufficient to penetrate into the main stream.

Fuel-preparation-system pressure drop is shown in Figure 43. At the design point, total pressure drop was less than 1.4%. This pressure drop was due mainly to the blockage of the perforated plate mounted in the pre-mixing-section inlet (Figures 2 and 10).

The entire fuel/air mixture-preparation system remained in excellent condition throughout the test series. A very thin coating of carbon was apparent at the fuel-injector exit and on the perforated plate, but no significant carbon buildup occurred.

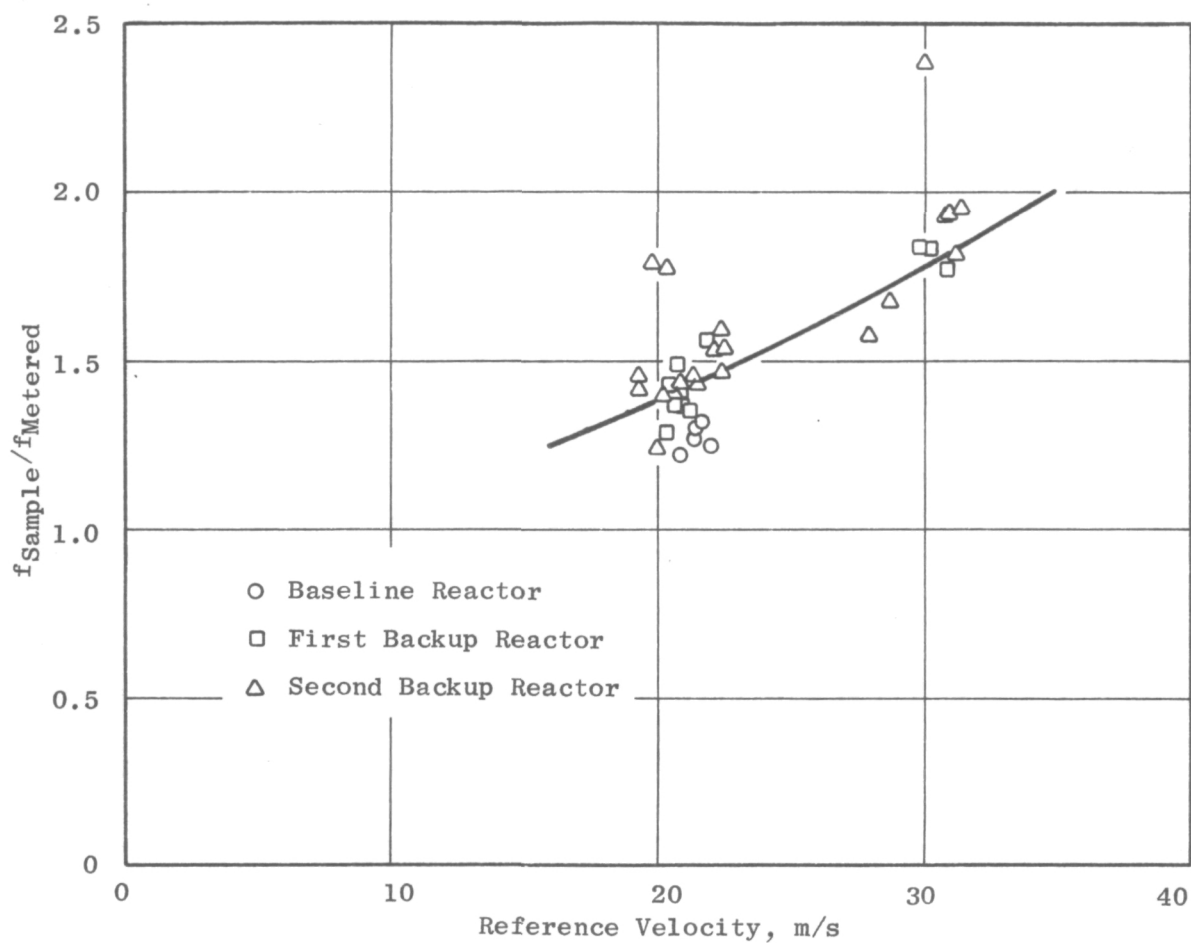


Figure 41. Effect of Reference Velocity on Fuel/Air Mixture Uniformity (No. 6 Oil).

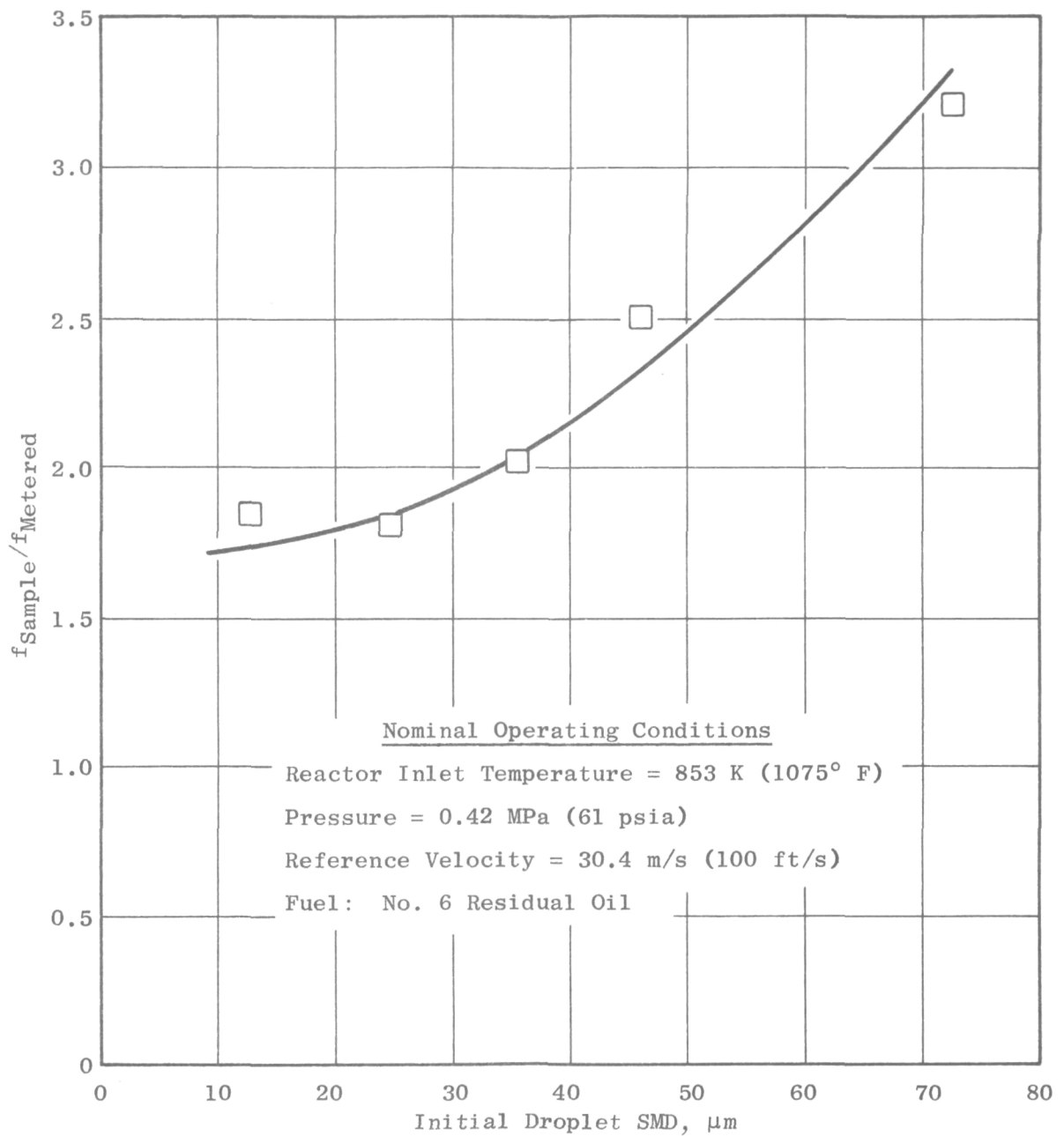


Figure 42. Effect of Initial Drop Size on Fuel/Air Mixture Uniformity (First Backup Reactor).

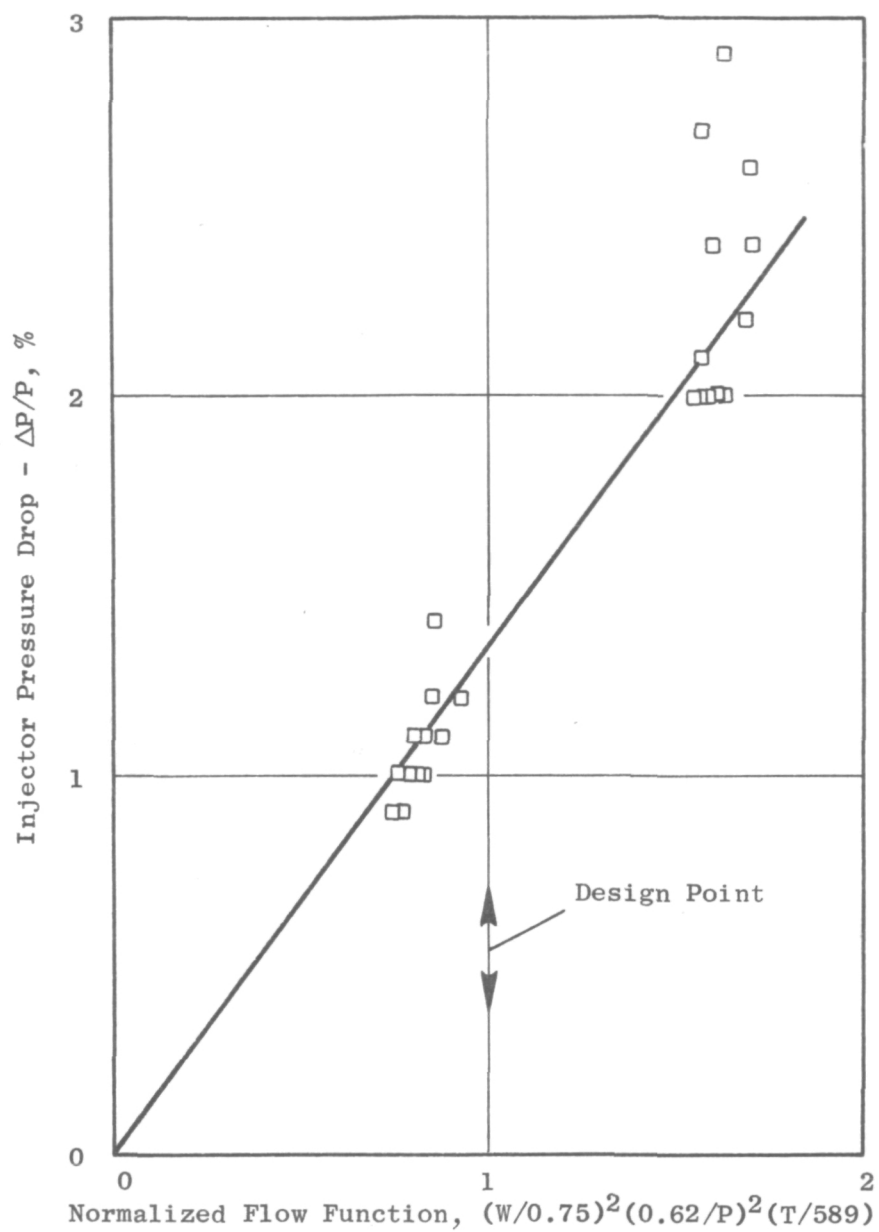


Figure 43. Fuel-Preparation-System Pressure Drop (First Backup Reactor).

6.0 CONCLUDING REMARKS

The stated objectives of this experimental program were to demonstrate lean catalytic combustion of a residual fuel oil, to determine if catalytic reactor performance is affected by incomplete fuel vaporization, and to determine if fuel-droplet size influences performance. Initially, the program was planned as a fairly straightforward demonstration of catalytic combustion at operating conditions typical of a large, industrial-gas-turbine combustor. However, due to operating difficulties with the residual fuel, it evolved into more of an exploratory test program to define and extend the range of catalytic combustor operation on the residual oil.

Steady-state operation on residual oil was successfully demonstrated. The combustion efficiency ($>99.5\%$) and pressure drop ($<5\%$) design goals were both met with considerable margins. However, the catalytic reactor operating range was rather narrow due to unsteady operation and/or reactor plugging as temperature was reduced.

Progress in extending the catalytic reactor operating range was made by increasing the catalyst channel diameters while also increasing reactor length to maintain performance, but operation at the original 589 K (600°F) design point was not obtained. Operation was demonstrated only at temperatures above 700 K (800°F).

The effects of incomplete fuel vaporization and variation in fuel-droplet size at the catalytic reactor inlet were not clearly demonstrated during this program. Initial fuel-droplet size was varied; however, at the inlet temperature levels required to maintain steady-state combustion with the residual oil, it is thought that the fuel-vaporization process was essentially complete over the range of initial drop sizes tested. Therefore, no strong fuel-atomization effects were to be expected, and none were observed.

One possible conclusion based on these test results is that residual oil must be completely vaporized (or completely devolatilized) to permit catalytic reactor operation. When vaporization is less than complete, droplets of thick, tar-like, partially evaporated fuel apparently impinge on and adhere to the reactor surface. If only a small proportion of the fuel is unvaporized, these droplets will vaporize on the reactor surface. But as the unvaporized proportion increases the rate of droplet deposition becomes greater than the rate of surface vaporization, and reactor plugging occurs. Thus, in this program, the catalytic reactor inlet temperature had to be well above the original 589 K (600°F) design value to maintain steady-state operation.

In terms of operation in an actual industrial-gas-turbine combustor, the high reactor inlet temperature required to successfully operate on residual oil would require the use of either a regenerator or a conventional preburner to increase the compressor exit temperature to the required level.

The fuel/air mixture-preparation system performed reliably throughout the test series. Improved mixture uniformity would be expected to result in better catalytic reactor performance and an increased operating range. The single-point injector system employed in this program was used with virtually no pre-test development. Significantly improved performance is expected with additional injector development. Fairly simple modifications, such as increasing the atomizing-air swirl angle or tailoring the inlet-velocity profile by changing the hole pattern in the perforated plate at the mixing-section inlet, should be sufficient to meet the design uniformity goal.

While the results of this study have shown that residual oil can be burned in a catalytic reactor, there are many more questions to be answered before this concept can be used in an actual gas-turbine-engine application. First, the long-term durability of a combustion catalyst operating on residual oil must be demonstrated. In the relatively short tests conducted in this program (the longest total operating time on any single reactor was about 13 hours on the second backup reactor), all of the catalytic reactors were damaged to some degree. This was not unexpected; it was the nature of the tests to operate at successively more difficult conditions until a limiting condition was observed. The limiting condition was usually defined by incomplete or partial coating and plugging of the reactor with the residual fuel. In each case, after plugging occurred, the coating of residual fuel burned off within a few minutes. It is believed that most of the observed damage to the catalytic reactor was the result of high local surface temperatures that occurred as the coating burned off. However, additional endurance testing would be required to determine if physical damage (erosion) to the substrate will occur during long-term, steady-state operation.

Catalyst poisoning during long-term operation must also be considered. One of the common metals found in residual oils is vanadium. Vanadium oxides created in the combustion process are extremely corrosive to hot turbine parts. Vanadium occurs in metal-organic compounds that are soluble in residual oil and practically cannot be removed. In order to control corrosion, magnesia or silica can be added to the fuel to raise the fusion point of the vanadium oxides. This generates large quantities of ash that deposit on surfaces within the engine and must be removed periodically. These deposits may also affect the combustion catalyst during extended operation.

The primary reason for using catalytic combustion is to achieve ultralow NO_x emissions. Levels of thermal NO_x measured during operation on Jet A fuel were extremely low. However, essentially 100% conversion of fuel-bound nitrogen to NO_x was observed during operation on residual oil.

In conclusion, lean catalytic combustion has shown some promise as a means of burning residual oil, but the demonstrated inlet temperature range for acceptable performance is not compatible with typical large industrial gas turbines. Significant additional development effort would be required to either extend the catalytic reactor operating range or to modify the engine (regenerative cycle) or combustor (preburner) to increase catalytic reactor inlet temperatures. Based on the results of this program, the required

increase in catalytic reactor operating range is unlikely to be obtained through reactor development alone. The use of a preburner or regenerative cycle to increase catalytic reactor inlet temperature appears to be more promising.

Before starting on any catalytic combustor development program, additional small-scale work should be conducted. Specific goals of this work would be: (1) to refine the fuel/air mixture-preparation system design to ensure reliable operation while providing more uniform fuel/air mixture and (2) to demonstrate long-term catalytic reactor durability without erosion or catalyst poisoning.

In consideration of the high conversion of fuel-bound nitrogen to NO_x , the environmental benefits of lean catalytic combustion of residual oil should be evaluated before any further work is conducted. The practicality of using residual oil in terms of cost and fuel availability should also be considered.

The above discussion applies primarily to the development of a gas turbine system specifically designed for operation on residual oil. A second possibility is the use of residual oils to temporarily supplement distillate fuels during a fuel shortage. Based on the results of this program, it is unlikely that a pure residual oil would work without major combustion-system modifications in a catalytic combustion system designed for distillate fuel. However, the case of residual/distillate blends could be a practical means to extend the available fuel supply. As practical catalytic combustion systems are designed and developed, the ability to use fuel blends containing residual oils should be considered.

APPENDIX A

TEST DATA SUMMARY

A total of eight test runs were conducted during this program; a total of 81 test readings were obtained. Detailed data for the baseline catalytic reactor are presented in Tables XV through XVIII. Data obtained with the first backup reactor are presented in Tables XIX through XXII, and test results with the second backup reactor are presented in Tables XXIII through XXVI. Reactor exit temperatures reported in these tables were measured with sheathed chromel-alumel thermocouples and are not corrected for radiation. Temperature corrections at the three stations in the exit section, for two different reference velocity levels, are shown in Figures 44 and 45.

● Baseline Reactor, Single-Point Injector

Table XV. Test Summary, Run 1.

Date: 9/18/80		Reactor Inlet Conditions						Injector Conditions							Calculations							
Reading Number	Test Fuel, % No. 6 Residual Oil (Remainder is Jet A)	W_C - Airflow, kg/s	$T_{1.5}$ - Calculated Temperature, K	$T_{1.5}$ - Measured Temperature, K	$P_{1.9}$ - Pressure, MPa	f_m - Metered Fuel/Air Ratio, g/kg	h - Humidity, g/kg	W_{AA} - Atomizing Airflow, kg/s	$T_{1.0}$ - Centerline Temperature, K	$T_{1.0}$ - Main-Stream Temperature at $r = 5$ cm, K	T_{AA} - Atomizing-Air Temperature, K	ΔP_{AA} - Atomizing-Air Pressure Drop, MPa	T_f - Fuel Temperature, K	ΔP_f - Fuel Pressure Drop, MPa	V_r - Reference Velocity, m/s	SMD - Calculated Fuel-Drop Size, μm	EICO - Carbon Monoxide Emission Index, g/kg	EIHC - Hydrocarbons Emission Index, g/kg	$EINO_x$ - Oxides of Nitrogen Emission Index, g/kg	f_s - Sample Fuel/Air Ratio, g/kg	η_g - Sample Combustion Efficiency, %	η_{tc} - Thermocouple Combustion Efficiency, %
1	Dry Loss	0.403	727	725	0.412	-	-	0.026	756	753	308	0.095	379	0.0	19.90	< 5	-	-	-	-	-	-
2	0	0.403	733	730	0.420	17.5	-	0.027	764	760	309	0.097	398	0.024	19.71	< 5	2.8	0.7	-	19.28	99.87	110.0
3	-	0.404	725	724	0.412	17.5	-	0.027	756	756	307	0.101	399	-	19.92	< 5	3.2	0.4	-	20.30	99.89	105.1
4	26	0.408	781	777	0.405	17.9	-	0.027	815	821	304	0.097	395	-	22.05	< 5	0.8	0.8	-	23.03	99.91	113.0
5*	42	0.407	771	778	0.375	17.3	-	0.024	800	812	302	0.084	393	0.048	23.39	< 5	0.6	0.4	-	22.64	99.95	116.4
6*	48	0.410	779	777	0.451	13.0	-	0.025	811	809	301	0.081	400	-	19.81	< 5	13.3	0.5	-	16.97	99.66	101.2
*Pressure Fluctuating																						

Table XVI. Temperatures and Exhaust-Gas Concentrations, Run 1.

Reading Number	ΔP_{fi} - Fuel Injector Pressure Drop, %	ΔP_c - Catalytic Reactor Pressure Drop, %	CO - Carbon Monoxide Concentration, ppm	CO ₂ - Carbon Dioxide Concentration, %	HC - Unburned Hydrocarbons Concentration, ppm	NO _x - Oxides of Nitrogen Concentration, ppm														
							Station	T _c - Reactor Substrate Temperature, K						T _{ex} - Reactor Exit Temperature, K (Uncorrected)						
								Radius, cm	2.0			2.5	3.0		3.1			4.0		4.1
								0.0	2.5	5.0	0.0	0.0	5.0	0.0	2.5	5.0	1.9	1.9	0.0	1.9
1	1.1	2.1	-	-	-	-		-	-	-	822	787	785	720	723	669	719	717	716	717
2	1.0	3.1	56.8	4.09	24.2	-		-	-	-	1416	1438	1127	1291	1266	747	1236	1235	1227	1271
3	1.1	3.4	68.2	4.34	16.1	-		-	-	-	1385	1432	1070	1266	1230	762	1234	1232	1200	1234
4	1.0	4.0	19.1	4.94	32.0	-		-	-	-	1598	1588	1106	1376	1311	777	1314	1301	1297	1354
5	1.2	4.8	15.0	4.86	16.1	-		-	-	-	1605	1587	1080	1380	1287	802	1316	1268	1273	1353
6	0.8	3.9	237.2	3.60	8.1	-		-	-	-	1337	1422	1030	1229	1088	834	1191	1129	1126	1217

Table XVII. Test Summary, Run 2.

● Baseline Reactor, Single-Point Injector

Date: 10/1/80

Date: 10/1/80		Reactor Inlet Conditions						Injector Conditions							Calculations									
Reading Number	Test Fuel, % No. 6 Residual Oil (Remainder is Jet A)	W_C - Airflow, kg/s	$T_{1.5}$ - Calculated Temperature, K	$T_{1.5}$ - Measured Temperature, K	$P_{1.9}$ - Pressure, MPa	f_m - Metered Fuel/Air Ratio, g/kg	h - Humidity, g/kg	W_{AA} - Atomizing Airflow, kg/s	$T_{1.0}$ - Centerline Temperature, K	$T_{1.0}$ - Main-Stream Temperature at $r = 5$ cm, K	T_{AA} - Atomizing-Air Temperature, K	ΔP_{AA} - Atomizing-Air Pressure Drop, MPa	T_f - Fuel Temperature, K	ΔP_f - Fuel Pressure Drop, MPa	V_r - Reference Velocity, m/s	SMD - Calculated Fuel-Drop Size, μm	EICO - Carbon Monoxide Emission Index, g/kg	EIHC - Hydrocarbons Emission Index, g/kg	E_{INO_x} - Oxides of Nitrogen Emission Index, g/kg	f_s - Sample Fuel/Air Ratio, g/kg	η_g - Sample Combustion Efficiency, %	η_{tc} - Thermocouple Combustion Efficiency, %		
7	Dry Loss	0.381	779	767	0.404	0.0	1.3	0.024	812	808	296	79.2	-	-	20.54	< 5	-	-	-	-	-	-		
8	0	0.382	777	773	0.418	11.2	1.3	0.027	813	810	299	94.1	315	-	19.86	< 5	363.6	23.2	0.30	12.6	89.49	96.2		
9	0	0.382	778	776	0.416	12.8	1.3	0.027	815	812	300	95.8	317	-	19.99	< 5	147.1	2.1	0.15	14.4	96.39	101.7		
10	50	0.386	790	794	0.420	15.1	1.3	0.027	828	825	303	97.9	389	-	20.33	< 5	7.2	1.0	3.91	16.9	99.75	109.1		
11	75	0.385	776	-	0.414	-	1.3	0.027	-	-	-	94.8	-	-	20.17	12.5	-	-	-	-	-	-		
12	0	0.369	847	832	0.411	10.4	1.3	0.015	870	866	305	34.5	412	-	21.28	< 5	7.8	1.2	0.14	15.6	99.71	117.3		
13	50	0.369	843	836	0.429	11.5	1.3	0.015	865	863	305	31.8	413	-	20.30	< 5	3.4	0.7	3.25	17.7	99.86	121.7		
14	100	0.370	843	808	0.414	15.2	1.3	0.015	866	863	305	33.9	411	-	21.04	20.7	5.6	1.2	7.14	17.9	99.76	101.3		
15	100	0.382	825	806	0.424	14.4	1.3	0.027	864	862	304	93.5	411	-	20.81	11.0	5.0	1.0	7.61	17.5	99.79	103.7		
16	100	0.535	838	-	0.414	-	1.3	0.027	-	-	-	94.8	411	-	30.31	-	5.8	1.4	5.81	18.3	99.74	-		
17	100	0.384	822	808	0.413	14.0	1.3	0.026	-	861	303	93.8	411	-	21.40	10.9	5.2	1.3	7.26	17.9	99.76	114.1		
18	100	0.384	823	-	0.413	12.9	1.3	0.026	862	859	302	93.1	411	-	21.44	10.5	17.2	0.7	7.12	16.7	99.53	93.7		
19	100	0.385	824	825	0.410	11.9	1.3	0.026	862	860	302	93.5	411	-	21.63	10.0	83.2	0.8	6.94	15.6	97.93	86.0		
20	100	0.385	824	814	0.403	10.8	1.3	0.026	863	860	302	94.5	411	-	21.98	9.4	412.9	18.7	5.38	13.4	88.51	82.1		

Table XVIII. Temperatures and Exhaust-Gas Concentrations, Run 2.

Reading Number	ΔP_{fi} - Fuel Injector Pressure Drop, %	ΔP_c - Catalytic Reactor Pressure Drop, %	CO - Carbon Monoxide Concentration, ppm	CO ₂ - Carbon Dioxide Concentration, %	HC - Unburned Hydrocarbons Concentration, ppm	NO _x - Oxides of Nitrogen Concentration, ppm		T _c - Reactor Substrate Temperature, K						T _{ex} - Reactor Exit Temperature, K (Uncorrected)							
								Station	2.0			2.5	3.0		3.1			4.0		4.1	
									Radius, cm	0.0	2.5	5.0	0.0	0.0	5.0	0.0	2.5	5.0	1.9	1.9	0.0
7	1.1	2.8	-	-	-	-	Catalytic Reactor Plugged	775	783	786	773	767	777	755	763	724	754	754	749	752	
8	1.0	3.3	4767.1	2.13	520.3	2.4		1030	947	911	1148	1212	985	1124	1053	874	1094	1030	1023	1118	
9	0.9	3.1	2216.4	2.83	53.3	1.3		1066	975	932	1208	1289	1014	1191	1107	896	1165	1087	1085	1187	
10	0.9	4.2	126.7	3.60	29.1	40.9		1074	969	942	1331	1409	1058	1275	1233	944	1274	1224	1193	1277	
11	-	-	-	-	-	-		-	-	-	-	-	-	-	-	-	-	-	-	-	
12	1.0	5.4	126.7	3.29	33.9	1.3		667	1249	920	1111	1361	986	1228	1144	893	1189	1152	1127	1218	
13	0.9	5.6	63.1	3.78	22.6	35.6		1195	1301	930	1123	1422	1001	1284	1179	911	1230	1182	1170	1265	
14	1.0	5.7	104.6	3.87	38.1	79.1	Catalytic Reactor Plugged	676	975	974	-	-	-	1285	1245	973	1228	1223	1190	1246	
15	1.0	6.5	91.6	3.78	32.0	82.4		-	1025	979	1036	1361	1124	1235	1243	1000	1266	1254	1228	1263	
16	-	~ 14.	110.5	3.96	45.2	65.9		-	-	-	-	-	-	-	-	-	-	-	-	-	
17	1.1	6.9	97.4	3.87	41.7	80.4		-	1192	987	1057	1434	1128	1281	1253	1018	1258	1256	1234	1261	
18	1.1	6.9	300.6	3.60	21.0	73.8		-	1123	949	997	1259	1115	1135	1185	1002	1229	1233	1207	1238	
19	1.2	6.9	1354.5	3.25	22.6	67.2		-	1099	948	976	1206	1064	1073	1143	971	1186	1211	1176	1191	
20	1.1	7.1	5759.3	3.28	446.7	44.8		-	981	942	960	1231	1034	1035	1105	949	1096	1145	1129	1103	

Table XIX. Test Summary, Run 3.

• First Backup Reactor, Single-Point Injector

Date: 10/7/80

Reading Number	Test Fuel, % No. 6 Residual Oil (Remainder is Jet A)	Reactor Inlet Conditions						Injector Conditions						Calculations								
		W_c - Airflow, kg/s	$T_{1.5}$ - Calculated Temperature, K	$T_{1.5}$ - Measured Temperature, K	$P_{1.9}$ - Pressure, MPa	f_m - Metered Fuel/Air Ratio, g/kg	h - Humidity, g/kg	W_{AA} - Atomizing Airflow, kg/s	$T_{1.0}$ - Centerline Temperature, K	$T_{1.0}$ - Main-Stream Temperature at $r = 5$ cm, K	T_{AA} - Atomizing-Air Temperature, K	ΔP_{AA} - Atomizing-Air Pressure Drop, MPa	T_f - Fuel Temperature, K	ΔP_f - Fuel Pressure Drop, MPa	V_r - Reference Velocity, m/s	SMD - Calculated Fuel-Drop Size, μm	EICO - Carbon Monoxide Emission Index, g/kg	EIHC - Hydrocarbons Emission Index, g/kg	EINO _x - Oxides of Nitrogen Emission Index, g/kg	f_s - Sample Fuel/Air Ratio, g/kg	η_g - Sample Combustion Efficiency, %	η_{tc} - Thermocouple Combustion Efficiency, %
21	Dry Loss	0.383	829	819	0.414	0.0	1.30	0.026	868	861	292	86.0	-	-	21.47	-	-	-	-	-	-	-
22	0	0.384	830	823	0.420	11.8	1.30	0.026	869	866	294	91.1	300	-	21.20	< 5	20.0	0.9	0.04	14.45	99.46	120.9
23	0	0.383	798	793	0.385	11.12	1.30	0.026	834	832	295	91.1	300	-	22.15	< 5	12.6	0.6	0.03	15.03	99.65	119.9
24	Dry Loss	0.391	816	806	0.421	0.0	0.76	0.027	855	852	288	94.5	-	-	21.23	-	-	-	-	-	-	-
25	0	0.388	836	831	0.412	11.06	0.76	0.027	876	872	292	93.1	300	-	22.01	< 5	10.6	0.7	0.03	14.90	99.69	138.6
26	0	0.386	825	824	0.414	12.75	0.79	0.027	866	863	294	95.5	401	-	21.54	< 5	13.1	0.4	0.03	14.91	99.66	86.3
27	50	0.384	822	827	0.423	12.45	0.89	0.026	862	859	296	90.1	404	-	20.87	< 5	16.4	0.3	3.64	15.22	99.59	118.8
28	100	0.382	828	824	0.430	11.20	1.14	0.027	868	865	300	93.1	405	-	20.58	9.6	62.8	0.2	7.98	15.33	98.47	135.4
29	100	0.381	829	962*	0.436	9.81	1.14	0.026	869	866	300	89.7	407	-	20.27	9.1	414.3	8.1	5.85	12.70	89.38	128.6
30	100	0.381	829	823	0.410	11.06	1.14	0.027	870	867	300	97.5	405	-	21.56	9.3	79.7	0.4	7.57	14.45	98.06	134.9
31	100	0.381	829	936*	0.421	12.15	1.14	0.027	870	867	301	95.8	404	-	21.03	9.8	7.8	0.1	5.47	16.54	99.80	139.8
32	100	0.405	765	719	0.410	13.34	1.14	0.027	798	800	301	93.1	405	-	21.15	10.8	8.0	0.6	7.69	18.02	99.76	107.0
33	100	0.542	841	827	0.421	9.36	1.14	0.027	869	866	303	93.6	403	-	30.33	10.5						148.7
34	100	0.538	844	810	0.421	9.04	1.14	0.022	868	865	304	67.7	403	-	30.20	12.6						149.0
35	100	0.531	850	867	0.421	8.92	1.14	0.015	866	864	305	33.7	403	-	30.00	18.9	Sampling Probe Failed					134.2
36	100	0.526	854	795	0.421	8.42	1.14	0.011	865	863	305	17.3	403	-	29.87	26.6						144.3
37	100	0.523	856	820	0.421	6.51	1.14	0.007	864	862	306	8.5	403	-	29.79	34.4						145.1

*Temperature Increased by Reaction Upstream of Catalytic Reactor

Table XX. Temperatures and Exhaust-Gas Concentrations, Run 3.

Reading Number	ΔP_{fi} - Fuel Injector Pressure Drop, %	ΔP_c - Catalytic Reactor Pressure Drop, %	CO - Carbon Monoxide Concentration, ppm	CO ₂ - Carbon Dioxide Concentration, %	HC - Unburned Hydrocarbons Concentration, ppm	NO _x - Oxides of Nitrogen Concentration, ppm														
							T _c - Reactor Substrate Temperature, K							T _{ex} - Reactor Exit Temperature, K (Uncorrected)						
							Station	2.0			2.5	3.0		3.1			4.0		4.1	
							Radius, cm	0.0	2.5	5.0	0.0	0.0	5.0	0.0	2.5	5.0	1.9	1.9	0.0	1.9
21	1.1	2.0	-	-	-	-		825	828	833	812	817	819	803	805	744	806	799	796	798
22	1.0	2.8	302.5	3.03	22.4	0.4		938	964	952	1214	1363	1023	1234	1185	952	1163	1160	1168	1226
23	1.2	3.3	198.0	3.16	17.0	0.3		907	937	921	1190	1345	1003	1202	1156	912	1116	1132	1147	1205
24	1.0	2.2	-	-	-	-		812	818	822	819	813	817	794	799	772	794	789	785	790
25	1.1	3.0	165.4	3.14	19.2	0.3		954	972	967	1220	1361	1050	1276	1257	1029	1209	1201	1187	1249
26	1.1	2.9	204.3	3.14	9.6	0.3		938	957	961	1217	1357	1064	1239	1202	1017	1158	1148	1150	1214
27	1.0	2.8	260.7	3.22	8.0	34.3		893	932	944	1183	1351	1061	1231	1244	1022	1167	1168	1168	1223
28	0.9	2.7	1003.2	3.22	6.4	75.9		884	916	921	1130	1332	1045	1225	1286	1024	1127	1221	1199	1207
29	0.9	2.5	5474.9	2.19	182.5	46.2		893	901	913	1084	1240	1019	1138	1234	993	1068	1166	1157	1164
30	1.1	2.9	1199.7	3.01	9.9	68.0		885	907	917	1118	1330	1042	1212	1288	1014	1122	1214	1195	1202
31	1.0	2.8	135.1	3.58	2.9	56.1		896	921	930	1159	1401	1075	1273	1338	1055	1175	1267	1245	1241
32	1.1	2.9	150.1	3.90	17.6	85.8		854	893	861	1100	1322	1010	1201	1150	979	1105	1186	1179	1193
33	2.0	4.9	Sampling Probe Failed					880	899	900	1148	1388	987	1258	1210	964	1175	1058	960	1198
34	2.0	4.8						885	898	898	1136	1393	989	1267	1168	961	1193	1103	996	1210
35	2.0	4.6						916	919	904	1124	1388	1009	1268	1105	977	1204	1092	1022	1199
36	2.0	4.4						948	943	897	1136	1393	972	1269	1122	949	1192	1070	1006	1198
37	2.0	4.3						877	938	884	1090	1328	919	1187	1057	909	1106	957	906	1169

Table XXI. Test Summary, Run 4.

• First Backup Reactor, Single-Point Injector

Date: 10/17/80

Date: 10/17/80		Reactor Inlet Conditions						Injector Conditions							Calculations								
Reading Number	Test Fuel, % No. 6 Residual Oil (Remainder is Jet A)	W_C - Airflow, kg/s	$T_{1.5}$ - Calculated Temperature, K	$T_{1.5}$ - Measured Temperature, K	$P_{1.9}$ - Pressure, MPa	f_m - Metered Fuel/Air Ratio, g/kg	h - Humidity, g/kg	W_{AA} - Atomizing Airflow, kg/s	$T_{1.0}$ - Centerline Temperature, K	$T_{1.0}$ - Main-Stream Temperature at $r = 5$ cm, K	T_{AA} - Atomizing-Air Temperature, K	ΔP_{AA} - Atomizing-Air Pressure Drop, MPa	T_f - Fuel Temperature, K	ΔP_f - Fuel Pressure Drop, MPa	V_r - Reference Velocity, m/s	SMD - Calculated Fuel-Drop Size, μm	EICO - Carbon Monoxide Emission Index, g/kg	EIHC - Hydrocarbons Emission Index, g/kg	EINO _x - Oxides of Nitrogen Emission Index, g/kg	f_s - Sample Fuel/Air Ratio, g/kg	η_g - Sample Combustion Efficiency, %	η_{tc} - Thermocouple Combustion Efficiency, %	
38	100	0.384	832	825	0.436	0.0	0.97	0.023	867	863	293	92.8	-	-	20.50	-	-	-	-	-	-	-	
39	100	0.382	834	865*	0.430	12.19	0.97	0.024	869	867	298	99.9	405	-	20.72	11.6	4.4	1.3	8.35	18.21	99.79	135.6	
40	100	0.381	827	819	0.405	10.99	0.97	0.022	860	861	297	94.8	405	-	21.78	11.5	6.7	0.9	8.08	17.09	99.77	130.0	
41	100	0.537	846	886*	0.420	9.81	0.97	0.023	871	868	299	95.2	405	-	30.30	12.9	6.7	0.4	7.85	18.01	99.81	130.0	
42	100	0.538	841	808	0.410	8.16	0.83	0.022	865	862	298	93.8	405	-	30.87	11.8	345.6	7.2	6.45	14.46	91.10	102.3	
43	100	0.539	841	794	0.424	8.96	0.83	0.022	864	862	298	89.1	405	-	29.88	12.8	38.5	0.6	7.85	16.51	99.03	119.3	
44	100	0.530	848	793	0.421	9.22	0.79	0.012	860	859	299	30.3	406	-	29.86	24.7	19.8	0.5	7.95	16.57	99.48	119.4	
45	100	0.526	855	915*	0.420	8.88	0.79	0.008	864	862	300	15.2	406	-	29.97	35.4	8.3	0.5	8.54	17.94	99.76	139.5	
46	100	0.524	861	836	0.406	6.78	0.79	0.006	867	865	301	7.5	408	-	31.09	45.9	14.6	0.5	8.53	16.94	99.61	146.2	
47	100	0.522	866	844	0.403	5.58	0.71	0.003	869	867	302	2.5	409	-	31.34	72.5	8.8	0.5	8.67	17.90	99.75	192.1	
48	100	0.376	778	734	0.402	13.54	0.79	0.022	808	806	294	90.8	402	-	20.36	13.1	4.1	0.5	7.87	19.19	99.86	121.5	
49	100	0.384	778	739	0.400	12.02	0.71	0.022	808	806	294	90.8	402	-	20.89	12.4	23.8	0.5	6.73	17.05	99.39	118.2	
50	100	0.374	793	713	0.400	13.90	0.71	0.012	-	810	296	33.9	401	-	20.77	24.2	3.6	0.5	8.05	19.59	99.88	104.5	
*Temperature Increased by Reaction Upstream of Catalytic Reactor																							

Table XXII. Temperatures and Exhaust-Gas Concentrations, Run 4.

Reading Number	ΔP_{fi} - Fuel Injector Pressure Drop, %	ΔP_c - Catalytic Reactor Pressure Drop, %	CO - Carbon Monoxide Concentration, ppm	CO ₂ - Carbon Dioxide Concentration, %	HC - Unburned Hydrocarbons Concentration, ppm	NO _x - Oxides of Nitrogen Concentration, ppm		T _c - Reactor Substrate Temperature, K						T _{ex} - Reactor Exit Temperature, K (Uncorrected)							
								Station	2.0			2.5	3.0		3.1			4.0		4.1	
								Radius, cm	0.0	2.5	5.0	0.0	0.0	5.0	0.0	2.5	5.0	1.9	1.9	0.0	1.9
38	1.0	2.3	-	-	-	-		-	829	831	824	819	819	804	813	799	803	806	799	799	
39	0.9	2.9	82.9	3.94	41.5	94.2		-	902	921	1182	1422	1073	1321	1272	1060	1288	1224	1211	1275	
40	1.4	3.1	119.1	3.69	25.9	85.6		-	902	904	1115	1356	1034	1270	1189	1017	1235	1160	1170	1250	
41	2.9	5.4	126.5	3.90	11.3	87.6		-	882	890	1093	1401	989	1301	1135	979	1258	1156	1189	1279	
42	2.6	5.6	5208.2	2.60	184.2	58.0		-	880	881	1059	1230	945	1129	1040	937	1119	1032	1051	1198	
43	2.4	5.3	663.2	3.51	16.2	80.4		-	877	884	1046	1307	958	1226	1093	948	1186	1091	1118	1240	
44	2.7	5.1	343.1	3.56	16.2	81.7		-	892	890	1093	1339	958	1238	1100	956	1238	1108	1179	1262	
45	2.1	4.9	156.4	3.88	15.2	94.9		-	909	886	1144	1423	940	1295	1138	942	1251	1197	1213	1293	
46	2.2	5.0	258.7	3.65	14.6	89.6		-	914	884	1138	1399	904	1264	1041	910	1182	1048	1118	1259	
47	2.4	4.9	164.0	3.87	14.6	96.2		-	892	878	1184	1450	893	1313	1053	899	1207	1049	1090	1269	
48	1.1	3.6	82.9	4.16	16.2	93.5		-	844	882	1077	1378	1038	1263	1231	998	1231	1244	1228	1257	
49	1.2	4.0	423.6	3.66	15.9	71.1		-	831	861	1043	1302	1013	1210	1163	977	1146	1118	1179	1210	
50	-	-	72.9	4.25	16.2	97.5		-	-	-	-	-	-	1310	1096	909	-	-	-	-	

Table XXIII. Test Summary, Run 5.

o Second Backup Reactor, Single-Point Injector

Date: 2/4/81

Reading Number	Test Fuel, % No. 6 Residual Oil (Remainder is Jet A)	Reactor Inlet Conditions						Injector Conditions						Calculations								
		W_C - Airflow, kg/s	$T_{1.5}$ - Calculated Temperature, K	$T_{1.5}$ - Measured Temperature, K *	$P_{1.9}$ - Pressure, MPa	f_m - Metered Fuel/Air Ratio, g/kg	h - Humidity, g/kg	W_{AA} - Atomizing Airflow, kg/s	$T_{1.0}$ - Centerline Temperature, K	$T_{1.0}$ - Main-Stream Temperature at $r = 5$ cm, K	T_{AA} - Atomizing-Air Temperature, K	ΔP_{AA} - Atomizing-Air Pressure Drop, MPa	T_f - Fuel Temperature, K	ΔP_f - Fuel Pressure Drop, MPa	V_r - Reference Velocity, m/s	SMD - Calculated Fuel-Drop Size, μm	EICO - Carbon Monoxide Emission Index, g/kg	EIHC - Hydrocarbons Emission Index, g/kg	EINO _x - Oxides of Nitrogen Emission Index, g/kg	f_s - Sample Fuel/Air Ratio, g/kg	η_g - Sample Combustion Efficiency, %	η_{tc} - Thermocouple Combustion Efficiency, %
51	Dry Loss	0.398	826	-	0.394	0.0	1.20	0.027	864	869	282	94.1	-	-	23.39	-	-	-	-	-	-	-
52	Dry Loss	0.394	822	807	0.414	0.0	1.20	0.027	864	859	288	92.1	-	-	21.85	-	-	-	-	-	-	-
53	100	0.399	811	820	0.404	12.52	1.20	0.028	845	857	289	99.2	402	-	22.42	10.1	1.2	0.0	8.03	18.39	99.97	141.2
54	100	0.399	820	823	0.411	8.89	1.20	0.028	854	865	288	97.5	405	-	22.30	8.5	20.6	0.1	7.37	14.17	99.50	139.2
55	100	0.396	826	822	0.414	7.67	1.20	0.027	868	865	288	95.5	407	-	22.15	7.9	280.1	1.1	6.27	11.87	93.19	128.9
56	100	0.399	823	820	0.411	6.63	1.20	0.027	860	865	288	96.2	407	-	22.37	7.3	402.4	54.9	5.17	10.27	85.70	125.2
57	100	0.551	836	830	0.418	8.00	1.20	0.027	867	863	288	94.5	403	-	30.83	9.7	26.9	0.1	7.56	15.45	99.34	129.7
58	100	0.549	829	827	0.407	6.26	1.20	0.027	853	861	288	96.2	406	-	31.31	8.4	558.8	67.7	4.33	12.29	80.86	119.8
59	100	0.551	834	827	0.418	7.29	1.20	0.027	865	861	288	95.5	405	-	30.78	9.2	234.2	0.8	6.62	14.17	94.32	122.9
60	100	0.549	855	851	0.421	9.45	1.20	0.028	885	885	289	95.2	403	-	31.19	10.5	3.9	0.3	7.71	17.34	99.88	148.4
61	100	0.543	833	820	0.424	9.06	1.20	0.017	-	850	292	42.0	403	-	29.83	16.9	60.3	0.1	7.15	14.89	98.54	116.0
62	100	0.539	837	812	0.419	9.09	1.20	0.013	852	849	294	24.1	402	-	30.14	23.0	103.8	0.1	6.81	14.41	97.50	120.1
63	100	0.557	771	778	0.419	10.60	1.20	0.029	798	798	287	101.9	399	-	28.71	10.8	13.9	0.1	7.19	17.85	99.66	117.2
64	100	0.554	777	787	0.432	12.11	1.20	0.029	801	807	286	99.9	397	-	27.89	11.6	4.5	0.1	7.69	19.08	99.89	140.6
65	100	0.556	772	776	0.401	8.98	1.20	0.029	797	800	286	104.3	399	-	29.94	9.8	856.4	4.6	5.99	21.49	79.06	105.7
66	100	0.385	778	786	0.390	12.61	1.20	0.028	819	814	286	101.6	401	-	21.44	9.9	5.7	0.2	7.52	18.21	99.85	135.8
67	100	0.385	780	783	0.414	9.15	1.20	0.029	823	816	287	101.6	407	-	20.31	8.2	688.5	2.8	4.69	16.17	83.25	123.9
68	100	0.384	777	780	0.421	8.87	1.20	0.028	817	815	287	96.9	407	-	19.84	8.3	702.9	4.0	4.72	15.85	82.80	118.9

*Surface-Mounted Thermocouple

Table XXIV. Temperatures and Exhaust-Gas Concentrations, Run 5.

Reading Number	ΔP_{fi} - Fuel Injector Pressure Drop, %	ΔP_c - Catalytic Reactor* Pressure Drop, %	CO - Carbon Monoxide Concentration, ppm	CO ₂ - Carbon Dioxide Concentration, %	HC - Unburned Hydrocarbons Concentration, ppm	NO _x - Oxides of Nitrogen Concentration, ppm	T _c - Reactor Substrate Temperature, K														T _{ex} - Reactor Exit Temperature, K (Uncorrected)					
							Station	2.0			2.5	3.0		3.1			4.0		4.1							
								Radius, cm	0.0	2.5		5.0	0.0	0.0	5.0	0.0	2.5	5.0	1.9	1.9	0.0	1.9				
51	1.4	2.4	-	-	-	-		825	830	838	822	819	826	824	830	831	820	828	820	825						
52	1.0	2.4	-	-	-	-		824	828	830	819	815	817	810	818	813	805	810	801	809						
53	-	3.8	23.0	3.99	1.6	91.4		1185	1168	1060	1374	1424	1205	1312	1306	1179	1276	1288	1290	1260						
54	-	3.3	303.8	3.04	1.6	64.9		1090	1073	995	1182	1278	1079	1190	1158	1047	1155	1145	1188	1133						
55	-	3.2	3458.3	2.23	22.6	46.4		1049	1035	975	1113	1198	1038	1120	1097	1003	1090	1076	1134	1066						
56	-	3.2	4288.0	1.70	1006.6	33.1		1016	1007	958	1066	1144	1003	1072	1048	974	1043	1026	1069	1015						
57	-	5.8	433.8	3.31	3.2	72.4		1091	1046	953	1154	1291	989	1177	1108	970	1151	1181	1225	1176						
58	-	6.2	7140.2	1.80	1485.9	33.1		1029	996	924	1076	1181	954	1075	1024	929	1036	1038	1101	1041						
59	-	5.8	3458.3	2.73	19.4	58.3		1061	1025	939	1121	1244	978	1133	1065	953	1099	1112	1190	1133						
60	-	5.9	70.8	3.76	9.4	82.8		1154	1105	991	1268	1416	1049	1288	1238	1025	1261	1279	1286	1258						
61	-	5.8	936.7	3.14	3.2	66.1		1079	1043	945	1146	1289	992	1184	1100	973	1206	1183	1222	1196						
62	-	5.8	1559.3	2.97	3.2	60.9		1100	1086	944	1160	1297	976	1183	1132	958	1215	1193	1221	1219						
63	-	6.1	258.7	3.85	1.6	79.5		1055	991	898	1170	1283	996	1181	1110	996	1199	1190	1248	1188						
64	-	5.7	89.4	4.14	1.9	90.7		1103	1043	935	1255	1396	1052	1282	1278	1040	1268	1296	1304	1274						
65	-	6.4	19292.9	2.73	175.8	79.5		975	957	866	1099	1701	958	1095	1023	936	1077	1033	1174	1077						
66	-	3.6	108.3	3.94	6.5	84.8		1111	1041	988	1255	1375	1154	1279	1255	1130	1252	1270	1264	1234						
67	-	-	11619.9	2.34	80.7	47.0		1003	988	933	1096	1191	1052	1125	1096	1021	1100	1081	1131	1063						
68	-	2.8	11619.9	2.26	113.0	46.4		981	994	922	1082	1169	1008	1105	1066	986	1081	1060	1120	1044						

*Includes Fuel Injector Plus Catalytic Reactor Pressure Drop

*Includes Fuel Injector Plus Catalytic Reactor Pressure Drop

Table XXV. Test Summary, Runs 6, 7, and 8.

● Second Backup Reactor, Single-Point Injector

Date: 2/5-9/81

Second Backup Reactor, Single Point Injector

Date: 2/5-9/81		Reactor Inlet Conditions						Injector Conditions							Calculations								
Reading Number	Test Fuel, % No. 6 Residual Oil (Remainder is Jet A)	W_C - Airflow, kg/s	$T_{1.5}$ - Calculated Temperature, K	$T_{1.5}$ - Measured Temperature, K*	$P_{1.9}$ - Pressure, MPa	f_m - Metered Fuel/Air Ratio, g/kg	h - Humidity, g/kg	W_{AA} - Atomizing Airflow, kg/s	$T_{1.0}$ - Centerline Temperature, K	$T_{1.0}$ - Main-Stream Temperature at $r = 5$ cm, K	T_{AA} - Atomizing-Air Temperature, K	ΔP_{AA} - Atomizing-Air Pressure Drop, MPa	T_f - Fuel Temperature, K	ΔP_f - Fuel Pressure Drop, MPa	V_r - Reference Velocity, m/s	SMD - Calculated Fuel-Drop Size, μm	EICO - Carbon Monoxide Emission Index, g/kg	EIHC - Hydrocarbons Emission Index, g/kg	$EINO_x$ - Oxides of Nitrogen Emission Index, g/kg	f_s - Sample Fuel/Air Ratio, g/kg	η_g - Sample Combustion Efficiency, %	η_{tc} - Thermocouple Combustion Efficiency, %	
69	Dry Loss	0.388	778	760	0.413	0.0	1.43	0.026	819	808	288	87.4	-	-	20.44	-	-	-	-	-	-	-	
70	100	0.384	765	782	0.427	13.29	1.43	0.027	796	805	290	91.8	401	-	19.21	10.6	2.6	0.2	8.14	19.38	99.92	136.3	
71	100	0.390	766	771	0.414	9.92	1.43	0.028	803	803	291	97.2	404	-	20.20	8.9	365.7	3.5	6.12	13.90	90.93	118.8	
72	100	0.387	771	779	0.411	11.71	1.43	0.027	807	809	291	96.9	403	-	20.31	9.7	19.9	0.1	7.60	16.53	99.51	125.4	
73	100	0.404	728	741	0.427	12.41	1.43	0.026	763	754	291	88.7	401	-	19.28	10.8	12.4	0.1	8.15	17.73	99.70	131.5	
74	100	0.627	726	739	0.636	11.46	1.43	0.032	745	753	288	89.7	395	-	20.01	11.8	230.9	0.3	9.84	12.84	94.44	126.3	
75	Dry Loss	0.613	731	720	0.616	0.0	1.43	0.031	755	751	292	87.0	-	-	20.34	-	-	-	-	-	-	-	
76	100	0.629	725	738	0.599	12.28	1.43	0.033	749	747	293	99.9	395	-	21.27	11.6	22.6	0.2	7.36	17.95	99.45	127.3	
77	100	0.622	736	748	0.620	13.97	1.43	0.032	761	759	293	95.2	394	-	20.67	12.7	2.6	0.1	7.96	19.96	99.93	138.2	
78	100	0.627	722	740	0.609	11.26	1.43	0.033	736	754	293	99.2	396	-	20.78	11.1	183.2	0.7	6.32	15.48	95.55	122.6	
79	Dry Loss	0.420	724	713	0.407	0.0	1.43	0.026	755	750	296	91.4	-	-	20.93	-	-	-	-	-	-	-	
80	100	0.420	714	728	0.416	13.89	1.43	0.027	740	743	299	95.2	401	-	20.14	11.2	-	-	-	-	-	135.7	
81	0	0.345	691	685	0.605	17.71	1.43	0.031	728	731	299	94.5	395	-	11.03	12.1	2.8	1.9	0.12	18.48	99.77	87.7	
*Surface-Mounted Thermocouple																							

Table XXVI. Temperatures and Exhaust-Gas Concentrations, Runs 6, 7, and 8.

Reading Number	ΔP_{fi} - Fuel Injector Pressure Drop, %	ΔP_c - Catalytic Reactor Pressure Drop, %	CO - Carbon Monoxide Concentration, ppm	CO ₂ - Carbon Dioxide Concentration, %	HC - Unburned Hydrocarbons Concentration, ppm	NO _x - Oxides of Nitrogen Concentration, ppm														
							T _c - Reactor Substrate Temperature, K							T _{ex} - Reactor Exit Temperature, K (Uncorrected)						
							Station	2.0			2.5	3.0		3.1			4.0		4.1	
							Radius, cm	0.0	2.5	5.0	0.0	0.0	5.0	0.0	2.5	5.0	1.9	1.9	0.0	1.9
69	0.8	1.6	-	-	-	-		776	780	780	767	765	765	763	770	760	760	765	756	759
70	0.7	2.4	51.9	4.21	6.4	97.5		1096	1055	1005	1233	1365	1051	1286	1280	1158	1244	1263	1258	1231
71	0.8	2.4	5292.1	2.48	86.9	52.8		959	946	904	1085	1185	1023	1129	1094	999	1078	1073	1128	1059
72	0.9	2.4	343.8	3.55	3.2	77.9		1011	978	953	1148	1286	1102	1214	1176	1060	1185	1180	1210	1160
73	0.9	2.7	228.9	3.83	2.9	89.4		968	918	856	1164	1281	1127	1204	1206	1096	1176	1186	1215	1174
74	1.0	2.6	3084.9	2.48	6.4	78.6		972	934	898	1085	1233	1059	1163	1172	990	1083	1119	1199	1081
75	0.8	1.4	-	-	-	-		723	724	733	716	714	725	720	725	719	717	721	714	718
76	1.0	2.7	423.7	3.85	4.8	81.7		1130	1311	1293	1207	1335	1080	1189	1206	1061	1141	1209	1226	1198
77	0.9	2.5	54.7	4.33	4.8	98.2		1229	-	1105	1515	1408	1185	1295	1319	1168	1253	1276	1294	1249
78	1.0	2.6	2957.9	3.06	19.4	60.6		1053	1139	978	1196	1275	1034	1136	1154	1026	1094	1129	1172	1138
79	0.9	1.8	-	-	-	-		724	724	725	714	714	714	713	718	701	710	713	707	709
80	0.9	3.3	-	-	-	-		1010	1140	989	1132	1340	1154	1249	1274	1190	1218	1241	1243	1200
81	0.2	0.9	53.8	3.91	62.1	1.4		1114	1095	1178	1218	1314	1306	1241	1250	1239	1225	1220	1213	1207

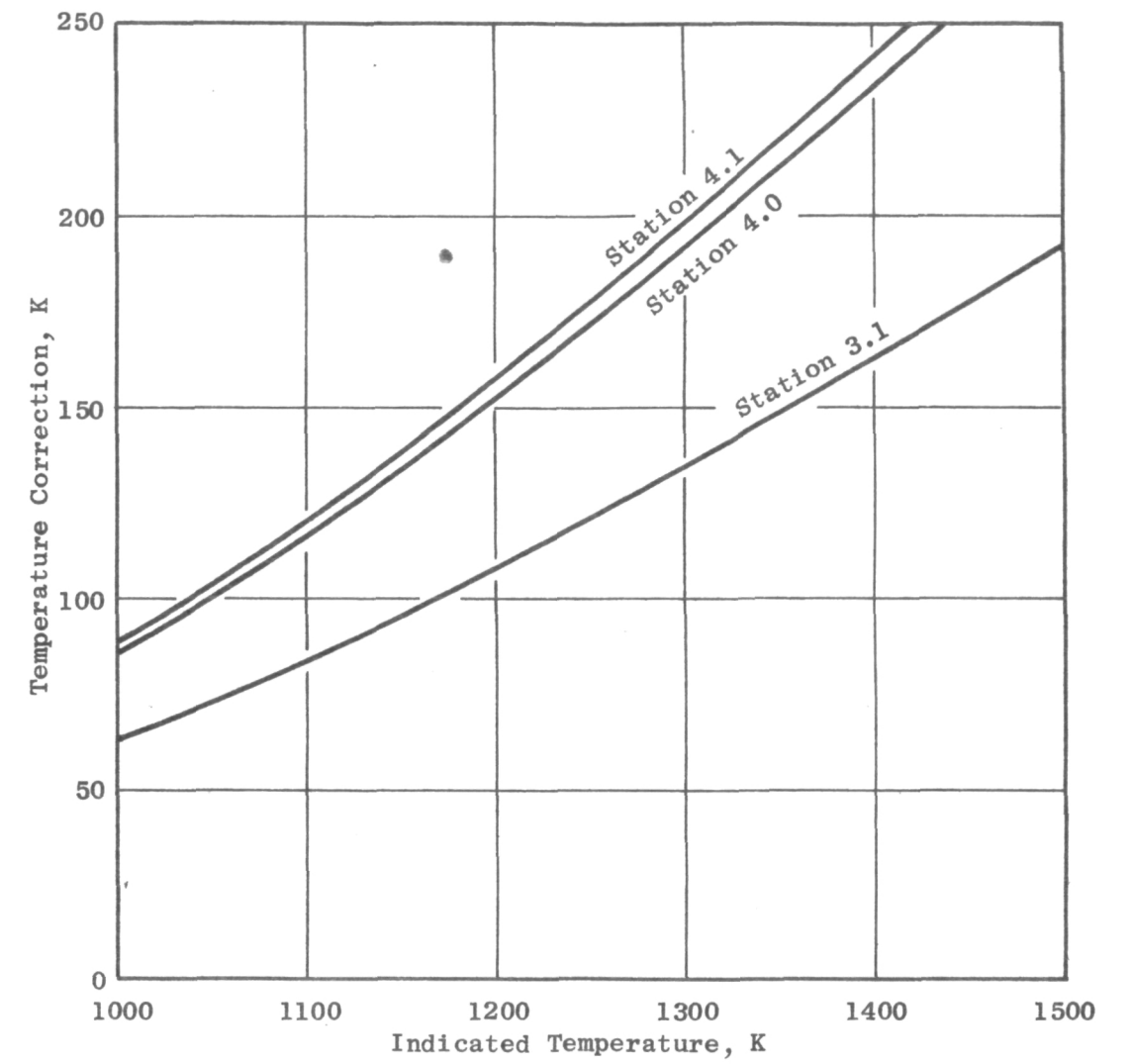


Figure 44. Temperature Corrections for $V_r = 19.8$ m/s.

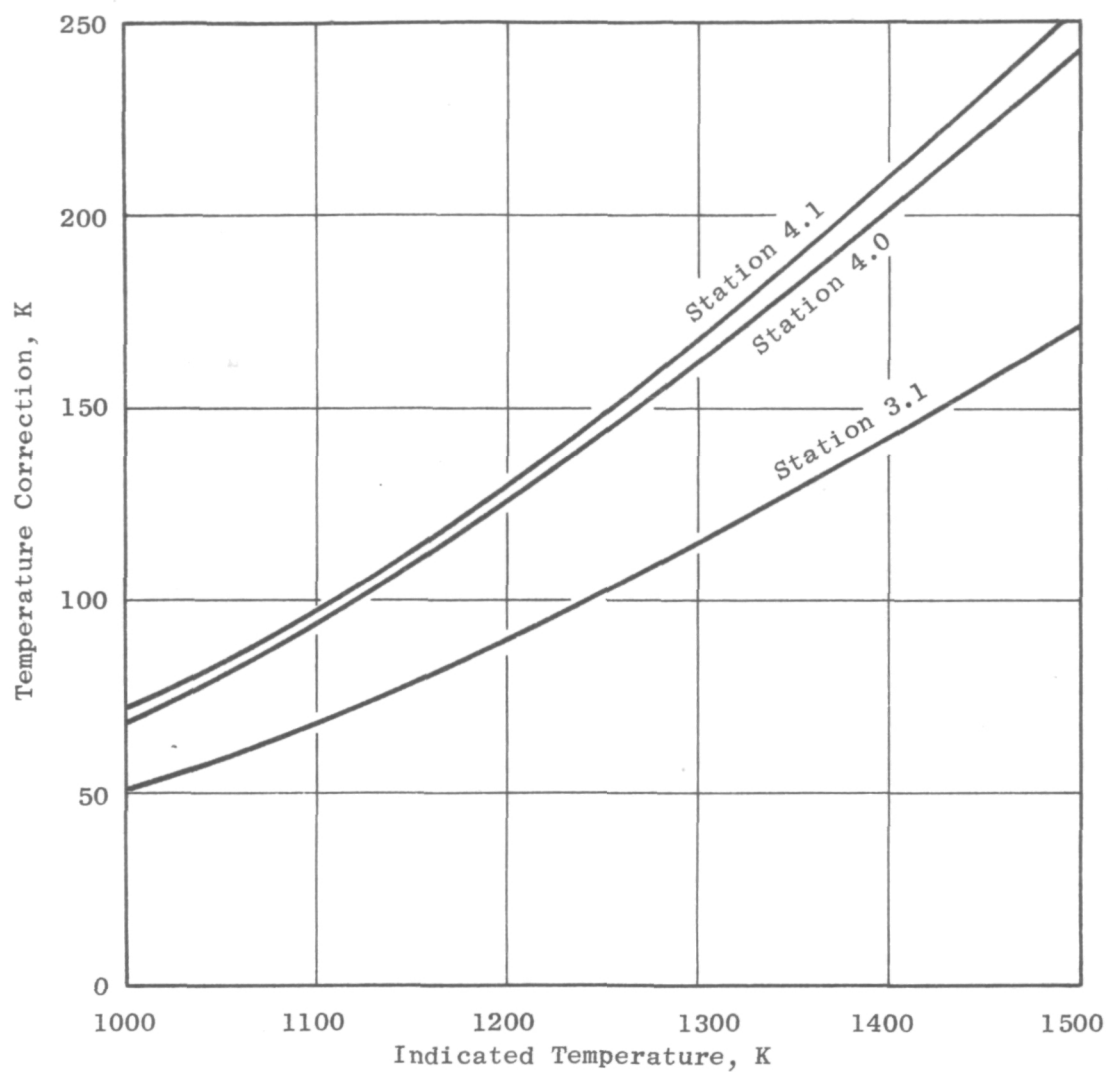


Figure 45. Temperature Corrections for $V_r = 30.5$ m/s.

APPENDIX B

MULTIPLE CONICAL TUBE INJECTOR

As described in Section 4.1, the baseline fuel/air mixture-preparation system used in this program consisted of a single-point, air-assisted, simplex injector mounted in a converging/diverging premixing duct. This system had not been tested previously, and there was some concern that additional system development would be required and cause a delay in the test program. Therefore, two additional injectors of the multiple-tube type (Reference 1) were designed and fabricated to serve as backup systems (Figure 46).

The two multiple-tube injectors were built to produce two average-drop sizes: the first range was less than 30 μm , and the second was between 70 and 150 μm . Cross-sectional views of these two injector designs are shown in Figure 47. Each of the multiple-tube injectors uses an array of 19 tubes as shown in Figure 48. In operation, fuel to each of the 19 tubes would be metered by orifices located at the tube inlet in order to ensure a uniform fuel-flow distribution. The fuel tubes are routed through a cavity that is isolated from the hot airstream. Details of the fuel-tube installation are shown in Figure 49. Temperature within the isolated cavity can be independently controlled to protect against fuel-tube fouling. The injector inlet is carefully radiused as shown in Figure 50 to provide a uniform air-velocity profile at the fuel-injection point. Each of the fuel tubes extends into the airstream to place the fuel in the center of the air tube, based on fuel penetration calculated with the correlations of Reference 1.

A summary of the multiple-conical-tube-injector design parameters is presented in Table XXVII. Drop size was predicted using an applicable drop-size correlation from Reference 12. This is a two-term correlation of the form:

$$\begin{aligned} \text{SMD} = & K_1 (\sigma_f)^{0.35} (\rho_f)^{-0.35} (V_a)^{-1} (\rho_a)^{-0.35} (1 + W_f/W_a)^{0.25} \\ & + K_2 \eta_f (D)^{0.5} (\sigma_f)^{-0.5} (\rho_f)^{-0.5} (1 + W_f/W_a) \end{aligned}$$

where σ_f , ρ_f , and η_f are the fuel surface tension, density, and viscosity respectively; V_a and ρ_a are airstream velocity and density; W_f and W_a are the injector fuel and air flows; D is the orifice diameter, and K_1 and K_2 are constants. The first term in this equation is controlled primarily by air velocity and density; the second term depends on the orifice diameter and fuel properties.

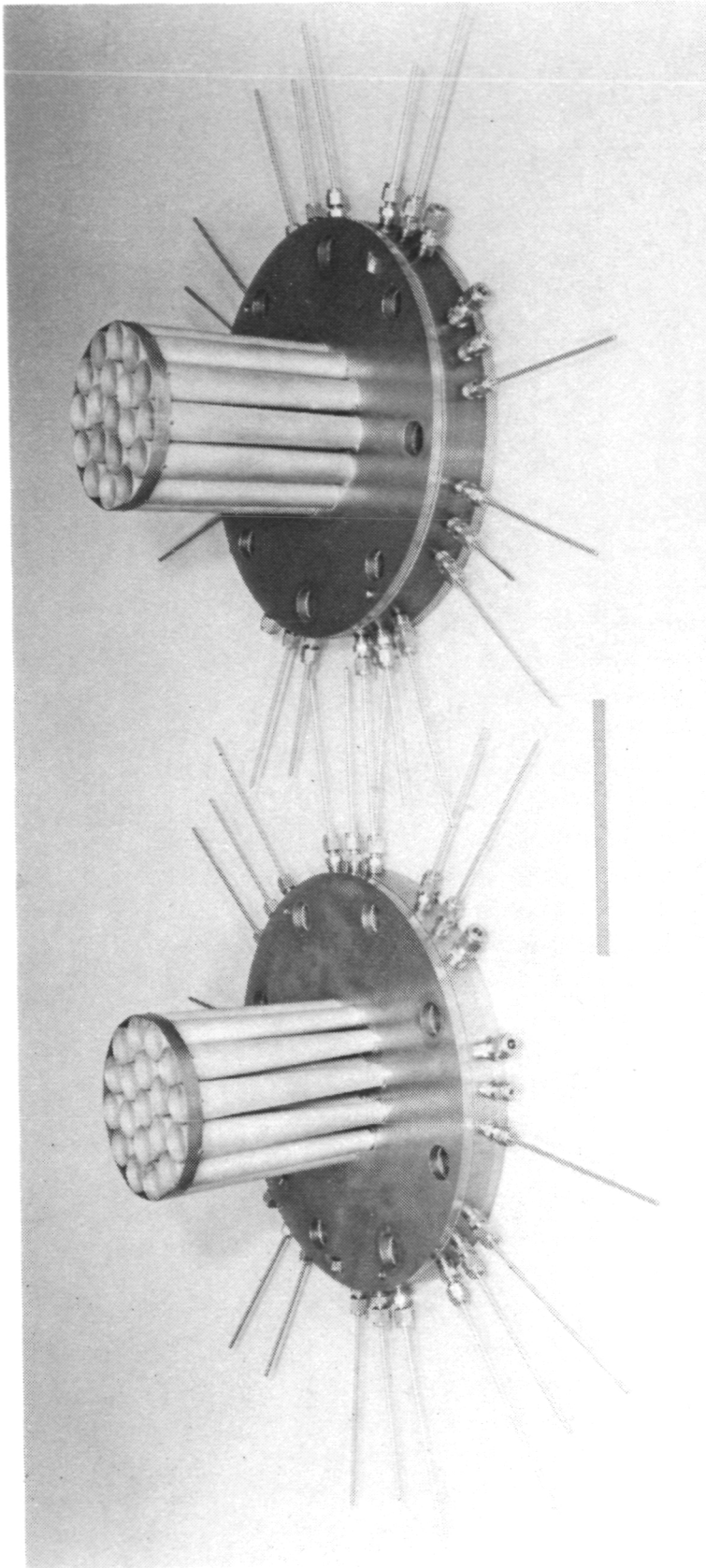


Figure 46. Multiple-Conical-Tube Fuel Injectors.

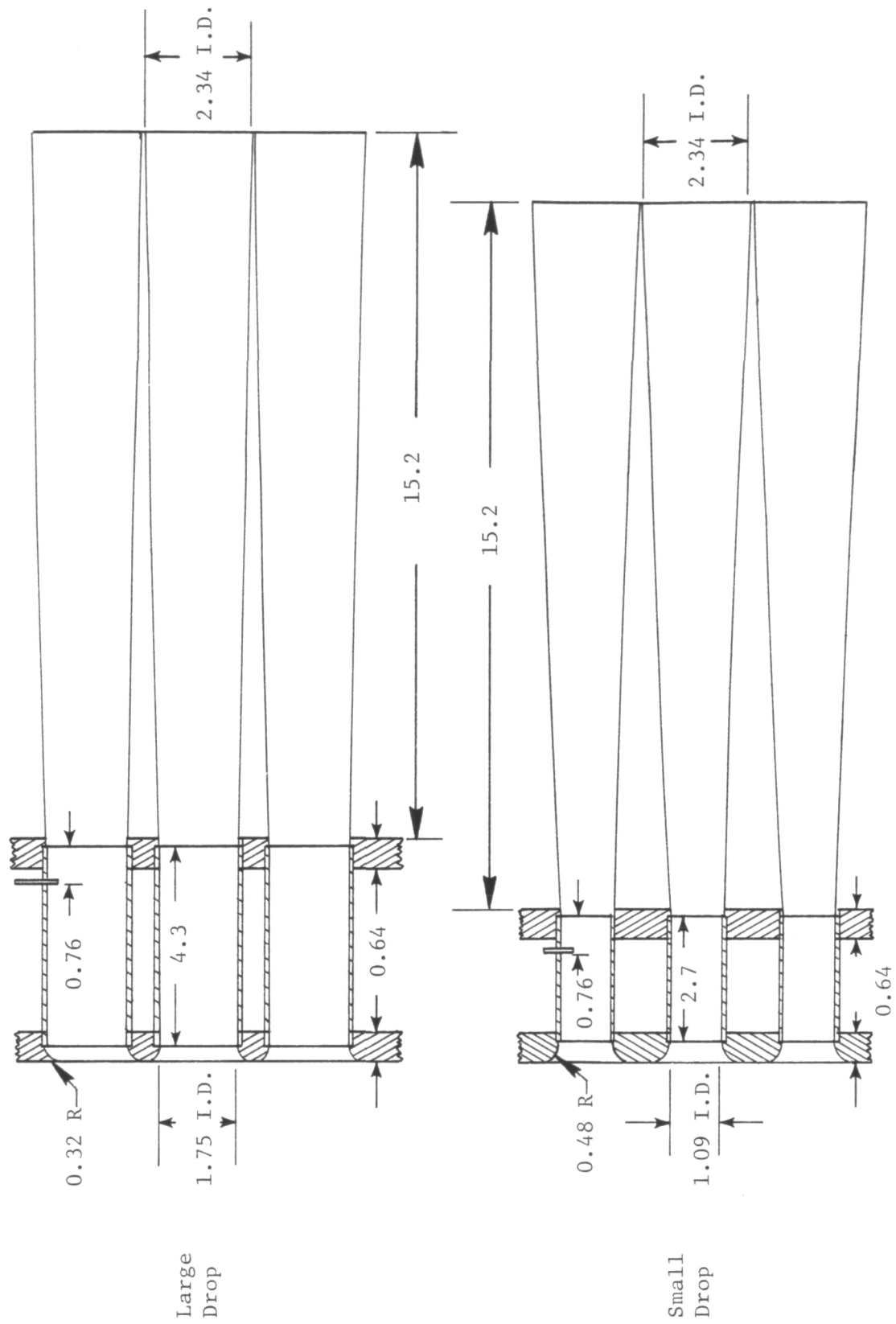


Figure 47. Multiple-Conical-Tube Injector Cross Sections,

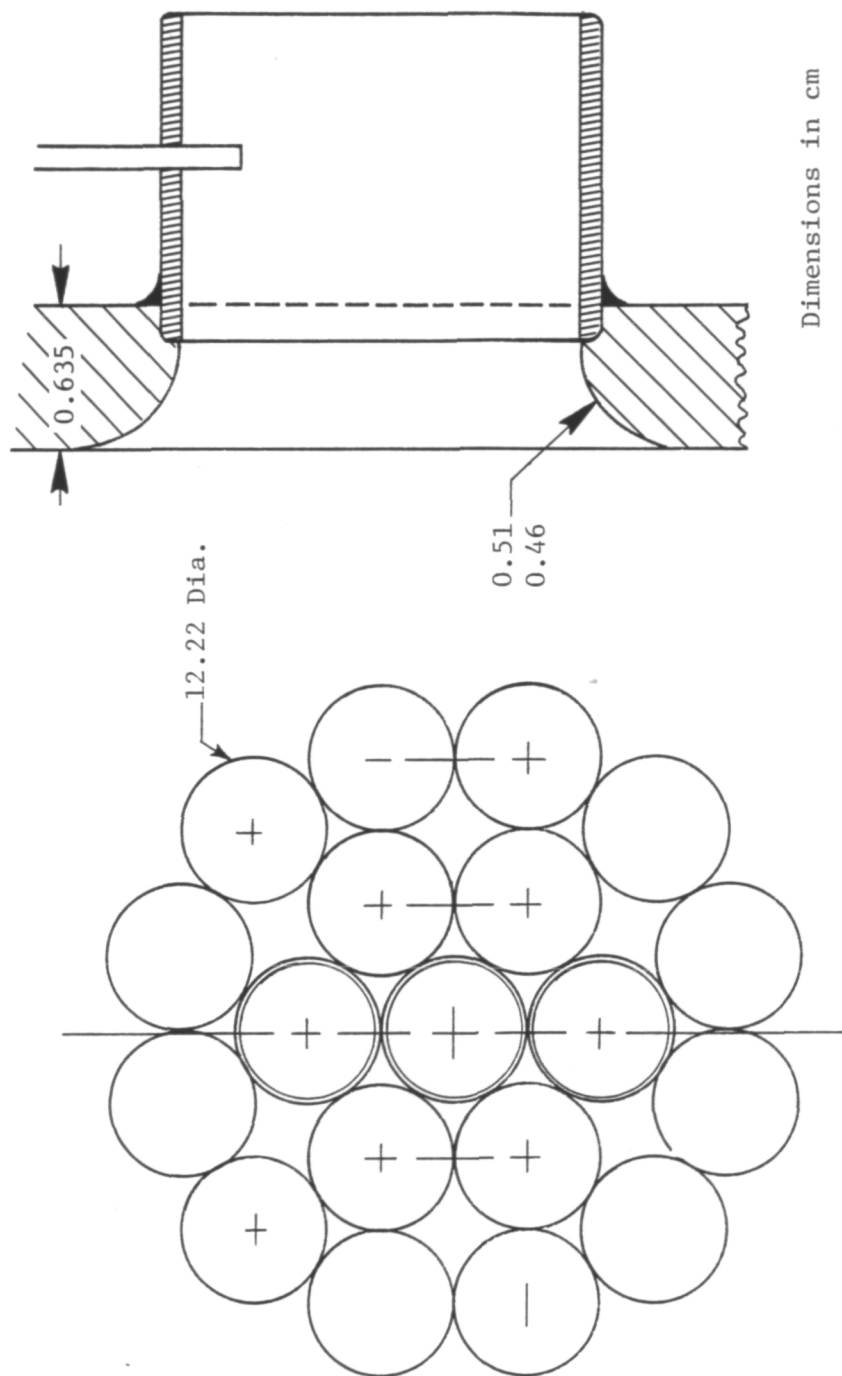


Figure 48. Multiple-Tube Injector Design Details.

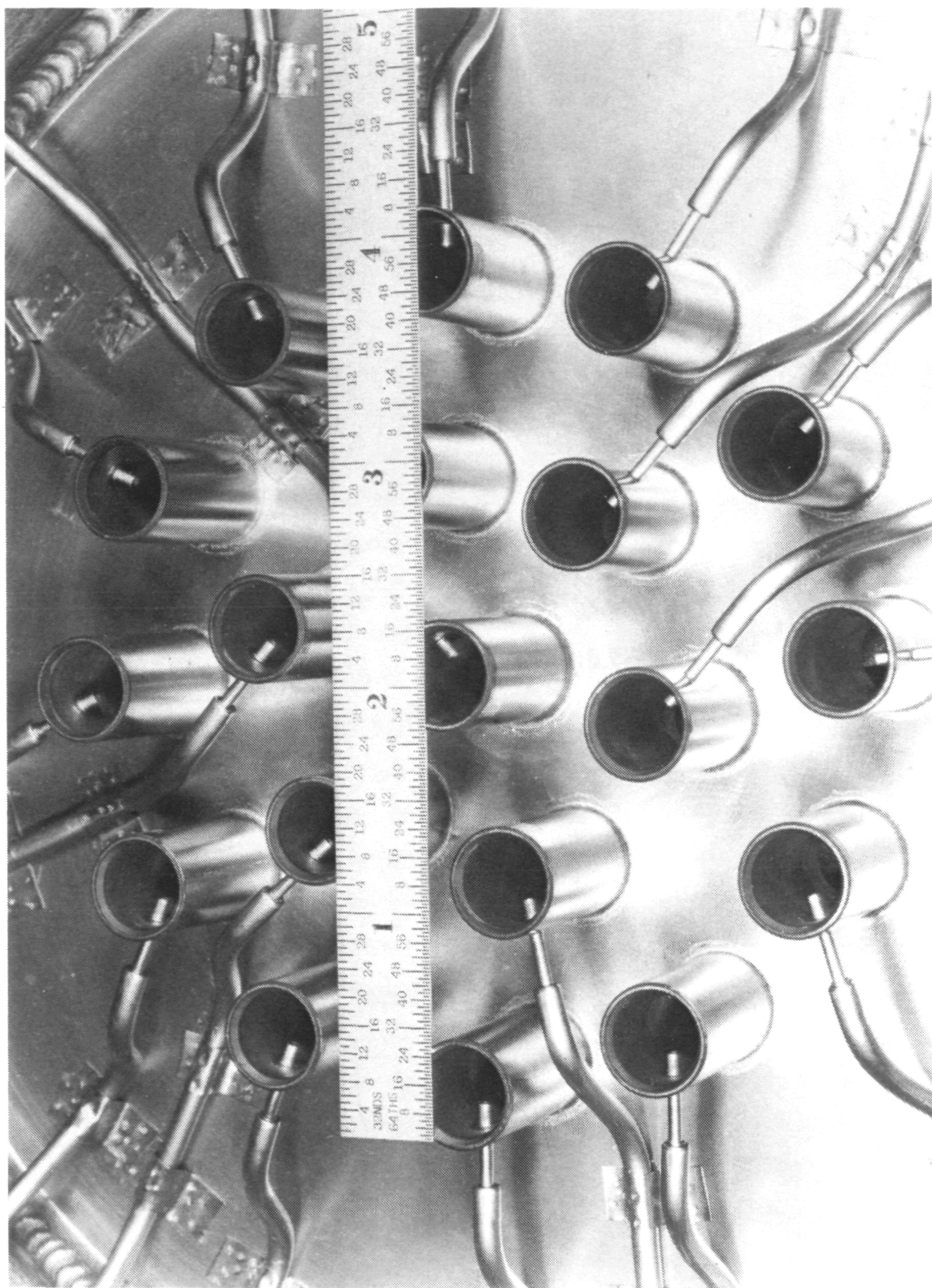


Figure 49. Multiple-Tube Injector Fuel Tube Installation.

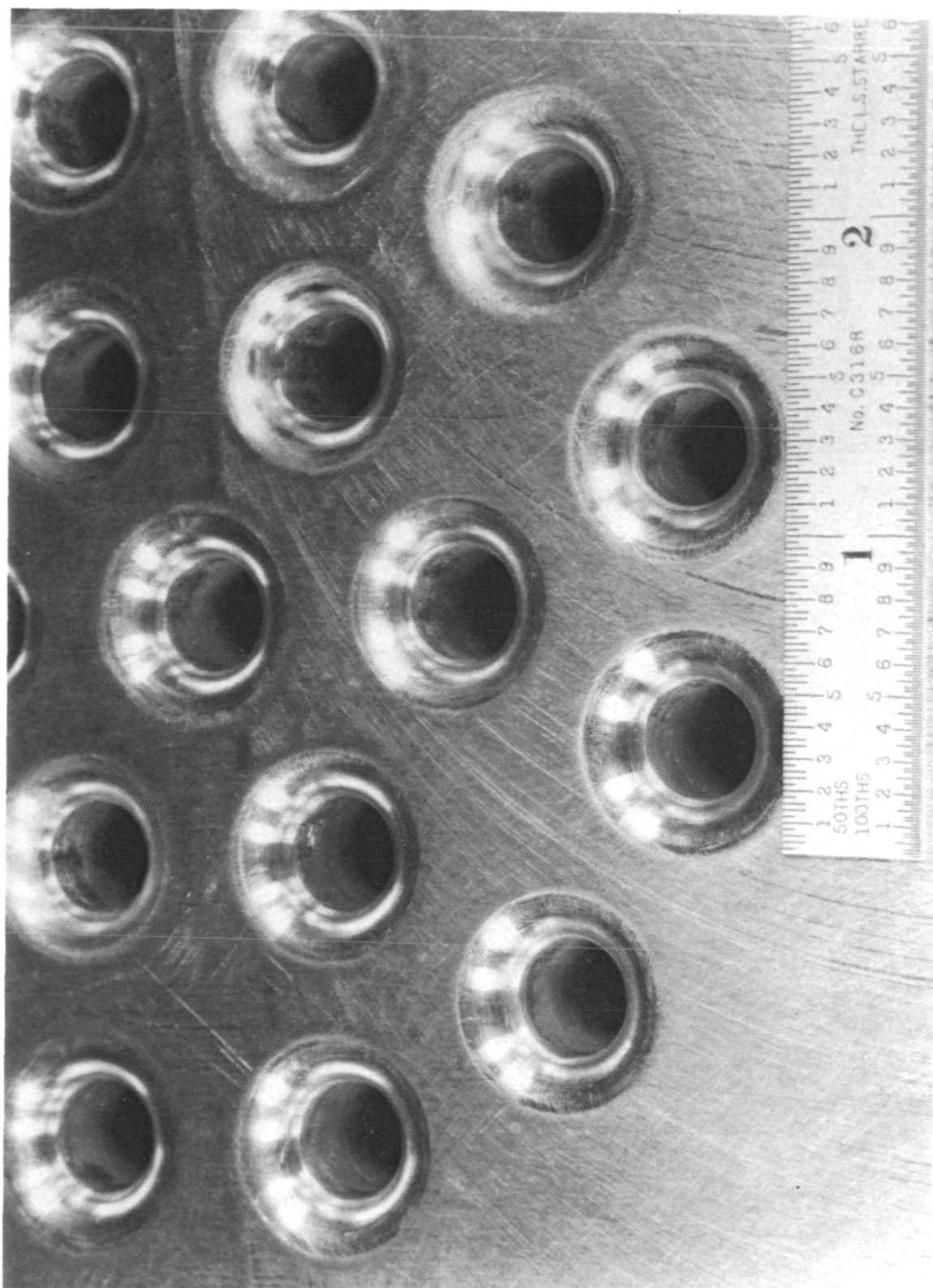


Figure 50. Multiple-Tube Injector Inlet.

The injector sizes and fuel temperatures for the two injector designs were selected such that each of the terms in the above equation are reduced by about 70% going from the large-drop injector to the small-drop design. The same percent reduction is predicted using a single-term correlation from Reference 13, but the predicted drop size is somewhat larger.

Since the performance of the single-point injector was adequate for all tests conducted during this program, the multiple-tube injectors were not tested.

Table XXVII. Multiple-Conical-Tube Injector Design Values.

Parameter	Small-Drop Injector	Large-Drop Injector
Fuel Temperature, K	400	360
Fuel Viscosity, ns/m ²	0.0101	0.0427
Fuel Surface Tension, N/m	0.0278	0.0311
Fuel Density, kg/m ³	882	909
Atomizing Air Velocity, m/s	145	45
Atomizing Air Density, kg/m ³	3.67	3.67
Fuel Orifice Size, mm	1.08	1.08
Predicted Drop Size, μ m	31	110

APPENDIX C


SYMBOLS

<u>Symbol</u>	<u>Description</u>	<u>Basic Units</u>
A	Area	m ²
CAROL	Contaminants Analyzed and Recorded On-Line	---
CO	Carbon Monoxide Concentration	ppm
CO ₂	Carbon Dioxide Concentration	%
D	Diameter	cm
D _H	Hydraulic Diameter	cm
d _o	Initial Droplet Sauter Mean Diameter	μm
EICO	Carbon Monoxide Emission Index	g CO/kg Fuel
EIHC	Unburned Hydrocarbon Emission Index	g HC/kg Fuel
EINO _x	Oxides of Nitrogen Emission Index	g NO _x /kg Fuel
f	Fuel/Air Ratio	g Fuel/kg Air
FBP	Final Burning Point	K
FID	Flame-Ionization Detector	---
h	Humidity	g H ₂ O/kg Air
IBP	Initial Burning Point	K
HC	Unburned Hydrocarbon Concentration	ppm
L	Length	cm
NO _x	Oxides of Nitrogen Concentration	ppm
P	Pressure	MPa
Pd	Palladium	---
P _s	Static Pressure	MPa
P _t	Total Pressure	MPa

APPENDIX C (Continued)

<u>Symbol</u>	<u>Description</u>	<u>Basic Units</u>
R,r	Radius	cm
SMD	Sauter Mean Diameter	μm
T	Temperature	K
T _{ad}	Adiabatic Flame Temperature (Normally Based on Gas Sample Fuel-Air Ratio)	K
T/c	Thermocouple	---
T _s	Static Temperature	K
T _t	Total Temperature	K
V _r	Reference Velocity	m/s
W	Airflow	kg/s
W _f	Fuel Flow	g/s
ΔP	Pressure Drop	% or kPa
η_f	Fuel Viscosity	Ns/m ²
η	Combustion Efficiency	%
ρ	Density	kg/m ³
σ	Surface Tension	N/m
ν	Fuel Kinematic Viscosity	cs
<u>Subscripts</u>		
a	Air	
AA	Atomizing Air	
ad	Adiabatic	
AR	Property Referenced to Air at Standard Temperature and Pressure	
b	Burning	

APPENDIX C (Concluded)

<u>Subscript</u>	<u>Description</u>
C,b	Catalytic Reactor
ex	Reactor Exit
f	Fuel
fi	Fuel Injector
FR	Property Referenced to Standard Calibration Fluid
g	Gas Sample
m	Metered
R,r	Reference
s	Gas Sample
tc	Thermocouple
1.0	 Test Section Axial Stations
1.5	
1.9	
2.0	
2.5	
3.0	
3.1	
4.0	
4.1	

REFERENCES

1. Tacina, R.R., "Experimental Evaluation of Fuel Preparation Systems for an Automotive Gas Turbine Catalytic Combustor," NASA TM 78856, June 1977.
2. Cutrone, M.B., Hilt, M.B., Goyal, A., Ekstedt, E.E., and Notardonato, J., "Evaluation of Advanced Combustors for Dry NO_x Suppression with Nitrogen Bearing Fuels in Utility and Industrial Gas Turbine Engines," ASME Paper 81-GT-125, March 1981.
3. Simmons, H.C., "The Prediction of Sauter Mean Diameter for Gas Turbine Fuel Nozzles of Different Types," ASME Paper 79-WA/GT-51, December 1979.
4. Spadaccini, L.J., "Autoignition Characteristics of Hydrocarbon Fuels at Elevated Temperatures and Pressures," ASME Paper 76-GT-3, March 1976.
5. El Wakil, M.M., Uyehara, D.A. and Myers, P.S., "A Theoretical Investigation of the Heating-Up Period of Injected Fuel Droplets Vaporizing in Air," Tech. Note 23179, NACA 1954.
6. Maxwell, J.B., Data Book on Hydrocarbons, D. Van Nostrand Co., 1950.
7. Barnett, H.C. and Hibbard, R.R., "Properties of Aircraft Fuels," NACA TN 3276, August 1956.
8. Tacina, R., "Experimental Evaluation of Premixing Prevaporizing Fuel Injection Concepts for a Gas Turbine Catalytic Combustor," NASA TM-73755, August 1977.
9. Roffe, G., "Development of a Catalytic Combustor Fuel-Air Carburetion System," AFAPL TR-77-19, 1977.
10. Retallick, W.B., "Preliminary Design of Catalytic Combustors," from Proceedings of the Fourth Workshop on Catalytic Combustion, EPA-600/9-80-035, August 1980.
11. Gleason, C.C., Rogers, D.W., and Bahr, D.W., "Experimental Clean Combustion Program, Phase II Final Report," NASA CR-134971, July 1976.
12. Jasuja, A.K., "Atomization of Crude and Residual Fuel Oils," ASME Paper 78-GT-83, April 1978.
13. Ingebo, R.D. and Foster, H.H., "Drop Size Distribution for Cross-Current Breakup of Liquid Jets in Air Streams," NACA TN 4087, 1957.

1. Report No. NASA CR-165369		2. Government Accession No.		3. Recipient's Catalog No.	
4. Title and Subtitle DEMONSTRATION OF CATALYTIC COMBUSTION WITH RESIDUAL FUEL				5. Report Date August 1981	
				6. Performing Organization Code	
7. Author(s) W.J. Dodds, and E.E. Ekstedt				8. Performing Organization Report No. R81AEG590	
9. Performing Organization Name and Address General Electric Company Aircraft Engine Business Group Cincinnati, Ohio 45215				10. Work Unit No.	
				11. Contract or Grant No. DEN 3-155	
12. Sponsoring Agency Name and Address U.S. Department of Energy Office of Coal Utilization Washington, D.C. 20546				13. Type of Report and Period Covered Final Report 10/79 - 4/81	
				14. Sponsoring Agency Code DOE/NASA/0155-1	
15. Supplementary Notes Final Report prepared under Interagency Agreement DE-AI01-77ET-10350 Project Manager - Dr. D.N. Anderson, Aerothermodynamics and Fuels Division NASA Lewis Research Center, Cleveland, Ohio 44135					
16. Abstract An experimental program was conducted to demonstrate catalytic combustion of a residual fuel oil. Three catalytic reactors, including a baseline configuration and two backup configurations based on baseline test results, were operated on No. 6 fuel oil. All reactors were multielement configurations consisting of ceramic honeycomb catalyzed with palladium on stabilized alumina. Stable operation on residual oil was demonstrated with the baseline configuration at a reactor inlet temperature of about 825 K (1025° F). At lower inlet temperatures, operation was precluded by apparent plugging of the catalytic reactor with residual oil. Reduced plugging tendency was demonstrated in the backup reactors by increasing the size of the catalyst channels at the reactor inlet, but plugging still occurred at inlet temperatures below 725 K (845° F). Operation at the original design inlet temperature of 589 K (600° F) could not be demonstrated. Combustion efficiency above 99.5% was obtained with less than 5% reactor pressure drop. Thermally formed NO _x levels were very low (less than 0.5 g NO ₂ /kg fuel), but nearly 100% conversion of fuel-bound nitrogen to NO _x was observed.					
17. Key Words (Suggested by Author(s)) Catalytic Combustion Residual Fuel Industrial Gas Turbine Combustor Emissions				18. Distribution Statement Unclassified - Unlimited Star Category 44 DOE Category UC-90d	
19. Security Classif. (of this report) Unclassified		20. Security Classif. (of this page) Unclassified		21. No. of Pages 106	
				22. Price*	

* For sale by the National Technical Information Service, Springfield, Virginia 22161